JAERI-M
8719

ANNUAL REPORT ON NEUTRON SCATTERING STUDIES IN JAERI, SEPTEMBER 1, 1978 - AUGUST 31, 1979

March, 1980

Masashi IIZUMI, Yasuo ENDOH* [eds.]

日本原子力研究所
Japan Atomic Energy Research Institute

この報告書は，日本原子力研究所が JAERI-M レポートとして，不定期に刊行している研究報告書です．入手，複製などのお問合わせは，日本原子力研究所技術情報部（茨城県那珂郡東海村）あて，お申しこしください．

JAERI-M reports, issued irregularly, describe the results of research works carried out in JAERI. Inquiries about the availability of reports and their reproduction should be addressed to Division of Technical Information, Japan Atomic Energy Research Institute, Tokai-mura, Naka-gun, Ibaraki-ken, Japan.

JAERI-M 8719

Annual Report on Neutron Scattering Studies in JAERI, September 1, 1978 - August 31, 1979

Masashi IIZUMI and Yasuo ENDOH* (eds.)

Division of Physics, Tokai Research Establishment, JAERI

(Received January 29, 1980)

Neutron scattering studies carried out from September 1978 to August 1979 by Division of Physics, JAERI, and universities with JRR-2 and -3 neutron beam facilities are described : 51 summary reports, and a list of publications.

Key words: Neutron Scattering, Neutron Diffraction, Neutron Optics, Solid State Physics, Condensed Matters, Crystal Structure, Lattice Dynamics, Structural Phase Transition, Magnetic Structure, Magnetic Moment Distribution, Spin Wave, Liquid, Solution, Research Reactor, JAERI.

---

* Tohoku University

JAERI－M 8719

日本原子力研究所における中性子散乱研究年次報告

（1978 年 9 月 1 日～1979 年 8 月 31 日）

日本原子力研究所東海研究所物理部

（編）飯泉　仁・遠藤康夫 *

（1980 年 1 月 29 日受理）

JRR－2，－3 を使い，日本原子力研究所物理部および諸大学研究機関によって行なわれた中性子散乱研究の，1 年間の成果をまとめたプログレス・レポートである。内容は，51 篇の小論文と，出版された文献のリストを収録している。

* 東北大学理学部

PREFACE

The present report follows the first and second issues, JAERI-M 7408 (Nov., 1977) and JAERI-M 8009 (Dec., 1978) and documents the current research activity in neutron scattering at Tokai Research Establishment in the period of the last twelve months from September 1, 1978 to August 31, 1979.

The report incudes 51 papers prepared by indivisual authors on the research done during the above period by the use of the neutron beam facilities in JRR-2 and 3. Considerable numbers of contributions are products of full activity assisted by the steady operation of the JRR-2 and 3.

The issuance of this report is not intended to constitute a publication in a usual sense. Final results will be submitted for publication in regular journals. Papers published during the period covered by this report are listed in the alphabetical order of the first authors at the end of this report.

M. Iizumi (JAERI)
and Y. Endoh (Tohoku Univ.),
Editors

CONTENTS

V. LIQUIDS AND SOLUTIONS

VI. NEUTRON OPTICS AND TECHNIQUES

APPENDIX

目　　次

Ⅰ・結　晶　構　造

Ⅱ・格子振動と構造相転移

Ⅲ．磁気構造とモーメント分布

Ⅳ・磁　気　励　起

V．液　体　溶　液

Ⅵ．中性子光学と技術

附　　録

I1 The Existence of the Order Phase and the Structure of Superionic Conductor Ag_3SBr

Takashi Sakuma* and Sadao Hoshino**

* Department of Physics, Faculty of Science, Ibaraki University ,
** Institute for Solid State Physics, The University of Tokyo.

The ordered phase (γ-phase) concerning the Ag distribution of superionic conductor Ag_3SBr was discovered below 128 K. The transition heat and the entropy change were measured to be 0.23 Kcal/mol and 1.77 cal/mol. deg. respectively.

The crystal structure of the newly found γ-phase and the room temperature phase (β-phase) were studied by X-ray and neutron diffraction methods. The neutron diffraction measurement was performed with the ISSP ND-1 diffractometer at JRR-2 and ISSP ND-2 diffractometer at JRR-3. The space group of γ-phase may be D_{2h}^{17}, different from that of γ-Ag_3SI[1]. The lattice constants were measured to be a(≈b) = 9.423±0.008A and c = 9.711± 0.009A at 118 K. Details will be submitted to J. Phys. Soc. Jpn.

	α-phase		β-phase[2]		γ-phase
Ag_3SBr :	(dissociation)	∿ 430°C	O_h^1-Pm3m	128K	D_{2h}^{17}-Cmcm
Ag_3SI :	O_h^9-Im3m	246°C	O_h^1-Pm3m	157K	C_3^4-R3

Table I Phase transition schemes for Ag_3SBr and Ag_3SI.

References

1) S. Hoshino, T. Sakuma and Y. Fujii : J. Phys. Soc. Jpn. 47 (1979)
2) B. Reuter and K. Hardel : Z. anorg. allgem. Chem. 340 (1965) 168.

I2 Refinement of the Structure of β-V_2D by Single Crystal Neutron Diffraction

Isao Okada*, Hajime Asano** and
Makoto Hirabayashi***

* Graduate School, Tohoku University, ** The Research Institute for Iron, Steel and Other Metals, Tohoku University, Now at Institute of Materials Science, University of Tsukuba and *** The Research Institute for Iron, Steel and Other Metals, Tohoku University.

Deuterium atoms in β-V_2D occupy preferentially one set of the octahedral z-sites (Oz_1) in a pseudotetragonal vanadium lattice with the axial ratio c/a ≃ 1.1 (Fig. 1)[1,2]. With increasing temperature, the deuterium atoms rearrange from the ordered occupation of Oz_1-sites to the random occupation of tetrahedral (T) sites at the β-α transition temperature Tc ≃ 130°C. It is noted, however, that the arrangement is not perfectly ordered at room temperature but the T-sites are fractionally occupied. The purpose of the present study is refinement of the β-V_2D structure by the Fourier anlysis; the distribution of deuterium can be readily determined taking advantage of the fact that vanadium is an almost perfect incoherent scatterer of thermal neutrons.

Two sections of the three-dimensional Fourier synthesis of the neutron scattering density are shown in Fig. 2. The deutrium atoms at Oz_1 sites exhibit appreciable peaks of the positive density with ellipsoidal contours, but the vanadium atoms are hardly seen. The deuterium distribution is extended to the neighboring T sites along the [010] direction, and seems to be almost continuous to the next neighboring Ox-sites. A similarly extended distribution appears around a small peak at the Oz_2-site. This result suggests jumping passes of deuterium in the sequences of Ox-T-Oz_1-T-Ox and T-Oz_2-T sites.

The occupation probabilities of deuterium p_1, p_2, p_3 and p_t for the Oz_1, Oz_2, Ox and T-sites, respectively, are evaluated from analyzing the observed intensities taking account of the anisotropic Debye parameters and the static displacement of vanadium U_z = 0.12 Å[3]. The results of p_1 = 0.84, p_2 = 0.03, p_3 = 0.01 and p_t = 0.12 are obtained for the minimun of $R = \Sigma||Fobs| - |Fcal||/\Sigma|Fobs| = 0.08$.

In addition to the Fourier analysis at room temperature, the temperature dependence of superlattice reflection intensities was measured at

temperatures up to 140°C. The long range order $S = p_1 - p_2$ as a function of temperature agrees well with the previous result of powder diffraction[4].

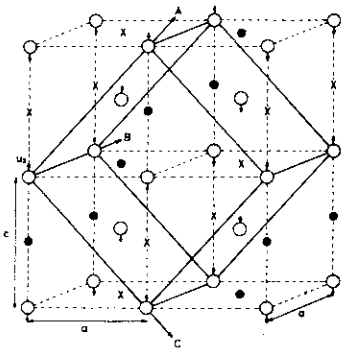

Fig.1 Structure of β-V_2D, o:V, ●:D at Oz_1 sites, ×:Oz_2 sites. Uz is the displacement of V along the c axis.

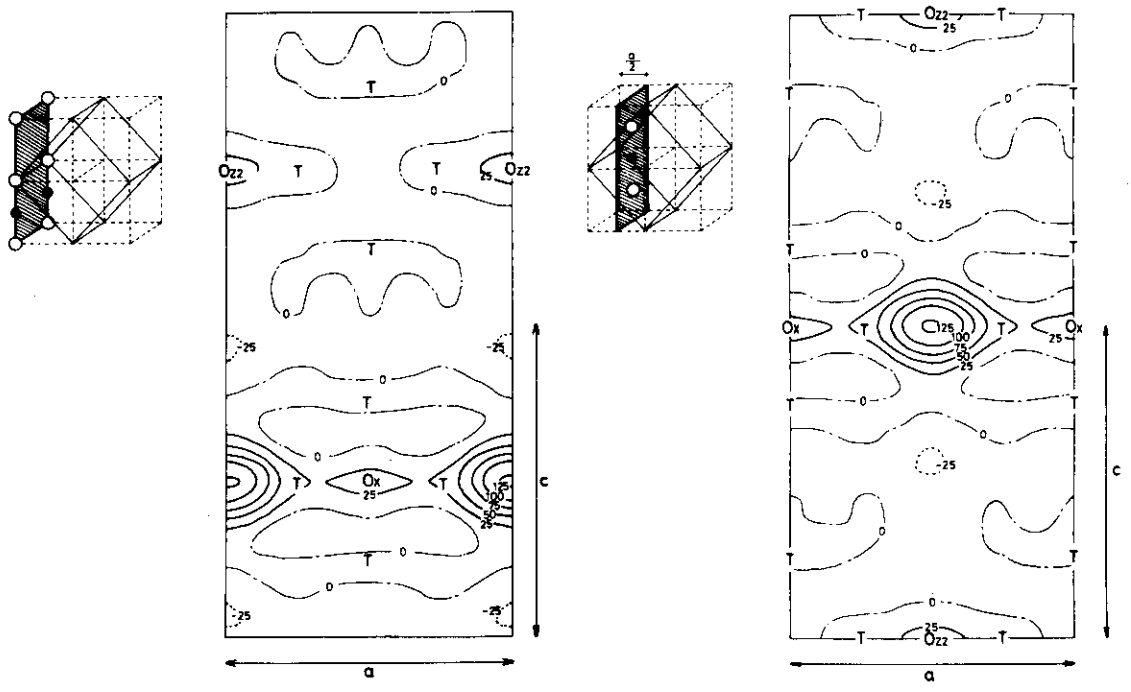

Fig.2 Sections of Fourier synthesis parallel to the (010) plane.

References

1) V. A. Somenkov, I. R. Entin, A. Yu. Chervyakov, S. Sh. Shil'shtein and A. A. Chertkov; Sov. Phys.-Solid State 13 (1972) 2178

2) H. Asano and M. Hirabayashi; phys. stat. solidi (a) 15 (1973) 267

3) H. Metzger, H. Jo, S. C. Moss and D. G. Westlake; phys. stat. sol. (a) 47 (1978) 631

4) H. Asano and M. Hirabayashi; 2nd Intern. Congr. Hydrogen in Metals, Paris 1977, 1D6

I3 Static Displacement of Ta. in Ta_2H by Single Crystal Neutron Diffraction

Hajime Asano*, Kazunori Kishi** and
Makoto Hirabayashi***

* The Research Institute for Iron, Steel and Other Metals, Tohoku University, Now at Institute of Materials Science, University of Tsukuba, ** Graduate School, Tohoku University and *** The Research Institute for Iron, Steel and Other Metals, Tohoku University.

The ordered structure of Ta_2H has been studied by single crystal neutron diffraction to determine the static displacement of tantalum atoms caused by the ordered distribution of hydrogen. The structure of Ta_2H is described by an orthorhombic unit cell (space group C 222) having

$A = a\{2(1+\cos\gamma)\}^{1/2}$, $B = a$ and $C = a\{2(1-\cos\gamma)\}^{1/2}$,

where $a \simeq 3.30$ Å is the lattice constant of the metal cell and $\gamma \simeq 90.5°$ is the monoclinic deformation (Fig. 1)[1,2,3]. The atomic coordinates are given as

(0, 0, 0; 1/2, 1/2, 0) +

4 Ta in 4 k: 1/4, 1/4, z; 1/4, 3/4, $\bar{z}$ with $z = 3/4 - \Delta$

2 H in 2 a: 0, 0, 0,

where Δ is the tantalum atom displacement.

A single crystal of pure tantalum ($5 \times 3 \times 0.3$ mm^3) was sealed in an evacuated glass tube together with an appropriate amount of a powdered sample $TaH_{0.72}$, kept at 350°C for 1 month and then followed by slow cooling to room temperature. During the above treatment, hydrogen was transferred from the powder to the tantalum crystal to form a single crystal of Ta_2H.

Neutron diffraction experiments were made for reflections on the reciprocal lattice section HOL. The crystal was proved to be composed of multiple domains with six orientations of the orthorhombic axes. We choose one domain and gathered the intensity data of superlattice reflections. After the correction of absorption effect and Lorentz factor, the observed structure factors are compared with calculations taking Δ as an adjustable parameter. A variation of R-factor which is given as $\Sigma||Fobs| - |Fcal||/\Sigma|Fobs|$ is shown in Fig. 2 as a function of Δ in comparison with the X-ray diffraction results[4]. It may be safe to determine Δ as 0.016 ± 0.002, although the R-factors for neutron and X-ray diffraction take minima at slightly different values of Δ. This

value is a little larger than that (0.012) for Ta_2D[1]. It is not clear at present whether the discrepancy is owing to the isotope effect or the degree of order attained in the crystals. A comparison of |Fobs| and |Fcal| with $\Delta = 0.016$ is given in Table 1. Agreement is satisfactory.

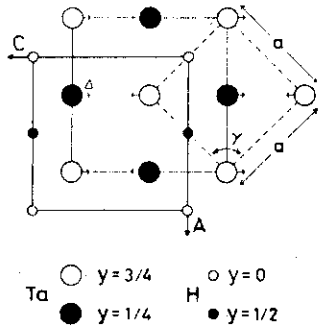

Fig.1 Structure of Ta_2H

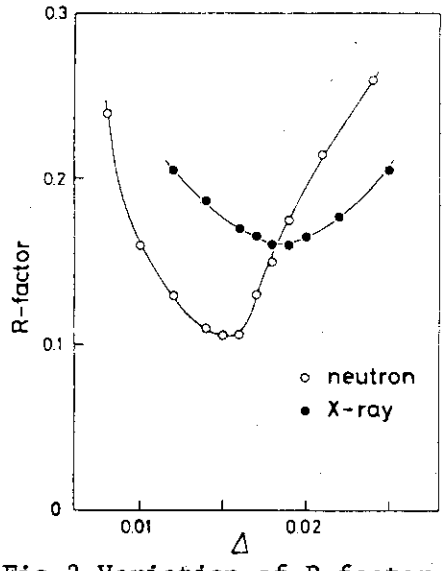

Fig.2 Variation of R-factor with Δ

Table 1 Comparison of |Fobs| and |Fcal|

	Neutron		X-ray	
HKL	|Fobs|	|Fcal|	|Fobs|	|Fcal|
200			167	212
400			192	153
001	10.8	10.1	20	23
201	5.4	4.4	27	21
401	9.1	8.8	18	15
601	4.0	2.5		
002			164	208
202			185	180
402			152	137
003	1.3	1.2	59	54
203	15.2	14.3	56	48
403	1.7	1.9	44	38
004			171	140
204			134	129
404			114	106
005	18.7	18.0	115	62
205	6.7	6.7	80	58
405	12.6	16.4		

References

1) V. F. Petrunin, V. A. Somenkov, S. Sh. Shil'shtein and A. A. Chertkov; Sov. Phys. - Crystallography 15 (1970) 137

2) J. Wanagel, S. L. Sass and B. W. Batterman; phys. stat. solidi (a) 11 (1972) K97

3) T. Schober and H. Wenzl: Script. Met., 10 (1976) 819

4) H. Asano, Y. Ishikawa and M. Hirabayashi: J. Appl. Cryst. 11 (1978) 681

I4 Lattice Location of Deuterium Dissolved in Vanadium

Sadae Yamaguchi*, Hajime Asano**,
Masahiro Koiwa*** and Makoto Hirabayashi***

* Department of Nuclear Engineering, Tohoku University, ** The Research Institute for Iron, Steel and Other Metals, Tohoku University; Now at Institute for Materials Science, University of Tsukuba and *** The Research Institute for Iron, Steel and Other Metals, Tohoku University.

Vanadium dissolves a large amount of hydrogen (deuterium) and oxygen in the interstitial sites of the bcc metal structure. It is important to know the behavior of hydrogen in the host metal in coexistence with other impurities such as oxygen atoms, since many kinds of interstitial impurities usually coexist in commercial metals. Since vanadium is an almost perfect incoherent scatterer of neutrons, neutron diffraction has a great advantage for determination of occupation sites of such interstitial atoms in the host lattice. Actually single crystal neutron diffraction studies have been performed to determine the occupation sites of carbon, nitrogen and oxygen atoms in vanadium[1].

In the present study, it is aimed to determine the location of deuterium in vanadium using single crystals of VD_x and $VD_xO_{0.02}$ with $x = 0.01 - 0.04$. The occupation probabilities of octahedral (O) and tetrahedral (T) sites are determined by analyzing the diffraction intensities. In ternary alloys $VD_xO_{0.02}$, neutron diffraction cannot determine uniquely these probabilities unless the location of oxygen is known. The O-site occupation of oxygen in $VD_xO_{0.02}$[2] as well as $VO_{0.02}$[3] was previously determined with the aid of ion channeling technique using the same crystals[2].

The structure factors for the random occupation of O and T-sites are listed in Table 1, where b_V and b_D are the scattering amplitudes of vanadium and deuterium atoms, respectively. The occupation at T or O-sites can be distinguished from the intensity of reflections other than 110, 310 and 400. Actually the T-site occupation of deuterium in $VD_{0.01}$ can be concluded from comparison of the observed data with the calculations.

For the ternary crystals $VD_xO_{0.02}$, the deuterium atoms are found to occupy statistically both T and O-sites as a result of the interaction with oxygen. The observed intensities are fitted with calculations taking the

occupation probability, p, of the O-sites as an adjustable parameter. In Fig.1 is shown a variation of R-factor with the probability. It is seen that the octahedral occupancy increases with the increase of deuterium content; p = 0.1, 0.2 and 0.5 for x = 0.02, 0.03 and 0.04, respectively. This may be connected with the fact that the terminal solubility of deuterium in vanadium increases with the addition of oxygen, which has been interpreted in terms of the trapping effect[4].

Table 1 Structure factors of VD_x

Index h k l	Structure factor $\|F\|/2$ O-site	T-site
1 1 0	$b_v - \frac{x}{3} b_D$	$b_v - \frac{x}{3} b_D$
2 0 0	$b_v + xb_D$	$b_v + \frac{x}{3} b_D$
2 1 1	$b_v - \frac{x}{3} b_D$	$b_v + \frac{x}{3} b_D$
2 2 0	$b_v + xb_D$	$b_v - \frac{x}{3} b_D$
3 1 0	$b_v - \frac{x}{3} b_D$	$b_v - \frac{x}{3} b_D$
2 2 2	$b_v + xb_D$	$b_v - xb_D$
3 2 1	$b_v - \frac{x}{3} b_D$	$b_v + \frac{x}{3} b_D$
4 0 0	$b_v + xb_D$	$b_v + xb_D$

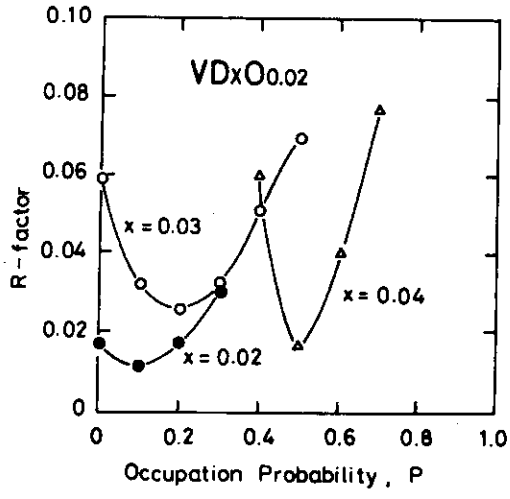

Fig.1 Variation of R-factor with the occupation probability of O-sites.

References

1) K. Hiraga, T. Onozuka and M. Hirabayashi; Materials Sci. and Eng. 27 (1977) 35

2) K. Ozawa, S. Yamaguchi, Y. Fujino, O. Yoshinari, M. Koiwa and M. Hirabayashi; Nucl. Inst. and Methods 149 (1978) 405

3) J. Takahashi, M. Koiwa, M. Hirabayashi, S. Yamaguchi, Y. Fujino, K. Ozawa and K. Doi; J. Phys. Soc. Japan 45 (1978) 1690

4) O. Yoshinari, M. Koiwa, H. Asano and M. Hirabayashi; Trans. Japan Inst. Met. 19 (1978) 171

III Neutron Scattering Study of the Phase Transition in Ag_3SI

Sadao Hoshino* and Takashi Sakuma**

* Institute for Solid State Physics, The University of Tokyo ,
** Department of Physics, Faculty of Science, Ibaraki University.

In the phase transition from the superionic β-phase to the pyroelectric γ-phase in Ag_3SI at 157 K, slight atomic displacements for S and I atoms and an order-disorder arrangement for the position of Ag atoms take place simultaneously.

In order to investigate a dynamical behaviour of atoms at the structural as well as the order-disorder phase transition in Ag_3SI, neutron inelastic scattering measurement has been carried out with the ISSP-ND-I spectrometer at JRR-2. Quasi-elastic central component and phonon peaks were measured at various temperatures between 120 K and 290 K. Up to the present, no soft modes were observed. However, a low energy mode with about 2 ∿ 2.5 meV was found to appear below the transition temperature, which is similar to those found in $RbAg_4I_5$ and AgI at low temperature, and may be the one due to the local vibrational mode for Ag atoms. Details of the phonon dispersion relation and its temperature dependence are now under investigation.

II2 Incommensurate-Commensurate Phase Transitions in K_2SeO_4-Type Ferroelectric Crystals

Kazuo Gesi and Masashi Iizumi

Division of Physics, Japan Atomic Energy Research Institute

Studies have been continued on incommensurate-commensurate phase transitions associated with ferroelectricity in the K_2SeO_4-type crystals. In addition to previously reported Rb_2ZnCl_4 and Rb_2ZnBr_4,[1] the incommensurate phases in K_2ZnCl_4 and $\{N(CH_3)_4\}_2ZnCl_4$ were studied by neutron scattering. Ferroelectricity in K_2ZnCl_4 was recently discovered by one of the present authors (KG),[2] and the reported superlattice structure[3] suggested that the ferroelectricity in this material is triggered by an incommensurate-commensurate phase transition as in the cases of K_2SeO_4,[4] Rb_2ZnCl_4,[1,5] and Rb_2ZnBr_4.[1,5]

In K_2ZnCl_4, neutron scattering study reveraled that there is an incommensurate phase in a temperature range from the ferroelectric Curie temperature of 130 °C to about 280 °C, where the satellite reflections appear at incommensurate positions of $(h,k,\ell \pm(1/3 - \delta))$ $(\delta \neq 0)$. The parameter δ which describes the deviation of the lattice modulation period from the commensurate one of $3c_0$ is about 0.027 at the normal commensurate-incommensurate transition temperature of T_{cI}. It almost lineraly decreases with decreasing temperature and reaches to about 0.012 just above the ferroelectric Curie temperature T_c. At T_c δ vanished discontinuously. The variation of δ with reduced temperature T/T_{cI} is shown in Fig. 2 together with results of other K_2SeO_4-type ferroelectrics.

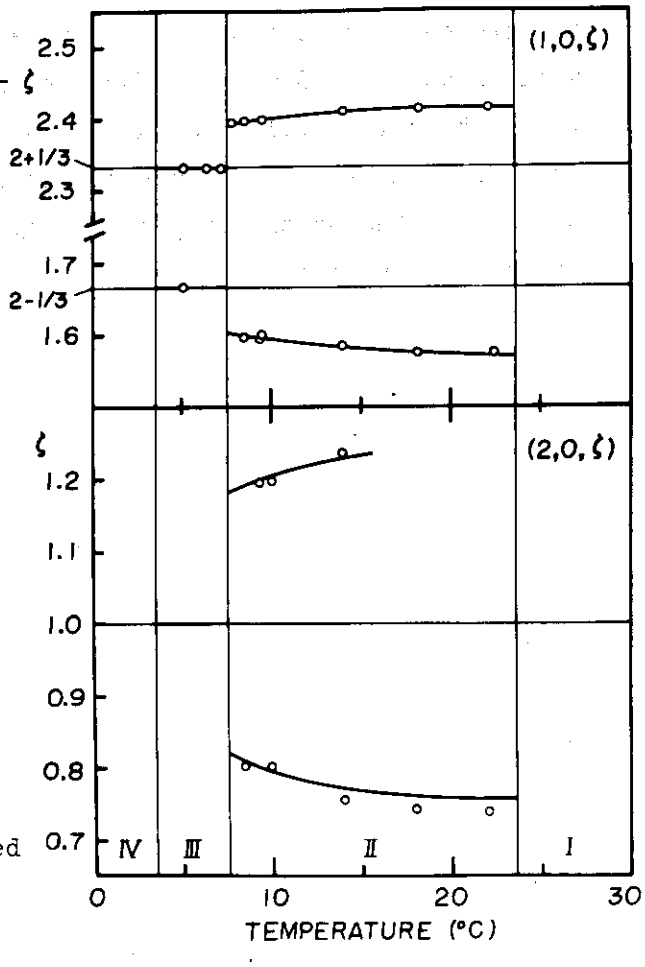

Fig. 1

The temperature variation of for K_2ZnCl_4 is quite similar to that found for K_2SeO_4.

In $\{N(CH_3)_4\}_2ZnCl_4$, the temperature dependence of the satellite positions which are found in the (h,0,ζ)-scans. In the lower portion of the figure the ranges of the successive phases are denoted by I, II, III, IV,··. The phase I takes β-K_2SO_4 type structure, and ferroelectricity is observed in phase III. In phase II the primary satellites are observed at incommensurate positions of $\zeta = 2 \pm (1/3 - \delta)$ ($\delta \neq 0$). In the ferroelectric phase III, they are observed at commensurate positions of $\zeta = 2 \pm 1/3$. Relatively intense third order harmonics are observed in the (2,0,ζ)-zone as shown in the lower part of the figure. The reduced temperature T/T_{cI} dependence of the parameter δ of $\{N(CH_3)_4\}_2ZnCl_4$ is shown in Fig. 2. Opposite sign of the parameter δ and large absolute value of it in comparison with other K_2SeO_4-type ferroelectrics characterize the incommensurate structure of $\{N(CH_3)_4\}_2ZnCl_4$. Further investigation is now in progress by using a deuterated crystal $\{N(CD_3)_4\}_2ZnCl_4$.

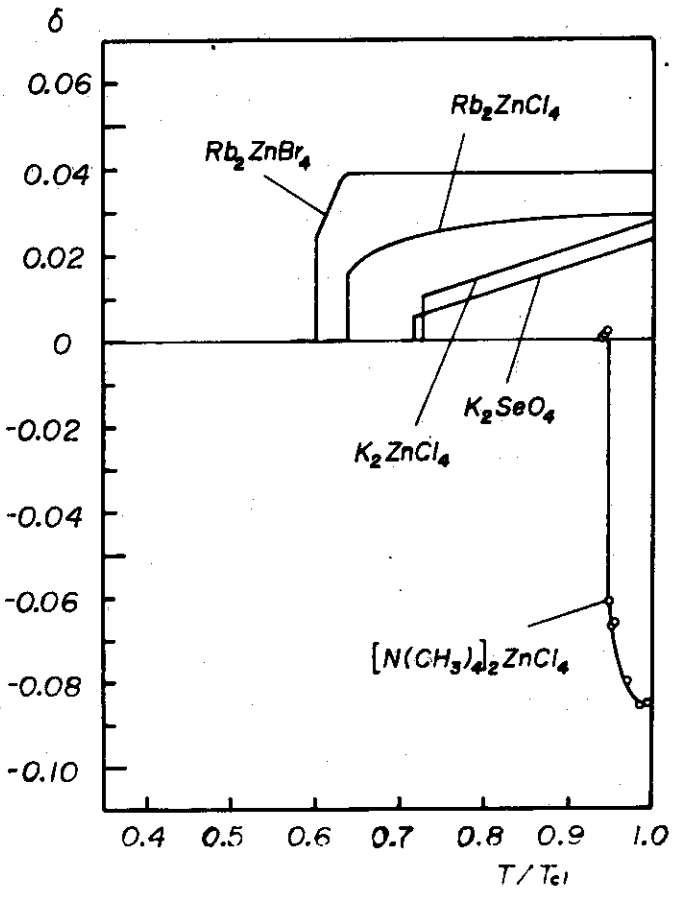

Fig. 2

1) Y. Hamaguchi, M. Iizumi, and Y. Endoh (eds.): Annual Report on Neutron Scattering Studies in JAERI, July 1, 1977-August 31, 1978, JAERI-M8009, p. 13.

2) K. Gesi: J. Phys. Soc. Jpn. 45 (1978) 1431.

3) H. P. Klug and G. W. Sears, Jr.: J. Amer. Chem. Soc. 67 (1945) 878.

4) M. Iizumi, J. D. Axe, G. Shirane, and K. Shimaoka: Phys. Rev. B 15 (1977) 4392.

5) K. Gesi and M. Iizumi: J. Phys. Soc. Jpn. 45 (1978) 1777, 46 (1979) 697.

II3 Incommensurate to Commensurate Phase Transition in Rb_2ZnBr_4

Masashi Iizumi and Kazuo Gesi

Division of Physics, Japan Atomic Energy Research Institute

Incommensurate (IC) structures in the family of compound with general formula A_2ZnX_4 with A = K,Rb or $N(CH_3)_4$ and X = Cl or Br have been studied[1-4] by the neutron diffraction method. The incommensurate structures are characterized by the wave vector given by $q_1 = (1/3 - \delta)c^*$ where δ indicates deviation from the commensurate (C) structure characterized by $q_c = c^*/3$. The temperature dependence of δ shows different behavior from one compound to another[3]. Among them the one for Rb_2ZnBr_4 is very peculiar: the parameter δ keeps the same value of 0.04 for an extremely wide temperature range from 70°C down to about -80°C and then δ suddenly starts to change and jumps to zero (the commensurate structure) within about 10°C. The intensity of satellite reflections also shows a break here. Therefore we have suggested[1] that this is another phase transition from one IC phase to another, namely from a clamped IC phase to a released and rapidly changing IC phase.

Recently we carried out more detailed measurements of this IC to C change in Rb_2ZnBr_4. In these measurements we observed closely the third order satellite reflections h k $\ell \pm 3\delta$. By this we could investigate the temperature change and splitting of the satellites three times more precisely than by observing the primary satellites. Diffraction profiles of both types of satellites are compared in Fig. 1, where those for the third order ones are shown by reducing the wave vector scale to one third and by taking the origin of the wave vector axis at the commensurate point for each type of satellites. The good resolution for the third order satellites are clearly indicated in this figure. Therefore what we had observed by looking at the first order satellites[1] were resolution-smeared profiles of the true satellite structure disclosed now by observing the third order satellites. The temperature change of the peak positions in the satellite structures are shown in Fig. 2, where the peak positions are supplemented by those of the primary satellites in the wave vector range where the peaks in the third order satellites merge into intense fundamental Bragg reflections.

These results indicate that apart from the original lattice modulation persisting from high temperature the second kind of lattice modulation appears below -70°C with the distinct wave vector given by $\delta = 0.03$ and this latter modulation becomes gradually dominant with the wave vector of modulation changing rapidly towards the commensurate value. The original modulation

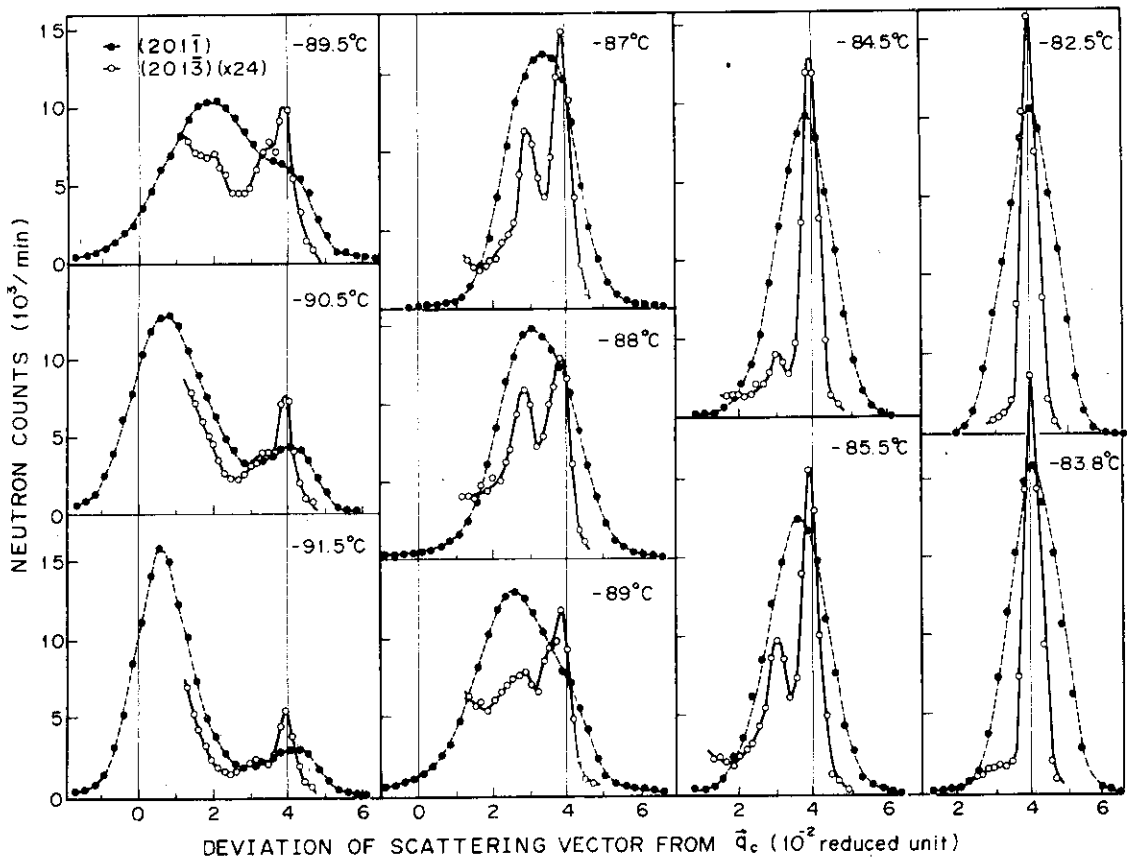

Fig. 1. Temperature change of diffraction profiles of the primary (201̄) and third order (201̄3) satellite reflections.

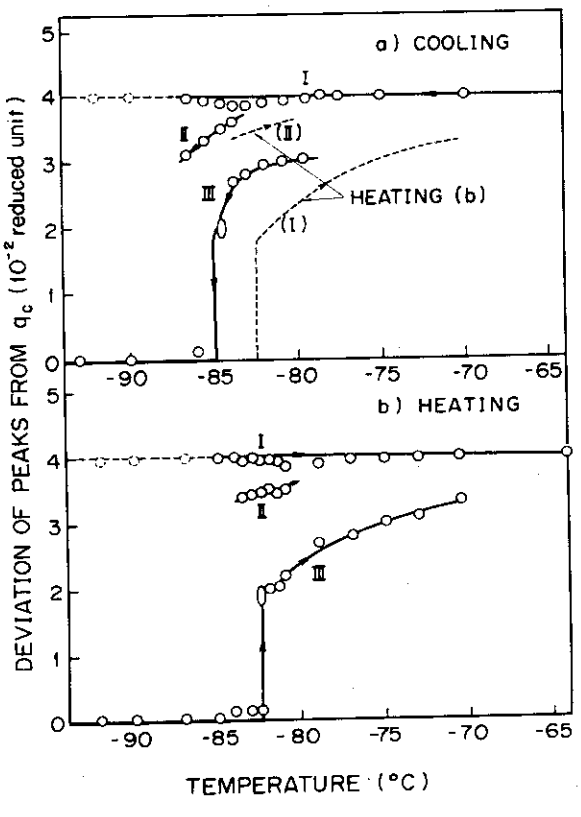

becomes less and less dominant keeping the constant wave vector. Moreover the third modulation is also seen within a limited temperature range. these behavior is very peculiar in comparison with the other incommensurate compounds. The confirmation of the overall behavior for specimen crystals of different origin is being planned.

1) K. Gesi and M.Iizumi, J.Phys. Soc. Jpn. 45 (1978) 1777.
2) K. Gesi and M.Iizumi, J.Phys. Soc. Jpn. 46 (1979) 697.
3) M. Iizumi and K. Gesi. AIP Conf. 53 (1979) 211.
4) K. Gesi and M. Iizumi, J.Phys.Soc. to be published .

Fig. 2. Temperature change of peak positions of satellite structure.

II4 Incommensurate Intermediate Phase in Rubidium Trideuterium Selenite $RbD_3(SeO_3)_2$

Kazuo Gesi and Masashi Iizumi

Division of Physics, Japan Atomic Energy Research Institute

Rubidium trihydrogen selenite $RbH_3(SeO_3)_2$ undergoes ferroelectric phase transition at about 150 K.[1] The crystal symmetry is orthorhombic $P2_12_12_1$ in the paraelectric phase and monoclinic $P2_1$ in the ferroelectric phase. The transition parameter is not the macroscopic polarization but belongs to a two dimensional irreducible representation of the space group $P2_12_12_1$ at $\vec{k} = \vec{b}_z/2$. Thus, this material is classified into the group of "improper" ferroelectrics. A group theoretical analysis predicted that there might be an incommensurate intermediate phase between the ferroelectric and paraelectric phases. Recent study of elastic properties of this material by Gladkii et al.[2] showed that an anomaly in the elastic compliance s^E_{55} exists at about 2 K above the ferroelectric Curie temperature T_c. They attributed the anomaly to the paraelectric-to-intermediate phase transition, but reproducibility of the result seemed not to be very good. We tried to detect the intermediate phase in the deuterated crystal $RbD_3(SeO_3)_2$.

A preliminary dielectric constant measurement along the b-direction showed that there are very slight breaks at about 146 K and 148 K. These anomalies should correspond to the paraelectric-to-intermediate and the intermediate-to-ferroelectric transitions. Figure 1 shows the line profile of the satellite reflection at around (2,0,0.5) in the (2,0,ζ)-scan at different temperatures around the Curie temperature T_c. In the ferroelectric phase ($T < 146$ K), the peak position exists just at $\zeta = 0.5$. On the other hand, in the intermedi-

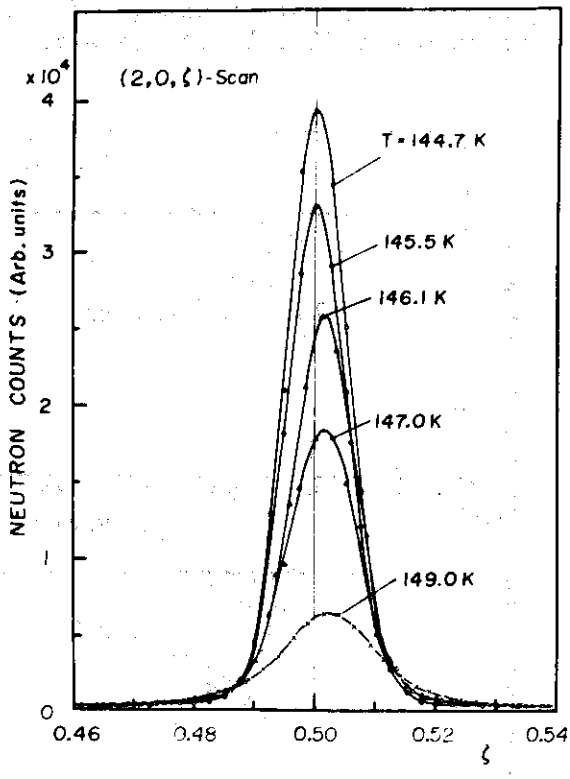

Fig. 1

Fig. 2

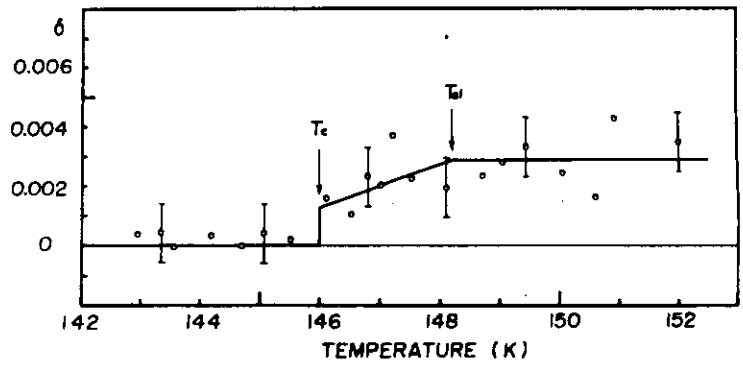

ate phase (146 K < T < 148 K), the peak position shifts from $\zeta = 0.5$ by δ ($\neq 0$). Above the paraelectric-to-intermediate transition temperature ($T_{cI} = 148$ K), the reflection becomes diffusive.

The above results indicate that there is an incommensurate intermediate phase in a temperature range of about 2 K above the ferroelectric Curie point in $RbD_3(SeO_3)_2$. In Fig. 2, the temperature dependence of the parameter δ is shown. In the figure the two transition temperatures are denoted by T_{cI} and T_c together with vertical arrows. It should be noted that above T_{cI} the parameter δ corresponds to the diffuse scattering peak. In the intermediate phase, the parameter δ is about 0.003 at T_{cI}, it decreases slightly with decreasing temperature and discontinuously vanishes at the Curie point. A marked characteristic of the incommensurate structure of this material is the smallness of the incommensurate parameter δ ; it is one order of magnitude smaller than the one typically found in $(ND_4)_2BeF_4$.[3] Also the range of the incommensurate phase is very narrow. It would be a problem to be solved in future to determine what is the microscopic mechanism which stabilizes the structure very slightly deviated from a commensurate one.

1) L. A. Shuvalov, N. R. Ivanov, N. V. Gordeyava, and L. F. Kirpichikova: Sov. Phys.-Crystallogr. 14 (1970) 554.
2) V. V. Gladkii, V. A. Kirikov, V. K. Magataev, and L. A. Shuvalov: Sov. Phys.-Solid State 19 (1977) 167.
3) M. Iizumi and K. Gesi: Solid State Commun. 22 (1977) 37.

II5 Quasielastic Neutron Scattering from Fe_2TiO_4

Y. Endoh and M. Kataoka*

Department of Physics, and *the Research Institute for Iron, Steel and Other Metals, Tohoku University

Ulvospinel, Fe_2TiO_4, exhibits a giant magnetostriction below its magnetic phase transition temperature, Tn[1]. The giant magnetostriction arises from the cooperative Jahn Teller effect (CJTE) of ferrous ions in A sites through the lattice vibrations[2]. Since the fictitious Jahn Teller transition temperature, Tt*, seems to be lower than the magnetic phase transition temperature, the Jahn Teller transition disappears. Instead, the Jahn Teller distortion behaves as if it were the giant magnetostriction. The diffuse scattering due to the local displacements produced by a single JT ion, being a typical example of the Huang effect, exhibits the critical behavior near above Tt*. Indeed, there have been reported such experimental results from many examples which show CJTE[3]. However in this Fe_2TiO_4 case, these two cooperative phenomena, the magnetic ordering and the JT distortion, interfere with each other. Thus it may not be clear whether the critical like behavior can be observed. Note that Fe^{2+} in the tetrahedral sites have electronic ground orbitals of doublet. Measurements were performed on the TUNS spectrometer from a single crystal of Fe_2TiO_4, which was grown by the floating zone melting method. The quasielastic scans around (400) reciprocal point, where both nuclear and magnetic amplitudes appear, show the double peak with respect to temperatures, one is a sharp peak at 135K corresponding to Tn and another is a rather broad one around 80K. This fact indicates clearly that the intensity of diffuse scattering due to CJTE diverses critically near Tt* as was seen in $NiCr_2O_4$ for instance[3]. This fact also means that the interference should not be strong, and that the theory based on the static JT effect, which is reasonable for the orbital triplet case of $NiCr_2O_4$, can be applicable even in this doublet case.

We compared the experimental results of quasielastic neutron scattering with the calculated correlation function[4], derived from the appropriate microscopic Hamiltonian for the lattice vibrations coupled with the localized electronic states[2]. Actually the latters are expressed in terms of the Pauli spin operators, and furthermore the static approximations as mentioned before were used in this calculation. A typical example of results is

illustrated in the figure. One can see from figure that agreement between observed and calculated contours is satisfactory, although we have encountered some difficulties in the resolution corrections.

References

1) Y. Ishikawa and Y. Shono: J. Phys. Soc. Japan 31 (1971) 452
2) M. Kataoka: J. Phys. Soc. Japan 36 (1974) 456
3) H. Trauchi, et al.: J. Phys. Soc. Japan 32 (1972) 1049
4) M. Kataoka and Y. Endoh: submitted to J. Phys. Soc. Japan

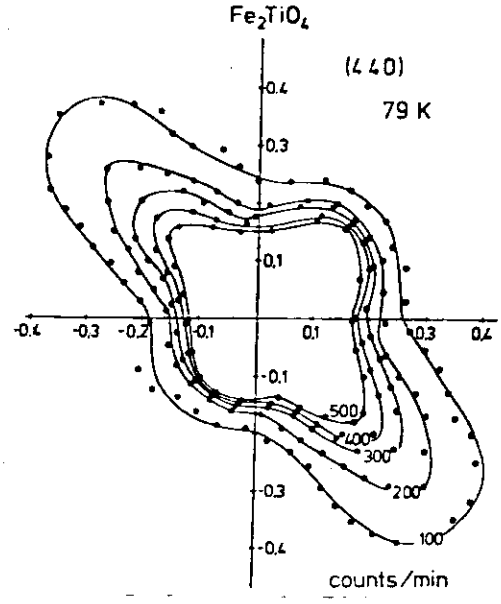

Fig.1.
Intensity contour of diffuse scattering around (440)

(a) calculated under fixed temperature of T=1.2Tc*, Elastic constants of Fe_3O_4

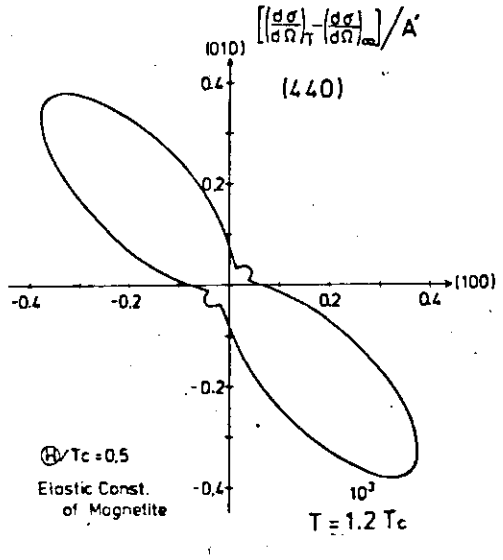

(b) Observed contour of quasi-elastic neutron scattering around (440), Resolution correction was not carried.

II6 Neutron diffuse scattering by 'molecular polarons' in Magnetite

Yasusada Yamada*, Masahiro Mori*, Yukio Noda* and Masashi Iizumi**

* Department of Physics, College of General Education, Osaka University,
** Physics Division, Japan Atomic Energy Research Institute

In this paper, we report the results of neutron diffuse scattering experiments on magnetite above its Verwey transition temperature (T_v). The obtained results are discussed in connection with a proposed model which describes the properties of valence fluctuations at the B-site Fe-ions.

Neutron diffuse scattering primarily gives informations on the properties of atomic fluctuations. In 1975, Fujii et al.[1] reported the observation of diffuse scatterings and analyzed the results in terms of the instability of the phonon modes with wave vector k=(1/2, 0, 0)[2]. Later, Shapiro et al.[3] performed more precise observation. They reported a new type of diffuse scattering which has different characteristics from the previously reported one due to soft phonons. It is widely spread in momentum space with its maximum at the Γ-points (the Brillouin zone center) and has a remarkable anisotropy in the reciprocal space. Moreover, its intensity is dependent on temperature only slightly, being still observable even at $T \sim T_v + 80K$. Observation of the same type diffuse streak pattern in an electron diffraction experiment was also reported by Chiba et al.[4] These characteristics does not allow the convensional interpretation as the 'critical diffuse scattering' at structural phase transitions. The critical diffuse scattering is usually interpreted as due to correlated fluctuations of an order parameter. Hence, it should have its maximum intensity at the position where the new Bragg reflections (superstructure lines) appear in the ordered phase. In the present case, the new Bragg reflections appear at (1/2, 0, 0) corresponding to the doubling of the unit cell along one of the cubic principal axes. Nevertheless, the maxima of the diffuse scattering are at the Γ-points. The origin of this type diffuse scattering has not been clarified yet.

In this paper, we tried to elucidate the origin of this diffuse scattering based on a model which describes the property of fluctuating valence electrons above T_v.

The model assumes the existence of 'molecular polarons' in the temperature region $T > T_v$. The 'molecular polaron' is a complex composed of two excess electrons and a local displacement mode of oxygens within the fcc

primitive cell. At sufficiently high temperatures, there are random distribution of molecular polarons, which are fluctuating independently by making hoppings through crystal or dissociating into smaller polarons. The life time of each molecular polaron is long enough to induce instantaneous strain field around it.

Based on this model, neutron diffuse scattering cross section due to independent dressed molecular polarons are calculated. In order to verify the model, a precise measurements of quasi-elastic scattering of neutrons have been carried out at 150 K making use of a triple axis neutron spectrometer installed at JRR-2 in JAERI. The experimental results show the characteristics predicted by the model.

References

1. FUJII Y., SHIRANE G. and YAMADA., Phys. Rev. 11B, 2036 (1975)
2. YAMADA Y., AIP Conf. Proc. NO.24 79 (1975)
3. SHAPIRO S. M., IIZUMI M. and SHIRANE G., Phys. Rev. 14B, 200 (1976)
4. CHIBA K., SUZUKI., and CHIKAZUMI S., J. Phys. Soc. Japan 39 839 (1975)

II7 Phonon Dispersion Relations of BCC Thallium

Masashi Iizumi

Division of Physics, Japan Atomic Energy Research Institute

Thallium undergoes a martensitic transformation at 230°C (T_M) taking the body-centered cubic (bcc) and hexagonal close-packed (hcp) structure above and below the transition temperature respectively. Although the phonon dispersion relations in the hcp structure have been mesured and their relation to the transition has been investigated by approaching the temperature from below[1], with a negative result, those in the bcc structure have not been studied.

We grew a single crystal of bcc thallium on the sample table of a triple axis neutron spectrometer and measured the phonon dispersion relations in the bcc phase maintaining the temperature of the crystal above T_M. Because the material is poisonous, grains of raw material were put in an alumina crucible and vacuum-sealed within a quartz tube and the latter was placed in a vacuum furnace for neutron diffraction. The upper and lower heaters of the furnace were controlled separately and the crystal was grown by the Bridgeman method. Melting point was 330°C (T_m). Neutron scattering measurements were carried out on the grown crystals leaving the crucible and quartz tube within beam. Quality and size of the grown crystal were checked by the standard neutron diffraction and polaroid photograph of the diffracted beam. About 5 cc single crystal of a certain orientation was obtained for each trial. Although the crystal orientation is accidental, it was not difficult to bring any one of the [100], [110] and [112] zone axes perpendicular to the scattering plane of the spectrometer by a moderate tilt of the furnace on a goniometer. Most of the measurements were carried out at 250°C by using incident neutrons of 14 meV. Mosaic spread of the crystals were always less than 0.3°. A brief test of the stability of the bcc structure below the martensitic transition temperature indicates that the single crystal is destroyed below T_M and then it was unable to restore the original crystal by raising temperature again above T_M, even though temperature was changed very slowly around T_M.

The dispersion relation were measured along the three principal directions of the cubic crystals. Two kinds of transverse phonon propagating along [110] with different polarization vectors (T_1 and T_2) were observed for the proper orientations of the crystals. The results of the measurements are summarized in Fig. 1. The most conspicuous feature of the results is the existence of a dip in the longitudinal branch along [111]. It occurs at

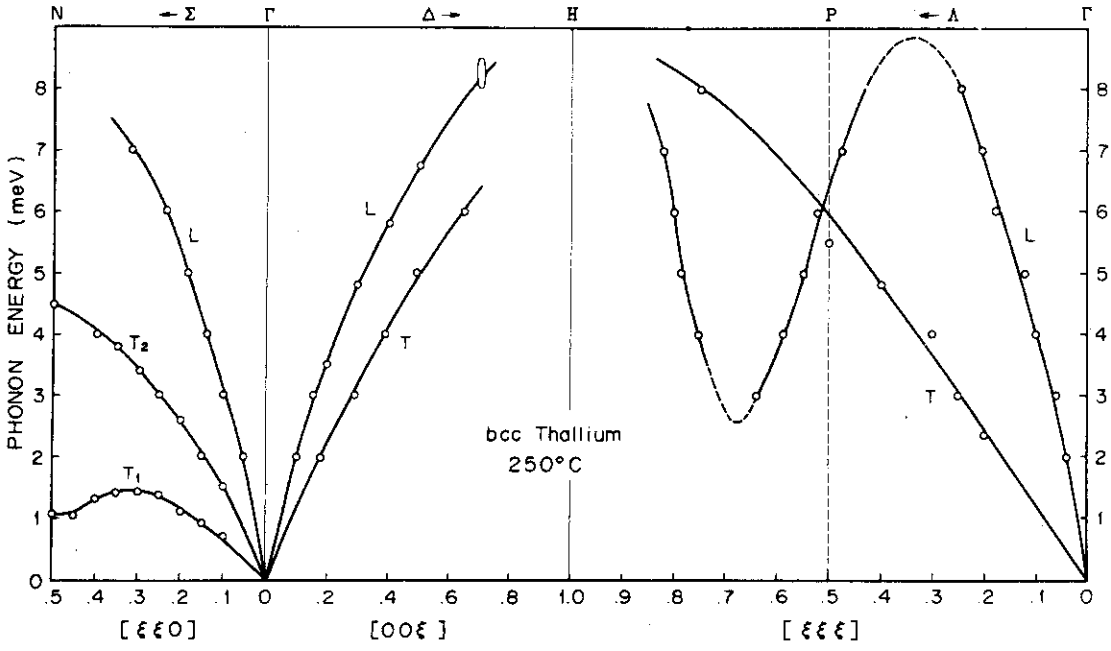

Fig. 1 Phonon dispersion relations of bcc Tl at 250°C

around $(\frac{2}{3},\frac{2}{3},\frac{2}{3})$. This kind of a pronounced minimum has been noticed for most of the bcc metals[2] and it has been related to the intrinsic instability of the bcc structure against the so-called ω-phase structure. Recently a striking dip of the similar nature was disclosed in zirconium in the bcc structure[3]. Another conspicuous feature is the existence of anomaly at N in the T_1 branch of transverse phonon (e//[1$\bar{1}$0]) propagating along [110] which retains low energy from the zone center to the boundary. The elastic constant $c_{11} - c_{12}$ corresponding to this branch is also very small. All the elastic constants derived from the initial slope of the acoustic branches are tabulated and compared with those of Pb.

The energies of some of the zone boundary phonons were difficult to determine by the measurements with relatively high resolution. Their measurements are going to be undertaken by the use of higher incident energy. Further measurements including the temperature-dependent behavior are now in progress.

Table 1 Elastic constants of Tl compared with those of Pb. (10^{12}dyne/cm^2)

	bcc Tl	fcc Pb
c_{11}	0.43	0.48
$\frac{1}{2}(c_{11}-c_{12})$	0.020	0.035
c_{44}	0.12	0.14

1) T. G. Worlton and R. E. Schmunk, Phys. Rev. B. 12(1971) 4115.
2) For example, A.D.B.Woods et al., Phys. Rev. 128 (1962) 1112.
3) C.Stassis J.Zarestky and N.Wakabayashi, Phys.Rev.Lett. 41 (1978) 1726.

II8 Acoustic Phonon Dispersion in $NiTe_2$ $

Masatoshi Sato* and Katsuhiko Abe**

*Institute for Solid State Physics, Tokyo University, Tokyo,
**Device Developement Center, Hitachi Ltd, Kodaira, Tokyo

Main Part of this work has already been published in J. Phys. C12 (1979) L613 and the detailed results can be seen in that paper. The acoustic phonon dispersion curves and the elastic constants are given in it. There can be seen some signs that suggest the existence of quasi-two dimentional character in the [ξ00] mode, which has a transverse out of plane character. It implies that the interlayer interaction is stll sufficiently weak in $NiTe_2$, even given the small value of c/a, for a tendency towards two-dimentional character to e seen. (a,c : usual notations of the lattice constants in the hexagonal type cell.)

The small kink in the LA phonon branches in the direction [ξ00] and [ξξ0] at a q value slightly smaller tha $0.3a^*$ ($a^*=4\pi/\sqrt{3}a$). It is interesting that this small kink, reminiscint of a Kohn anomaly, has been observed near the same region of the reciprocal space in many materials of similar structure such as 1T-TaS_2 [1]. Here we would like to refer to the recent developement of the understandings of the anomalies of the transition metal carbide and nitride. The work by Terakura emphasised the importance of the q dependence of the electron-phonon interactions. This q dependence is known to be mainly determined by the geometricalalignment of the atoms in a cnit cell. Although this is studied for the metallic compounds with NaCl type structure, it is tempting to connect this idea to the present layer structure matallic compounds. Further experiment using a compound with the same structure and the larger electron phonon coupling is now planned.

1) K. R. A. Ziebeck, B. Dorner, W. G. Stirling and R. Schollhorn, J. Phys. F7 (1977) 1139
2) K. terakura, J. Phys. C11 (1978) 469

$Main Part of this work was done at Harwell. However, many preliminary experiments were carried out at JRR-2, at Tokai.

II9

Phonon Dispersion Relation of a Precipitation Alloy $Al_{98}Cu_2$

Nobuhiko Kunitomi*, Hiroshi Shiraishi*, Yorihiko Tsunoda*,
Mitsuzo Osamura**

* Department of Physics, Faculty of Science, Osaka University

** Department of Metallurgy, Faculty of Engineering, Kyoto University

An Al alloy with the dilute concentration of Cu is one of the well-known precipitation alloys and has become a subject of the physical and metallurgical investigations. In the early stage of the precipitation, a precipitate with the two dimensional shape called as the Guinier-Preston zone (G-P zone) is formed by the room temperature anneal. This precipitate produces lattice distorsion around it and may cause a characteristic change of the phonon dispersion relation. In order to observe this effect, we previously made a measurement of phonon dispersion relation on $Al_{99}Cu_1$ and found some variation before and after the aging.(1) However, more accurate measurement made by using HFIR at Oak Ridge National Laboratory has revealed that the phonon variation observed once is a fictitious one probably due to the imperfectness of the single crystal specimen which was grown by the Bridgeman method. In this note, we report a new result obtained by using a single crystal specimen with Cu concentration of 2 at.% which was grown by strain anneal method. In order to dissolve Cu into Al the specimen was annealed at 550°C for 1 hr. and quenched into water. However, as will be mentioned later, a complete solid solution specimen could not be obtained and a trace of the formation of the G-P zone was observed even though the specimen was kept at the dry ice temperature until just before the phonon measurement.

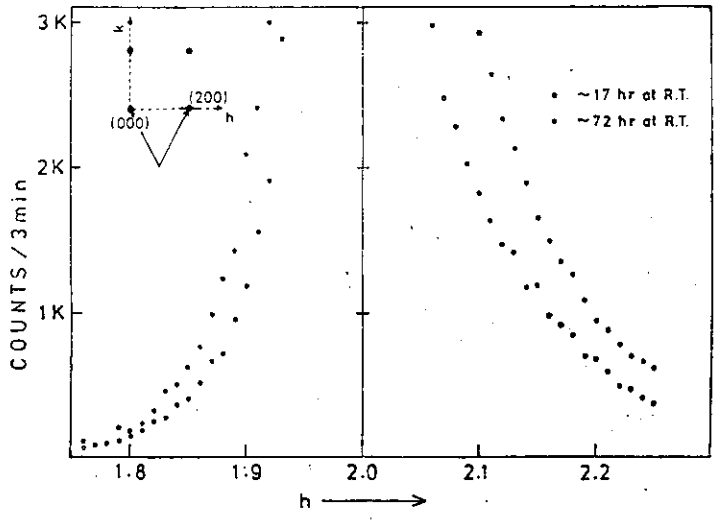

Fig. 1.

The phonon dispersion relation was measured at room temperature on the Triple Axis Spectrometer TUNS installed at JRR-2. In Fig.1 are shown line profiles of the (200) Bragg reflection observed by the specimen kept in room temperature for 17 and 72 hrs.

During this period, the neutron inelastic scattering measurement was made. Although the intensity of the scattered neutron is very lowcompared to the peak intensity of the (200) Bragg reflection (about 5,000 kc/min.), a typical evidence of the development of the G-P zone that the stronger diffuse tail appears in the positive direction from (200) is found even in the case of the 17 hrs aging. This G-P zone formation may be attributed both to the effect of the room temperature aging and to the limited speed of the quenching.

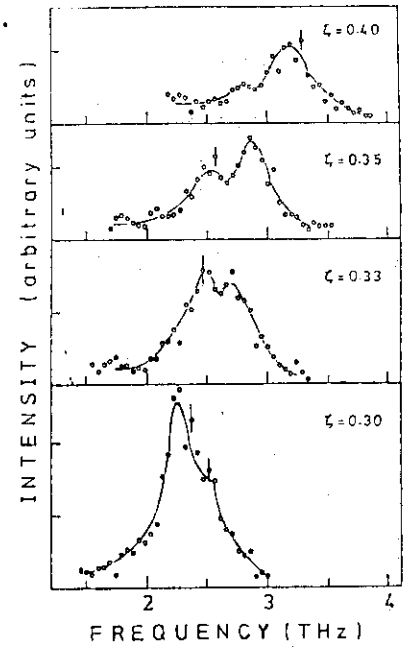

Fig. 2

In Fig. 2, the intensity spectra of scattered neutrons for the measurement of [ζ00]T phonons are shown, where one can see the double peak structue typical to the existence of the resonance mode. As shown in this figure and in Fig.3 the resonance mode appears at around E 2.5 THz or at 0.35. In Fig.3, the dispersion relation of the [ζ00]T branch is drawn which almost agree with that for pure Al except the apparent double branch structure at the resonance. In this figure is also shown the theoretical dispersion relation of the mass defect model calculated under the dilute approximation. Since the impurity concentration is very low, the theoretical result indicates only a small variation of the slope of the dispersion curve at the resonance which can hardly be observed by the usual experimental method. It has been known experimentally in various mass defect substances such as Au(Cu), Ni(Pt) and Ni(Pd) that the observed magnitudes of the energy gap observed at the resonance agree with the calculated values quantitatively. Therefore, we can conclude that the resonance effect found in this Al(Cu) alloy with the G-P zone is extraordinarily strong in [ζ00]T branch.

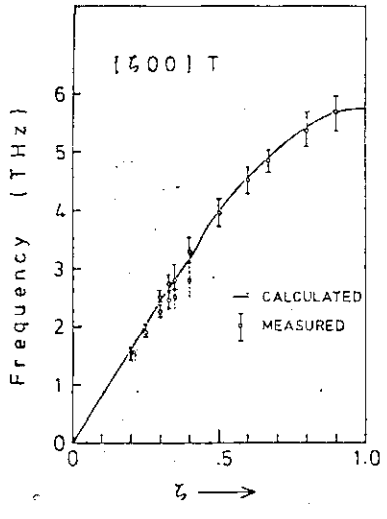

Fig.3

The dispersion relation was also observed for [$\zeta\zeta$0]T branch and the results are shown in Fig.4 together with the theoretical one. In this branch, the resonance mode was hardly detected as expected the retically. These experimental results imply that the phonon dispersion relation and the behavior of the resonance mode in this specimen is anisotropic.

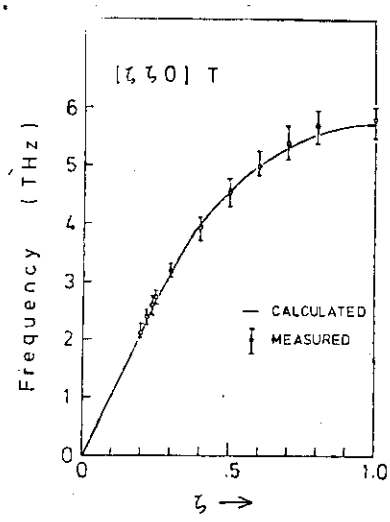

Fig. 4

(1) N.Kunitomi, M.Hamada, Y.Nakai; Ann. Report Neutron Scatt. JAERI, 1977, p29

II10 Resonance-like Phonon Mode in a Force Constant Disorder System $Pd_{70}Ag_{30}$

Yorihiko Tsunoda and Nobuhiko Kunitomi

Faculty of Science, Osaka University

Since an atomic mass and a force constant have dual symmetry in the formulation of the lattice vibration, it will be expected in principle that the introduction of the impurities with large difference of the force constant also leads to the resonance or the localized phonon modes. Recently, Katayama and Kanamori[1] developed the CPA theory of the lattice vibration in a substitutional disordered alloy with the force constant disorder within a single site approximation. Present measurements were carried out on the basis of their prediction about the possibility of the existence of resonance-like phonon anomaly in the Pd-Ag system.

The Pd-Ag alloy seems to be the best sample for the study of the resonance phonon mode associated with the force constant disorder from the following reasons. 1) The atomic force constant in Pd metal is about 1.8 times larger than that of Ag metal for the nearest neighbor pairs[2,3], whereas the mass difference of these atoms is only 1.4%. 2) Both have a f.c.c. structure and form a continuous series of solid solutions. Since the existence of atomic superlattice structure has not been reported, we need not bother about the contamination by the short range order. 3) General shape of phonon dispersion curves for both of the metals has almost perfect similarities[2,3]. We can anticipate that the atomic force constants will change homogeneously in this alloy. 4) The difference of the lattice parameters between Pd and Ag metals is rather small compared with the systems for which the resonance phonon modes have been investigated. The increase of the lattice constant has linear dependence to Ag concentration. 5) The experimental noise caused by the incoherent scattering of neutrons is very small because the coherent scattering amplitudes for Pd and Ag atoms are almost the same.

The sigle crystal specimen with the volume of about 0.5 cc was cut off from an ingot which was melt in an alumina crucible by the Bridgeman method in an Ar atmosphere. The measurements were carried out by using TUNS triple axis spectrometer installed at JRR-2 reactor, JAERI, Tokai. Constant-Q mode of operation was used throughout the course of the

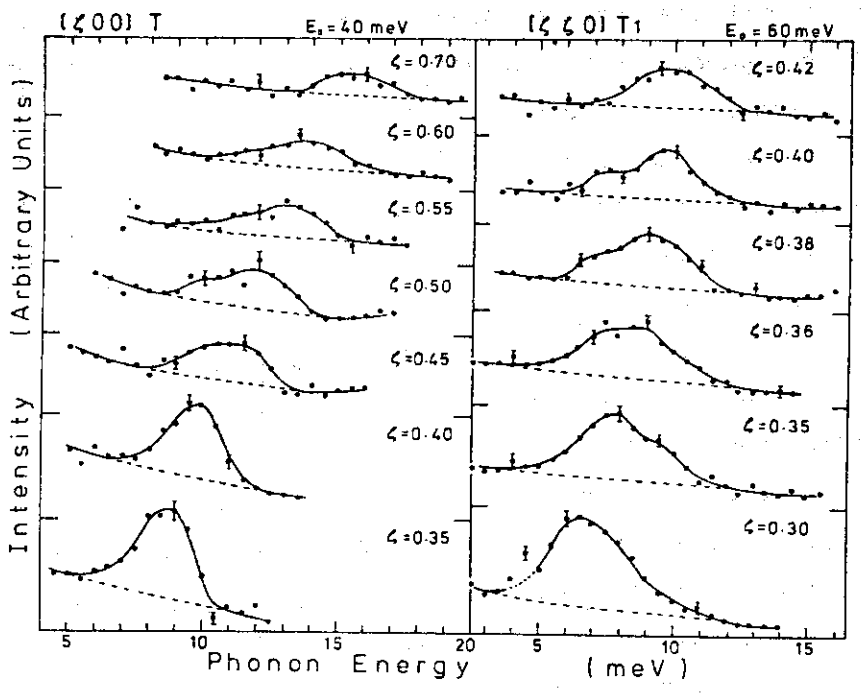

Fig. 1 Scattered neutron groups of constant-Q scan for the [ζ 0 0] T and the [ζ ζ 0] T_1 branches. Data were taken by E_0 = 40 meV for the former and 60 meV for the latter. Dashed lines are estimated backgrounds and solid lines are drawn for guides to the eye.

experiments.

Phonon perturbation was measured for both transverse (T) branch in the [ζ 0 0] direction and T_1 branch in the [ζ ζ 0] direction. A portion of the experimental results obtained for several wave vectors is shown in Fig. 1 for these two symmetry directions. Asymmetric phonon line shapes which seem to have double peak structure were observed around ζ = 0.45 ∿ 0.55 for the [ζ 0 0] T branch and ζ = 0.35 ∿ 0.40 for the [ζ ζ 0] T_1 branch. Anomalous behavior for the [ζ 0 0] T branch was checked for different crystal settings and incident neutron energies. The first one was carried out by using 60 meV incident neutrons and the scanning was made in the (0 0 1) reciprocal plane, thus the polarization of phonon lies along [1 0 0] direction. The second was made by 40 meV neutrons and scanning was made in the (1 $\bar{1}$ 0) reciprocal plane, thus the polarization vector lies along [1 1 0]. The consistent results were obtained for both crystal settings. In Fig. 2, observed FWHM of the phonon peaks for the [ζ 0 0] T branch is shown. Increase of the phonon line width suddenly takes place around 11 meV. These changes of the observed phonon profile with the wave vectors are quite similar to those of the resonance mode observed in mass defect alloys. Further evidence that the unusual phonon peaks observed here seem certainly to be the resonance-like behaviors

associated with the force constant disorder is the phonon energy at which the anomaly takes place. These roughly agree with the value calculated from the CPA theory in which the appreciable energy shift and line broadening are expected to appear at around 10 meV.

Since the present experiments were performed under the conditions with rather poor energy resolution in order to obtain the strong scattering intensity, the quantitative comparison with the theory was not made here. Qualitatively, however, the agreement between the experimental results and the theoretical calculations by Katayama and Kanamori[1] is satisfactory.

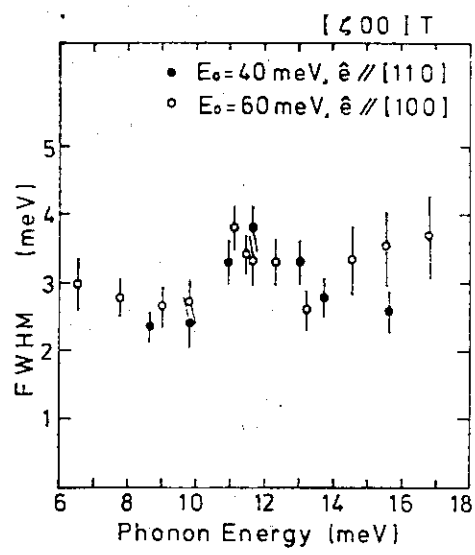

Fig. 2 Observed FWHM for the [ζ 0 0] T branch plotted against the phonon peak energy.

In the concentrated alloy, especially for the force constant disorder system, it is not so easy to picture out what happens in the specimen as in the case of a dilute alloy because the atomic force constant in metallic system is generally considered to extend to rather long distance. Actually, 6-th or 8-th neighbor force constants have to be taken into account in order to reproduce the observed phonon dispersion curves satisfactorily. However, to point out the followings may be worthwhile. In the present case, the first nearest neighbor force constans for both Pd and Ag metals are more than 10 times larger than those of the second nearest neighbor. The phonon perturbation will be mainly determined by the first nearest neighbor force constants and may spatially localize even for the system with the force constant disorder.

Acknowledgement - The authors are indebted to Prof. J.Kanamori and Dr. H. Katayama for valuable discussions. We also appreciate to Profs. Y.Ishikawa and Y.Endoh for providing their spectrometer to our experiments.

1) H.Katayama and J.Kanamori, J. Phys. Soc. Japan 45 1157 (1978).
2) A.P.Miiller and B.N.Brockhouse, Can. J. Phys. 49 704 (1971).
3) W.A.Kamitakahara and B.N.Brockhouse, Phys. Lett. 29A 639 (1969).

III1 Inelastic Neutron Scattering from Fe_2TiO_4

Y. Endoh, Y. Noda**, H. Takei*, S. Saito, and Y. Ishikawa

Department of Physics, and *the Research Institute for Iron, Steel and Other Metals, Tohoku University, and **Sendai College of Radio Technology.

The sound velocity of the transverse mode propagating 110 direction in Fe_2TiO_4 decreases substantially upon cooling from room temperature towards Tn ($\sim$ 135 K).[1] The anomalous slowing down of the sound velocity might be associated with the structural transition from cubic to tetragonal due to the cooperative Jahn Teller effect.[2] However the developing of the magnetic long range order interfere with the CJTE transition. In fact, the soft mode transition at which sound velocity approaches zero does not occur.

The inelastic neutron scattering experiments have been carried in order to clarify the soft mode behavior in this crystal. Since the frequency difference between ultra sound and thermal neutrons is as large as $\sim 10^5$ H_z, two results concerning to the velocity of sound do not necessarily coincide with each other. In fact, phonon velocity detected by INS experiments from many JT crystals is much larger than sound velocity detected by ultrasound measurements in the vicinity of CJTE transition. The criterion of this difference should be related to the relaxation speed of the local electronic entropy through phonons with respect to the velocity of probes.

We are also much interested in the dynamical response in this particular case of CJTE for the doublet electronic orbitals, because the electronic states even in the tetragonal field are of the mixed orbitals of doublet, and thus unique axis is not specified. The unique axis of Fe_2TiO_4 in the tetragonal phase rotates with the quantized axis of the magnetic moments in A site.[3]

Measurements have been performed on TUNS spectrometer using large single crystals which have been grown by zone melting technique with the image focuss of xenon lamp by gold reflectors. The phonon velocity at various temperatures has been detected by the derivative of the phonon dispersion at small $\vec{q}$. Scans have been made for three acoustic modes of [100] T, L and [110] T_1. Anomalous softening is seen clearly for [110] T_1 mode, which agrees with the ultrasonic measurements. However the difference of two values enlarges upon cooling down to Tn.

The temperature variation of phonon velocity is found to be due to the temperature shift of the dispersion relation with temperature independent

zone boundary energy. The similar effect was observed in the phonon dispersion relation in FeNi Invar alloy.[4] It must be emphasized that the spoon like dispersion relation which shows a broad dip in the dispersion curve implies either $\vec{q}$ dependent effective electron-phonon coupling or thermal effects, which should be clarified by further studies.

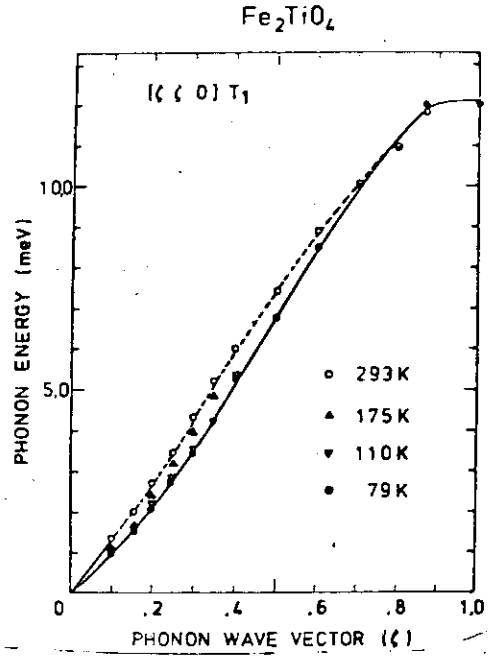

The phonon dispersion relation of [110] T_A, mode at several temperatures below 300 K.

References

(1) Y. Syono, U. Fukai and Y. Ishikawa. J. Phys. Soc. Japan 31 (1971) 471

(2) M. Kataoka. ibid 36 (1974) 456

(3) Y. Ishikawa and Y. Shono. ibid 31 (1971) 461

(4) Y. Endoh, Y. Noda and Y. Ishikawa. Solid State Commun. 18 (1976) 509

II12 Phonon Density of States in FeNi Invar Alloy

Y. Endoh and Y. Noda*

Department of Physics, Tohoku University and Sendai College of Radio Technology.

Lattice dynamics of Invar alloy of $Fe_{65}Ni_{35}$ have been studied extensively by inelastic neutron scattering experiments[1] A remarkable aspect in the lattice dynamical property is the unusual temperature dependent dispersion curve particularly for [110] T_1 mode. This fact reflects softening of the sound velocity or the unusual temperature shift of the shear modulus in the Invar alloys.[2]

We could interprete phenomenologically the temperature shift of the elastic modulus by introducing the spin dependent electron-phonon coupling, which seems to be proportional to the order parameter of the magnetization.[1]

Now we tested the effect of the temperature dependent phonon dispersion relation on the phonon density of states, which must be an important basis for the thermodynamical quantities such as Debye Waller factor, lattice specific heat and so on. We have been carried out the phonon density of states computation from the observed phonon dispersions at several temperatures. We have found the shift of the density towards low frequency upon cooling, due to the dominant contribution from the temperature dependent [110] T mode in the small frequency region. Typical demonstration is illustrated by the change of the phonon density of states with temperatures.

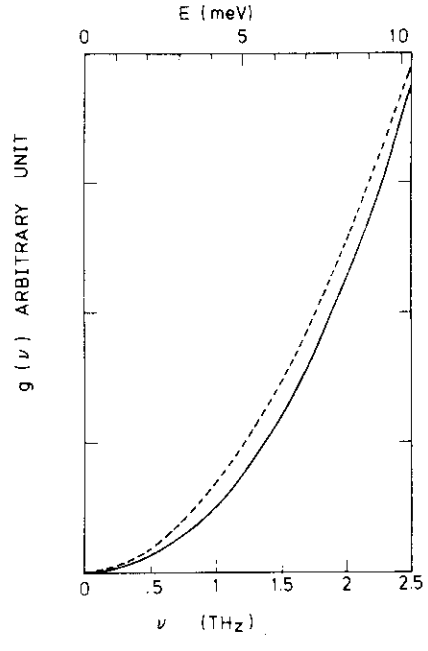

Fig. 1. Phonon density of states in the low frequency region. Solid line is in the paramagnetic state 500 K, while dotted line, the ferromagnetic state at 300 K.

References

(1) Y. Endoh. JMMM 10 (1979) 177

(2) G. Hausch and H. Warlimont, Acta Met. 21 (1973) 401

IIIl

Magnetic Structure of V_5S_8

Satoru FUNAHASHI*, Hiroshi NOZAKI** and Isao KAWADA**

*Physics Division, Japan Atomic Energy Research Institute

**National Institute for Researches in Inorganic Materials

The compound V_5S_8 has a monoclinic crystal structure derived from metal deficient Ni-As type structure. It has been considered from NMR[1,2] and magnetic measurements[3] that only the vanadium atoms in the metal deficient layers, called type 1, have magnetic moments in the magnetically ordered state.

We measured neutron diffraction of a single crystal of the mass of a few milligrams grown by chemical transport.[4] Superlattice reflections were detected at low temperature at the positions defined as $h\pm\frac{1}{2}\ k\ \ell$ with even k and ℓ. Integrated intensities along the θ-2θ scanning were measured in detail for the reflections in the a*-b* plane as well as in the a*-c* plane. Square root of the integrated intensity corrected for the Lorentz factor(i.e.$\sqrt{I\sin 2\theta}$) is shown in Fig.1 as a function of $\sin\theta/\lambda$ for the diffractions in the a*-b* plane. The result is proportional to the form factor of V^{2+}(denoted by f_{V2+}) calculated by Watson and Freeman. This means that $\sqrt{I\sin 2\theta}/f_{V2+}$ is constant in the a*-b* plane. On the other hand, this quantity changed greatly in the a*-c* plane as a function of angle Ψ between the scattering vector and the a*-axis as shown in Fig.2. The solid curve in the figure represents a function $\alpha\sin|\Psi-\Psi_0|$ with the best fit value of α and Ψ_0. The direction $\Psi=\Psi_0$ is 8.9° deviated from the c*-axis toward the a*-axis and coincides with the easy direction observed in the torque and the magnetoresistance experiment.[3] The magnetic structure is considered to be collinear because the susceptibility along the direction described above becomes very small at low temperature. Therefore, possible magnetic structure which satisfies the following assumptions were examined. 1)Only type 1 vanadium atoms have magnetic moments. 2)Magnetic moments are aligned collinearly along the easy direction described above. 3)Magnetic periodicity along the a*-axis is twice as the periodicity of the crystal. 4)The structure factor is equal for all superlattice reflections. 5)The structure factor vanishes unless both k and ℓ are even.

The structure which satisfies them is shown in Fig.3. The magnitude of the moments was estimated to be $1.4\mu_B$ per type 1 vanadium atom by comparing the magnetic reflection intensities with the nuclear ones.

In addition to this general feature, a fine structure as shown in Fig.4 was observed around the $\frac{1}{2}00$ and $\frac{3}{2}00$ reflections. (In the analyses described above, the integrated intensity over the fine structures was taken into account.) The side peaks were not so clearly resolved at higher scattering angles. Therefore the magnetic structure will have a small incommensurate modification if we look into the structure in further detail.

Another question left unresolved is that the magnitude of the moment of the present result is too large compared with the value of about $0.3\mu_B$ estimated by Kitaoka from NMR experiment.[5] The discrepancy cannot be explained on the basis of the present neutron results unless we abandon the assumption that only the type 1 vanadium atoms have the moments.

The temperature dependence of the square root of the $\frac{1}{2}00$ scattering intensity shown in Fig.5 is similar to that of NMR[5] and seems to indicate the localized magnetic moments character.

References

1) De Vries A.B. and Haas C., J.Phys.Chem.Solids 34,651(1973).
2) Silbernagel B.G.,Levy R.B. and Gamble F.R., Phys.Rev.B 11,4563(1975).
3) Nozaki H., Umehara M., Ishizawa Y., Saeki M., Mizoguchi T. and Nakahira M. J.Phys.Chem.Solids 39,851(1978).
4) Saeki M., Nakano M. and Nakahira M., J.Cryst.Growth 24/25,154(1974).
5) Kitaoka Y. and Yasuoka H., Private communications.

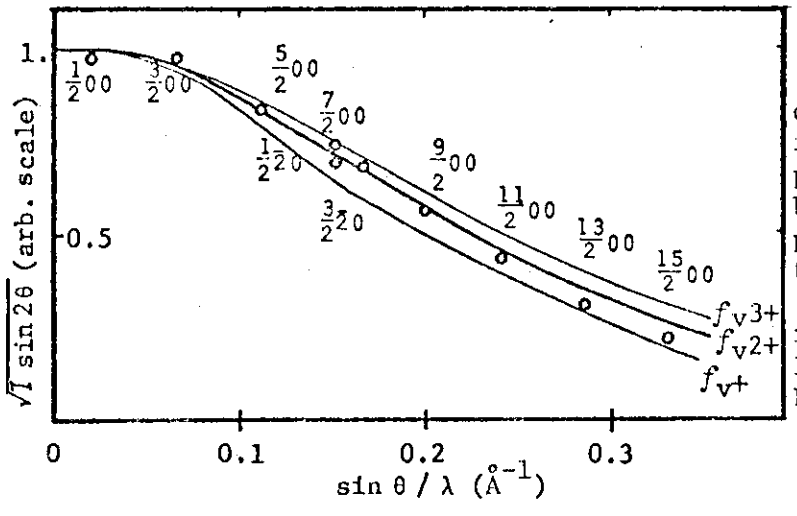

Fig.1 Square root of the integrated intensities in a*-b* plane corrected for Lorentz factor is plotted as a function of sinθ λ. Curves represent form factors calculated by Watson and Freeman.

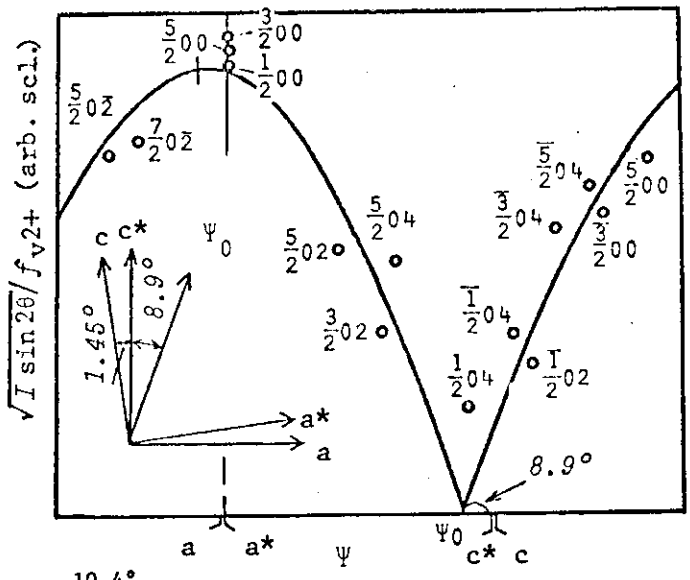

Fig.2 The values of $\sqrt{I \sin 2\theta}/f_{V2+}$ for the scatterings in the a*-c* plane are plotted as a function of the direction of the scattering vector.

The curve represents $a \sin|\Psi-\Psi_0|$ with the best fit a and Ψ_0.

The direction Ψ_0 is 8.9° away from the c*. (i.e. 10.4° away from the c axis.)

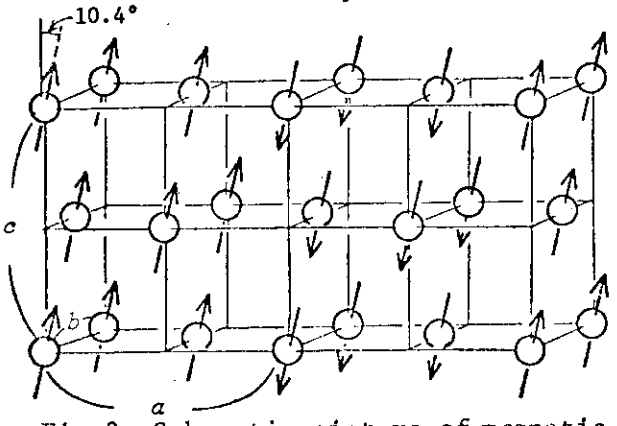

Fig.3 Schematic picture of magnetic structure of V_5S_8. Only the type 1 vanadium atoms are drawn. The easy direction is inclined toward the a-axis at an angle of about 10.4°.

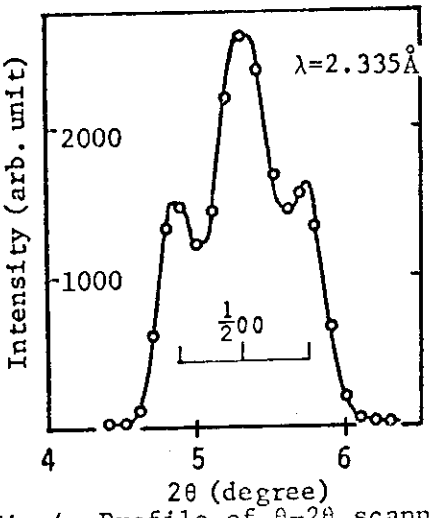

Fig.4 Profile of θ-2θ scanning through $\frac{1}{2}00$. Side peak positions are described as $\frac{1}{2}\pm0.041\ 0\ 0$.

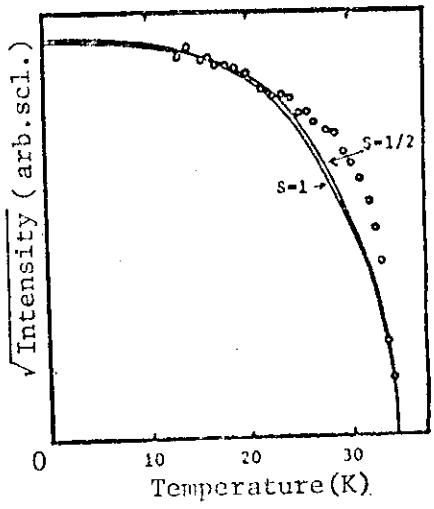

Fig.5 Temperature dependence of the square root of the peak intensity of $\frac{1}{2}00$. Solid curves represent molecular field magnetization for S=1/2 and 1.

III2 Magnetic Structure of $Fe_{1-x}O$

Masako Akimitsu*, Jun Akimitsu**, Tadashi Mizoguchi* and Shigeyuki Kimura***

*Department of Physics, Gakushuin University, **Department of Physics, Aoyama Gakuin University, ***National Institute for Researches in Inorganic Materials.

A non-stoichiometric $Fe_{1-x}O$ has a defect NaCl type structure which is stable above 570°C. From X-ray diffraction studies[1] on the quenched samples of iron content 1-x=0.92 to 0.88, there exist the defect clusters which include 13 Fe site vacancies and 4 interstitial ferric irons (Koch-Cohen cluster), and the cluster forms the superlattice with periodicity of about three times longer than that of the basic unit cell. The stoichiometric ferrous oxide is antiferromagnetic[2] below its Néel temperature of 198K. The magnetic structure in the Koch-Cohen cluster of $Fe_{1-x}O$ has not been reported for the lack of the large single crystal. We report in this note the possible magnetic structure of $Fe_{1-x}O$ using the neutron diffraction technique.

The single crystal used in the present experiment was deoxidized from magnetite by changing the oxygen partial pressure at 1250°C. Neutron diffraction measurements were performed by a double axis spectrometer at the JRR-3 reactor of J.A.E.R.I., Tokai. The intensities of both fundamental and superlattice magnetic reflections were examined at 77K. Fig 1 is a typical example of magnetic reflections. The experimental results as well as the calculated intensities assuming the different magnetic structures are shown in Table. The experimental

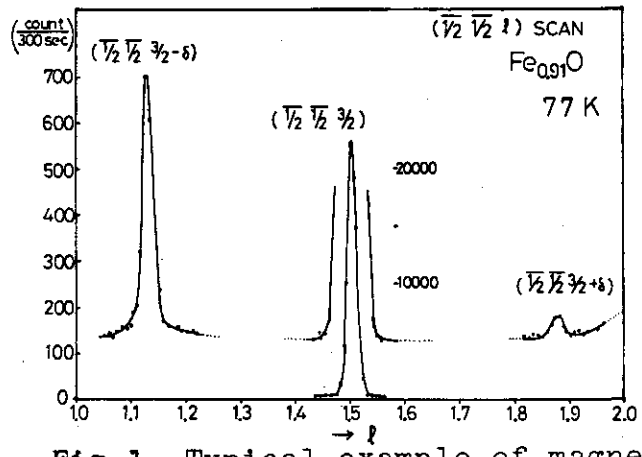

Fig. 1 Typical example of magnetic reflections at 77K.

values are situated inbetween the calculated value of model 1 and model 2. The spin configurations of both models are shown schematically in Fig 2. Fig 2 shows that the magnetic moments of three interstitial Fe^{3+} ions (Nspins) ordered ferromagnetically, and the up and down spin in the one Fe^{3+} interstitial site (M spin) correspond to the model 1 and model 2, respectively. The ferromagnetic component of the magnetic moments in the cluster are arranged antiferromagnetically with the periodicity of twice that of the atomic superstructure.

h k l	model 1	model 2	model 3	experimental
$\frac{1}{2}\ \frac{1}{2}\ \frac{3}{2}-\delta$	1.00	1.00	1.00	1.000±0.024
$\frac{1}{2}\ \frac{1}{2}\ \frac{3}{2}+\delta$	0.049	0.058	0.011	0.052±0.011
$\frac{1}{2}\ \frac{1}{2}\ \frac{1}{2}+\delta$	0.056	0.069	0.030	0.053±0.007
$\frac{1}{2}+\delta\ \frac{1}{2}+\delta\ \frac{1}{2}$	0.070	0.039	0.026	0.173±0.024
$\frac{1}{2}-\delta\ \frac{1}{2}-\delta\ \frac{3}{2}$	0.245	0.164	0.105	0.059±0.013

Table The experimental and caluculated intensities of the magnetic satellites. The values are normalized to $(\frac{1}{2}\ \frac{1}{2}\ \frac{3}{2}-\delta)$

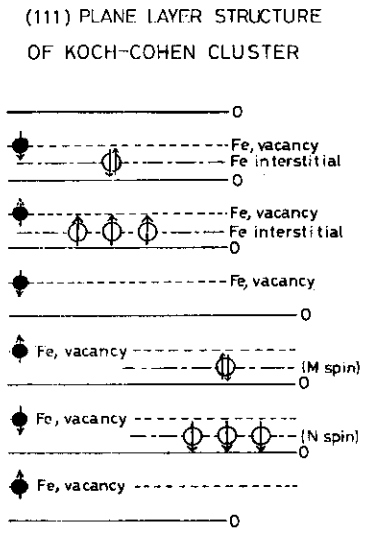

Fig. 2 The possible magnetic structure of Koch-Cohen cluster in $Fe_{1-x}O$. Solid and open circles show octahedral and tetrahedral interstitial Fe ions, respectively. Arrows indicate the spin configulations as discribed in the main text.

References

1) F. Koch and J. B. Cohen: Acta Cryst. B25 (1969) 275.

2) W. L. Roth: Acta Cryst. 13 (1960) 140.

III3 Neutron Diffraction Study of $MnSe_2$

Katsuya Kikuchi, Tomonao Miyadai and Hiroki Ito

Department of Physics, Faculty of Science, Hokkaido University

$MnSe_2$ has the cubic pyrite structure, isomorphous with NiS_2 etc.. Neutron diffraction study by J.M.Hastings et al.[1] has shown that this compound exhibits a complicated antiferromagnetic ordering with the magnetic unit cell which is equal to three times the chemical unit cell along one of ⟨100⟩ axes. Such a structure, however, can not be stabilized by the Heisenberg type interaction.[2)]

The magnetic susceptibility and the thermal expansion were measured by H. Ito and S. Miyahara, and showed discontinuous changes at T_N (=47.4 K)[3)], indicating a first order transition.

In order to investigate the magnetic structure and the properties of the phase transition, we performed neutron diffraction measurements on the powdered specimen used for measurements of the susceptibility and the thermal expansion.

The measurements were performed using the neutron diffractometer of ISSP installed at JRR-3.

Neutron diffraction pattern was taken at 5 K and at a wavelength of 1.851 Å. The observed magnetic pattern is the same as that observed by Hastings et al.[1)], and also a fit is obtained between calculated and observed intensities, if a spin direction is assumed to be parallel to the long axis of the magnetic cell. It is interesting what mechanism stabilizes such a magnetic structure.

The (010), (101) and (210)magnetic

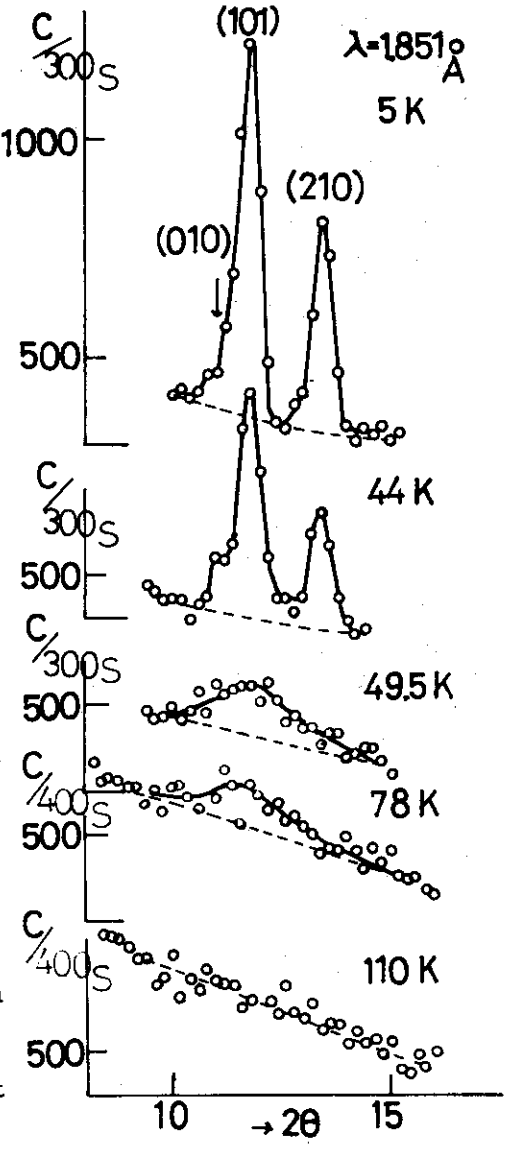

Fig.1. The diffracted peaks at various temperatures.

reflection*) were measured from 5 K to 110 K. Typical diffraction peaks are shown in Fig.1. Up to 48 K, the diffraction peaks are similiar to that obtained at 5 K. Above 48 K, a broad peak was observed, instead of sharp Bragg reflections. T_N(=48 K) determined by neutron diffraction agrees well with that determined from the magnetic susceptibility. The line-width of the broad peak increases gradualy with increasing temperatures, and it could not be observed at 110 K. A simple calculation from the observed linewidth suggests that there are at 49.5 K regions with the magnetic short range order extending over about 50 Å.

In Fig.2, the temperature variation of the sublattice magnetization is shown; the experimental points were taken from the (101)reflection and the solid curve is a Brillouin function for J=5/2. As can be seen, the sublattice magnetization varies anomalously with temperatures and disappears sharply at T_N. The transition seems to be of the first order, being consistent with the results of the susceptibility and the thermal expansion.

*) The index is referred to (3a,a,a)cell, where a is the chemical cell.

The authors would like to express their sincere thanks to Prof. K. Hirakawa and Dr. M. Sato for the measurement of neutron diffraction.

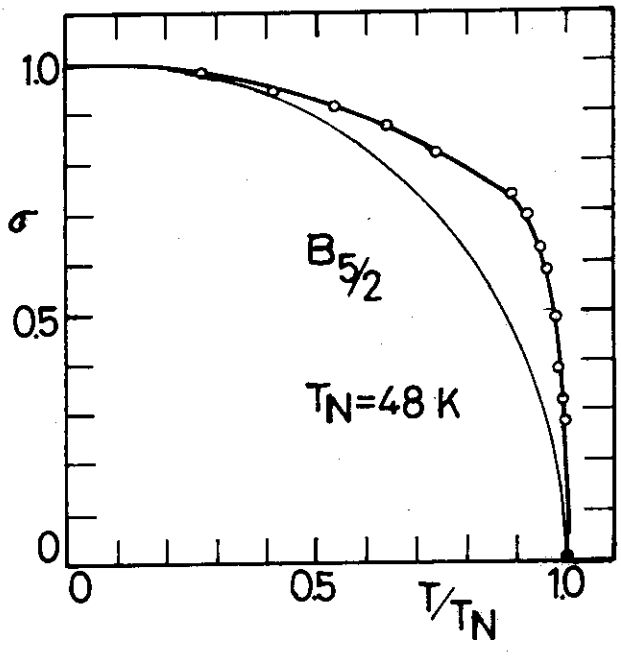

Fig.2. Temperature variation of the sublattice magnetization.

1) J.M.Hastings, N.Elliot and L.M.Corliss: Phys. Rev. 115 (1959) 13.
2) Y.Yamamoto and T.Nagamiya: J. Phys. Soc. Japan 32 (1972) 1248.
3) H.Ito and S.Miyahara: J. Phys. Soc. Japan 42 (1977) 470.
4) L.M.Corliss and J.M.Hastings: J. Phys. (France) 25 (1964) 557.

III4 Antiferromagnetic Structure of $Fe_{1.75}Mn_{1.25}Si$

Masayoshi Ohashi, Fumiaki Ohwe, Yasuo Yamaguchi and Hiroshi Watanabe

The Research Institute for Iron, Steel and Other Metals,
Tohoku University, Sendai

According to Yoon and Booth[1] on the basis of the neutron diffraction and magnetic measurements, the ferromagnet Fe_3Si and the antiferromagnet Mn_3Si conbine to form a series of solid solution, $Fe_{3-x}Mn_xSi$, (except at x=0, and x=1.0) with $L2_1$ structure which consist of four interpenetrating f.c.c. sublattices A,B,C and D with the origins at the points (0,0,0), $(\frac{1}{2},\frac{1}{2},\frac{1}{2})$, $(\frac{1}{2},\frac{1}{2},\frac{1}{2})$, and (3/4,3/4,3/4). In this structure Mn atoms strongly favour the B site with Si atoms favouring the D site. The alloys with Mn concentration less than 0.75 were found to be ferromagnetic with a bulk magnetization and a Curie temperature, T_c, decreasing monotonically with increasing Mn concentration. The alloys in the range $0.75<x\leq1.75$ exhibited the complex magnetization, as shown in Fig. 1, which showed a decrease as temperature fell below T_R~68K. In addition the slope of the high field part of the magnetization curve increased below T_R. The neutron diffraction of powder sample suggested not only a ferromagnetic but also antiferromagnetic components.[2]

In order to determine the magnetic structure, neutron diffraction was carried out by using TOG diffractometer installed at JRR-3. The single crystal of $Fe_{3-x}Mn_xSi$, which took the composition x=1.25 as the B sites were almost occupied by Mn atoms, was grown by the Bridgeman method from a homogenized powder sample. The structure characteristics were obtained by the nuclear reflections at R.T. (paramagnetic state), using the values, 0.96, -0.36 and 0.42 in units of 10^{-12} cm for nuclear scattering amplitudes of Fe, Mn and Si atoms, respectively. The fraction of the B sites occupied by Mn atoms take the value 98%, on the assumption that the D sites are occupied by Si atoms only and Fe and remains Mn atoms have statistically

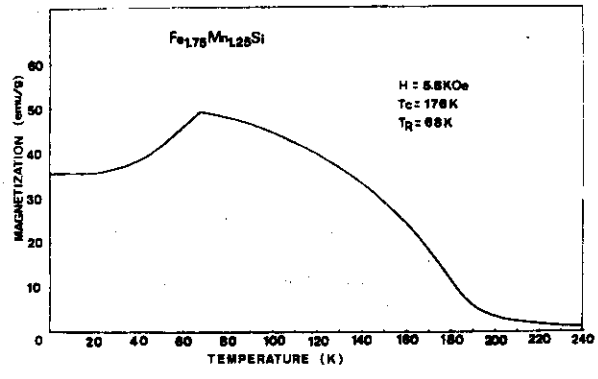

the A and C sites.

The magnetic scattering due to antiferromagnetic components observed at 4.2K, shown in Table I, are indexed using a unit cell doubled in each direction with the antiferromagnetic components being arranged in [111] direction. The magnetic moments of B and A(C) sites which take the values 2.3 μ_B and 0.16 μ_B respectively are obtained from the intensity analysis using the [$\pi\pi\pi$] model in which the antiferromagnetic components of the A(C) sites points to the opposite direction of that of the B sites. The magnetic form factors for the B site (Mn^{2+}) and the A(C) sites (Fe^{3+} and Mn^{2+}) calculated by Watson and Freeman were used.

The temperature dependence of the (1/2,1/2,3/2) antiferromagnetic reflection as shown in Fig. 2, are in close agreement with the Brillouin function for S=1 and take T_R=68K. Fig. 2, also, shows the temperature variation of the (111) reflection due to the ferromagnetic component.

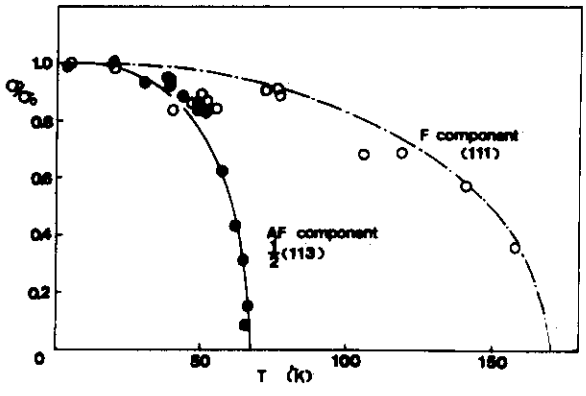

Fig. 2. The temperature variation of the $\frac{1}{2}$(113) antiferromagnetic and (111) ferromagnetic reflection.

h k l	F^2_{obs}	F^2_{calc}
1/2,1/2,3/2	6650	6953
1/2,1/2,1/2	0	0
3/2,3/2,1/2	4336	4431
3/2,3/2,3/2	0	0
1/2,1/2,5/2	1308	1490
3/2,3/2,5/2	1622	2128
5/2,5/2,1/2	557	549
1/2,1/2,7/2	2329	2195
5/2,5/2,3/2	626	910
5/2,5/2,5/2	0	0
3/2,3/2,7/2	193	253
1/2,1/2,9/2	688	507

Table I. Comparison of the calculated and observed antiferromagnetic intensities.

References

(1) S. Yoon and J.G. Booth, J. Phys. F: Metal Phys., 7 (1977) 1079.

(2) K.R.A. Ziebeck and P.J. Webster, Phil. Mag., 34 (1976) 973.

III5 Two Dimensional Spin Ordering in YFe_2O_4

Jun Akimitsu*, Youichi Inada*, Kiiti Siratori**,
Isamu Shindo*** and Noboru Kimizuka***

*Department of Physics, Aoyama Gakuin University, **Department of Physics, Osaka University, ***National Institute for Researches in Inorganic Materials.

In this note, we report the observation of completely two demensional magnetic long range order in an Ising system YFe_2O_4, a new compound systhesized by Kimizuka and Katsura[1]. The crystal has a hexagonal layered structure, a = 6.090Å c = 24.788Å at room temperature, R3m[2]. As is shown in Fig 1, Fe sites form triangular nets in planes perpendicular to the c axis and two adjacent layers form a honeycomb lattice. These honeycomb nets are separated by a triangular net of Y^{3+} ions. The lattice of spins is similar to that of ilmenite and two dimensional spin correlation is expected[3].

Single crystals were grown by the floating zone melting method under controlled oxygen partial pressure. Details were reported already[4]. As grown single crystals were not stoichiometric but were found slightly reduced. Measurements of elastic scattering of neutrons were performed by a double axis spectrometer at the JRR-3 reactor of J.A.E.R.I., Tokai.

Measurements in (h, h, l) reciprocal plane at 77K showed that the magnetic reflections at (n/3, n/3, 0) (n ≠ 3m) spread parallel to the c axis. The line profile of (1/3, 1/3, ℓ) along the c axis is shown in Fig 2. There is no fine structure except the slow decrease due to the magnetic form factor. When the measurement was made across the line, the width of the magnetic scattering was the same as that of the nuclear reflections. The continuous magnetic scattering spikes observed in this specimen of YFe_2O_4 are, thus, due to spin ordering in two dimensions. No magnetic scattering other than (n/3, n/3, ℓ) was observed by the scanning in (h, h, ℓ) and (h, 0, ℓ) reciprocal planes. Strong anisotropy of spins being considered, such a

diffraction pattern suggests that the spin structure in the (0 0 l) plane of YFe_2O_4 is commensurate sinusoidal with wave vector [1/3, 1/3, 0] and there is no spin correlation along the c axis.

The two dimensional long range order cannot be expected in a perfect three dimensional lattice. In the present case, inhomogeneities due to the non-stoichiometry seems to be responsible. The crystal used in the present study was known to be non-stoichiometric. Studies on the effect of the stoichiometry are now in progress.

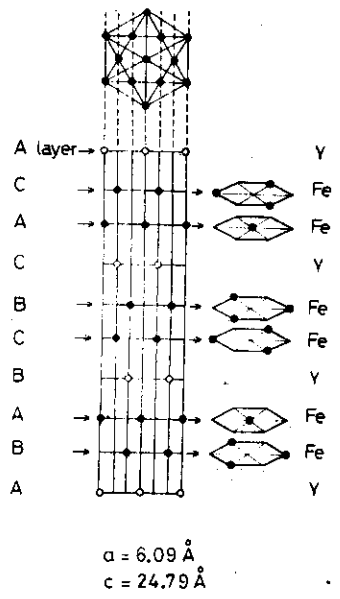

Fig 1 Crystal structure of YFe_2O_4. Oxygens are omitted in this figure.

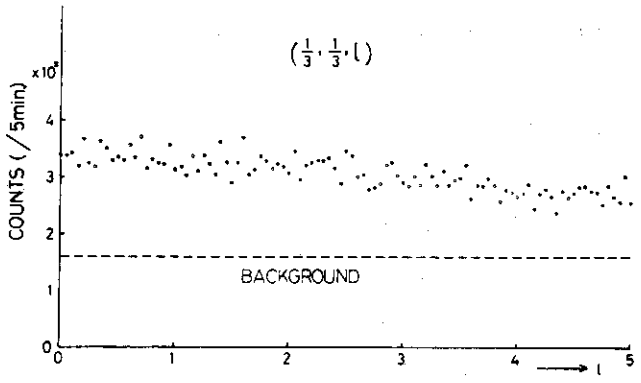

Fig 2 (1/3, 1/3, ℓ) reflection scanned along the c axis at 77K.

References

1) N. Kimizuka and T. Katsura: J. Solid State Chem. 15 (1975) 151.
2) N. Kato, I. Kawada, N. Kimizuka and T. Katsura: Z. Krest. 141 (1975) 314.
3) J. Akimitsu and Y. Ishikawa: J. Phy. Soc. Jpn 42 (1977) 462.
4) I Shindo, N. Kimizuka and S. Kimura: Mat. Res. Bull. 11 (1976) 637.

III6 Magnetic Phase Diagram of a Cr Alloy with Dilute Concentration of Be

Tsutomu Sano, Shuzo Kawarazaki, Satoshi Iida, Nobuhiko Kunitomi

Department of physics, Osaka University, Toyonaka, Osaka, 560

In recent years, the magnetic properties of dilute Cr alloys containing non-transition elements such as Al, Si, Ge, Sb and Ga were studied extensively by many investigators[1]-[5]. In these alloys, the magnetic structure changes from incommensurate to commensurate antiferromagnetic structure with increasing concentration of the impurities. In all alloys except Cr-Si, the Nèel temperature tends to increase with the impurity concentration. Akai and Kanamori theoretically discussed the effect of vacancies or non-transition element on the energy bands of Cr and on the antiferromagnetic susceptibility. According to them, the introduction of these kinds of lattice defects into a Cr lattice causes the modification of the bonding band as the density of states near the Fermi level increases.[6] As the results of this band modification due to the decrease of Cr atom pairs, the antiferromagnetic susceptibility, magnetic moment and Nèel temperature increase. They, therefore, have explained the experimental results above mentioned as well as the increase of T_N in a cold worked Cr and in thin Cr films, comprehensively.

The purpose of the present work is to examine the general applicability of their theory to Cr alloys containing any kind of non-transition element. Be seems to be a suitable candidate as a solute atom for this purpose because it has a quite different atomic nature compared to all the other elements examined hitherto. It belongs to IIa series without p-electron while the others to IIIb-Vb series with 1-3 p electrons.

Since the solid solubility of Be into Cr has been reported as 2.8 at.% at 1160°C, the specimens containing 0.5, 0.92, 1.3 and 2.4 at.% Be were prepared by melting proper amounts of 99.996% pure Iochrom and 99.9% pure Be in an argon arc furnace. Single crystals with the dimensions of about 1.5x1.5x2 mm^3 were cut from the ingots. The powder samples for neutron diffraction were prepared by crushing the ingots into powders with the particle size of about 0.3 mm in a Cu-Be piston and cylinder unit. The Be contents were determined by means of chemical analysis. The neutron diffraction experiment was performed on the TOG neutron diffractometer installed at JRR-3, JAERI.

The observed magnetic phase diagram of the Cr-Be alloy is shown in Fig.1. The Nèel temperature T_N was determined by the measurements of neutron diffraction (shown by open circles) and electrical resistivity (solid circles). The both results agree well with each other. The transverse to longitudinal spin flip temperature T_f obtained by neutron diffraction is also shown in the figure but it falls down below the liquid N_2 temperature for the specimens containing Be more than 0.92 at.%. It is apparent that both T_N and T_f decrease monotonously with Be concentration.

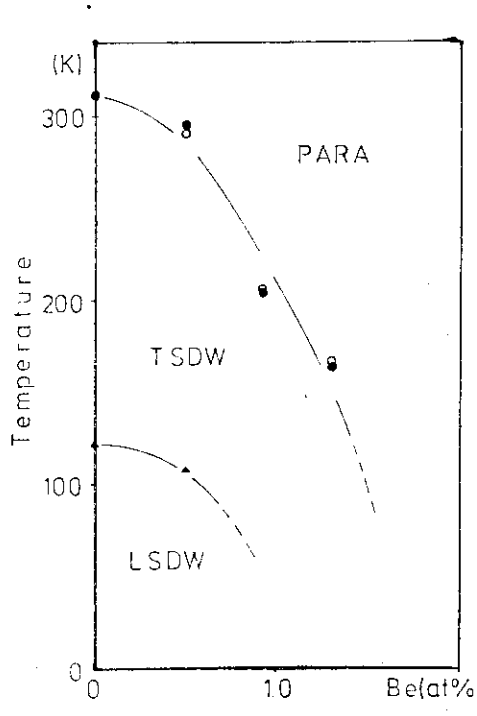

Fig. 1. Magnetic phase diagram in Cr-Be

Fig.2 shows the temperature dependence of the magnitude of the wave vector $Q=1-\delta$ expressed in the unit of $(2\pi/a)$. The values of Q were estimated from the position difference of two satellite reflections $(1\pm\delta,0,0)$. As the temperature raises up, the values of Q in Cr-Be increase similar to the behavior of Q observed in pure Cr. As the concentration of Be increases, the magnitude of Q decreases. This fact indicates that the magnetic structure of Cr-Be goes far away from the antiferromagnetic structure.

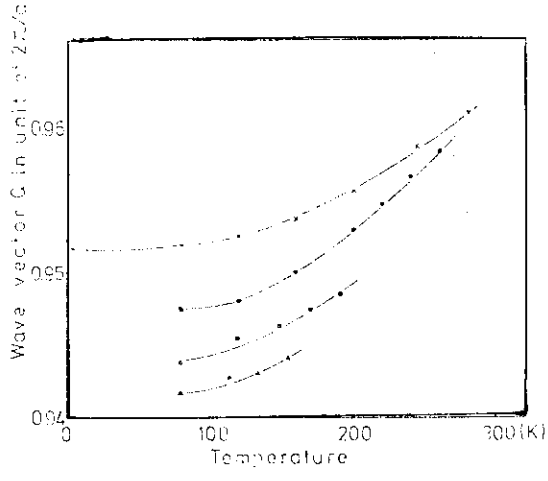

Fig. 2. Temperature dependence of the wave vector Q

The maximum amplitude of the magnetic moment μ_{max} in Fig.3 was obtained from the intensity ratio of the magnetic scattering around (1,0,0) and the nuclear (2,0,0) intensities obtained by powder neutron diffraction. Powder specimens were used in order to avoid the errors due to the

secondary extinction effect and to the inhomogeneous distribution of the magnetic Q-domains.

It was found by the present investigation that the magnetic structure of the Cr-Be alloy has sinusoidal antiferromagnetic structure up to 1.3 at.% Be. The effect of the addition of Be to Cr is to decrease T_N,T_f,Q and μ_{max}. This behavior is quite different from that observed in Cr alloys with the other non-transition elements in which antiferromagnetic structure appears and Q increases by increasing solute concentration. It can be considered, therefore, that the properties of Cr-Be cannot be explained by the general theory of Akai and Kanamori even in qualitatively, although Be forms a magnetic void in Cr.

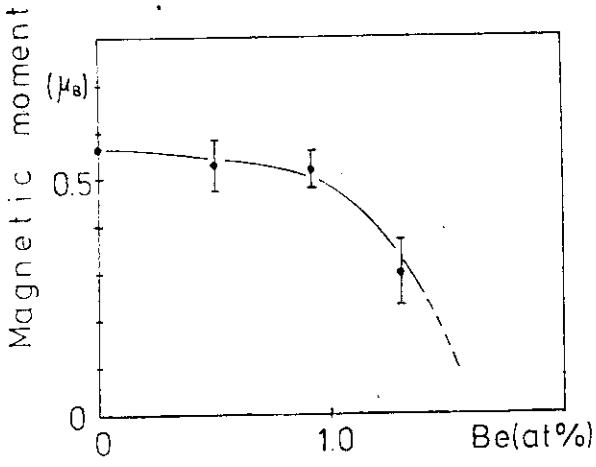

Fig. 3. Maximum amplitude of magnetic moment in Cr-Be at the liquid N_2 temperature

References

1) A.Kallel, F.De Bergevin; Sol.St.Comm. 5, 955 (1967)
2) J.W.Cable; J.Mag.Magn.Mat. 5, 112 (1977)
3) T.Suzuki; J. Phys. Soc. Jap. 45, 1852 (1978)
4) K.Fukamichi; phys.stat.sol. (a) 49, K47 (1978)
5) K.Fukamichi; J.Phys. F; Metal Phys. 9, L85 (1979)
6) H.Akai, J.Kanamori; Bulletin, Ann. Meeting, Phys.Soc. Japan 1978 April, 3pLC1 (in Japanese)

III7 Phase Relation between Primary and 3rd Harmonics of Spin Density Wave

Satoshi Iida, Yorihiko Tsunoda, Yutaka Nakai and Nobuhiko Kunitomi

Department of Physics, Faculty of Science, Osaka University

Pynn, et.al.[1] observed the existence of the 3rd harmonics of the spin density wave (SDW) in pure Cr, and determined its amplitude and the temperature dependece. But they did not discuss the phase relation between the 3rd harmonics and the primary SDW. In this report the experimental investigation about phase relation is presented. The possible phase relations make the envelope of the SDW to be antiphase (Fig.1a) or triangular type(Fig.1b). The 3rd harmonics of SDW make the satellite peaks at the ($1\pm3\delta$ 0 0) position in the reciprocal lattice space, where δ means the (1-Q) and Q is the wave number of SDW in units of $2\pi/a$. The phase modulation of the primary SDW by the strain wave (sinusoidal periodic lattice distortion) also produces a diffraction harmonics at the same position ($1\pm3\delta$ 0 0). The phase relation can be determined by the interference effect between the 3rd harmonics of SDW and the diffraction harmonics which were neglected by the previous authors[(1)]. Two models for the SDW state are considered when the strain wave is existing. The first one is as follows;

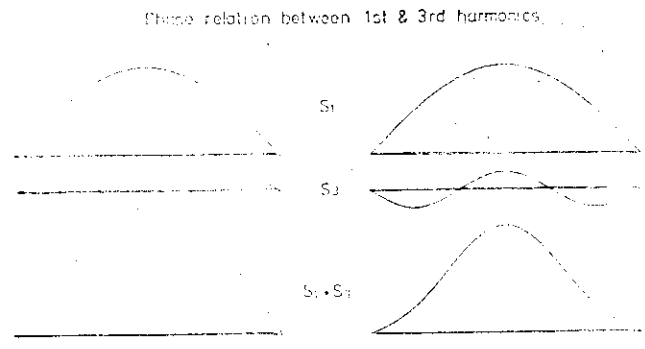

(a) (b)

Fig.1. The envelope of the SDW in the antiphase (a) and the triangular (b) type phase relation.

$$S_{1j}=S_1\cos\, Q\cdot R_j^0,$$

$$S_{3j}=S_3\cos\, 3Q\cdot R_j^0,$$

$$R_j=R_j^0-\Delta\sin\, 2Q\cdot R_j^0,$$

where S_1 and S_3 is the maximum amplitude of primary and 3rd harmonics of SDW, respectively. R_j is the jth atomic site, Δ is the strain wave amplitude and R_j^0 is the equilibrium lattice position without strain wave. In this model the magnitude of the magnetic moment at each atomic site is not

affected by the displacement due to the strain wave. Hereafter we refer this model as the rigid spin model. In this case the satellite intensities observed at (1±3δ 0 0) can be written as follows;

$$I(1-3\delta\ 0\ 0\ ) \propto |F(K)|^2|\pm S_3+S_1(1-3\delta)\pi\Delta/a|^2\cdot L\cdot e^{-2W},$$

$$I(1+3\delta\ 0\ 0\ ) \propto |F(K)|^2|\pm S_3-S_1(1+3\delta)\pi\Delta/a|^2\cdot L\cdot e^{-2W}.$$

The magnetic form factor F(K) for primary and 3rd harmonics of SDW are assumed to be the same, and K is the scattering vector, L is the Lorentz factor and e^{-2W} is the Debye-Waller factor. The plus sign of S_3 corresponds to the triangler type phase relation and the minus sign to the antiphase type. The second model is that the magnitude of the magnetic moment at each site varies so that its sinusoidal envelope is held unchanged when atoms displace from their equilibrium positions due to the existence of the strain wave. This model will be referred as the deformable spin model. In this case, the SDW and the atomic position for the jth atom can be written as

$$S_{1j} = S_1\cos\ Q\cdot R_j,$$

$$S_{3j} = S_3\cos\ 3Q\cdot R_j,$$

$$R_j = R_j^0 - \Delta\sin\ 2Q\cdot R_j^0.$$

The satellite intensities at (1±3δ 0 0) can be written as

$$I(1-3\delta\ 0\ 0\ ) \propto |F(K)|^2|\pm S_3-S_1(2\delta)\pi\Delta/a|^2\cdot L\cdot e^{-2W},$$

$$I(1+3\delta\ 0\ 0\ ) \propto |F(K)|^2|\pm S_3-S_1(2+2\delta)\pi\Delta/a|^2\cdot L\cdot e^{-2W}.$$

Since S_3/S_1 is estimated as $(1.65\pm0.05)\times10^{-2}$ [1] and Δ/a is reported to be $(1.3\pm0.3)\times10^{-3}$ [1] or $(1.6\pm0.3)\times10^{-3}$ [2], the ratio of the second term (diffraction harmonics) to the first term (3rd harmonics of SDW) of the scattering amplitude is about 10% and the phase relation can be determined by comparing the scattering intensities of I(1-3δ 0 0) and I(1+3δ 0 0).

The experiments were carried out by using the triple axis neutron spectrometer TUNS installed at JRR-2 in JAERI. Two single crystals were grown by arc-melting Iochromium. One composed of multi Q domains was measured at 144K and another of nearly single Q domain at 200K. The diffraction pattern at 144K is shown in Fig.2. The observed intensity I(1+3δ 0 0) has almost the same magnitude as I(1-3δ 0 0) in spite that the magnetic form factor and the Lorentz factor make the former appreciably less than the latter. In order to make the difference between two (1±3δ 0 0) satellite intensities clear, the observed scattering intensities are devided by the square of the magnetic form factor, the Lorentz factor and Debye-Waller

factor. These reduced intensities normalized at the value of (1−δ 0 0) are given in table.1.

Comparison of the reduced intensities at (1±3δ 0 0) indicates that the minus sign for S_3 is valid in either rigid or deformable spin model, i.e. the phase relation between the 3rd and primary SDW is antiphase type. This phase relation in pure Cr may be reasonable by considering that the antiphase type phase relation is expected theoretically[3] near the commensurate-incommensurate transition observed in the Cr alloys with small amounts of Mn or other elements. The reduced intensities for the two different temperature have almost the same value within the experimental error.

Table.1.

	$I' = I/F^2 \, L \, e^{-2W}$	
(1−δ 0 0)	1.00	1.00
(1+δ 0 0)	0.89±0.02	0.90±0.01
(1−3δ 0 0)	$(1.8\pm0.2)\times10^{-4}$	$(1.8\pm0.2)\times10^{-4}$
(1+3δ 0 0)	$(3.6\pm0.3)\times10^{-4}$	$(3.7\pm0.4)\times10^{-4}$
	(T=144K)	(T=200K)

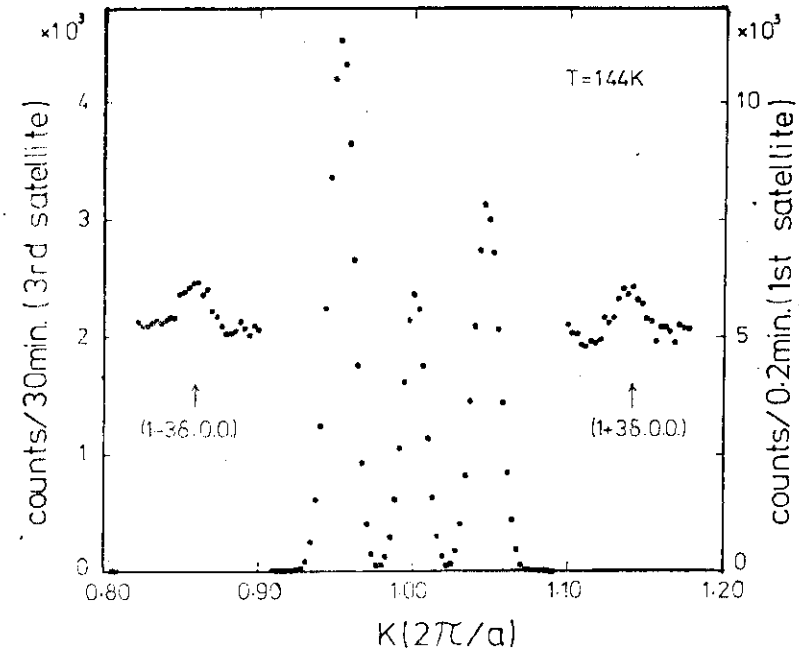

Fig.2. The scattering intensities of the primary and 3rd harmonics of SDW.

This results are consistent with the previous report in which the change of the 3rd satellite intensities is small at low temperature.[1] From the reduced intensity ratio of $I'(1-3\delta\ 0\ 0)/I'(1-\delta\ 0\ 0)$, S_3/S_1 is estimated to be $(1.6\pm0.1)\times10^{-2}$ and Δ/a to be $(0.9\pm0.2)\times10^{-3}$ within the rigid spin model. On the other hand the deformable spin model is adopted, S_3/S_1 and Δ/a are calculated to be $(1.3\pm0.1)\times10^{-2}$ and $(0.9\pm0.1)\times10^{-3}$, respectively. It was not determined definitely whether the SDW with the strain wave was rigid spin type or deformable spin type in this experiments.

(1) R.Pynn, W.Press, S.M.Shapiro and S.A.Werner: Phys. Rev. B13 (1976) 295.
(2) C.F.Eagen and S.A.Werner: Solid State Commun. 16 (1975) 1113.

III8 A Neutron Study of Spin Density Wave in CrGe Alloys

Satoshi Iida, Shuzo Kawarazaki and Nobuhiko Kunitomi

Department of Physics, Faculty of Science, Osaka University

In order to study the magnetic properties of Cr alloys with nonmagnetic impurities, we carried out neutron diffraction measurements for several CrGe alloys in single and polycrystalline forms. The polycrystalline samples were made by arc-melting 5N electrolytic Cr and 4N Ge, and the ingots were annealed at 1200°C for 20 hours. These samples were used for the determination of the amplitude of the magnetic moment by the powder diffraction method. The single crystals with the dimension of about 4×4×4 mm^3 were cut from the ingots made by melting 4N iodide Cr and 4N Ge. The magnetic phase diagram and the temperature dependence of the wave number Q of spin density wave (SDW) were determined using these single crystals. The experiments were done by using the double axis neutron diffractmeter TOG installed at JRR-3 in JAERI.

Magnetic Phase Diagram

The temperature dependence of the (100) peak intensity for the 0.5 at% Ge sample is shown in Fig.1, where one can see typical changes of the intensity at the temperature of longitudinal- transverse SDW (T_{SF}), incommensurate-commensurate SDW (T_{CI}) and antiferromagnetic-paramagnetic (T_N) phase transitions. The magnetic phase diagram of CrGe alloys determined by the present experiments is shown in Fig.2(a) by the closed circles, where data obtained from the thermal expansion measurements are also shown by open circles. As seen in the figure T_N increases with Ge concentration. T_{CI} decreases with Ge concentration

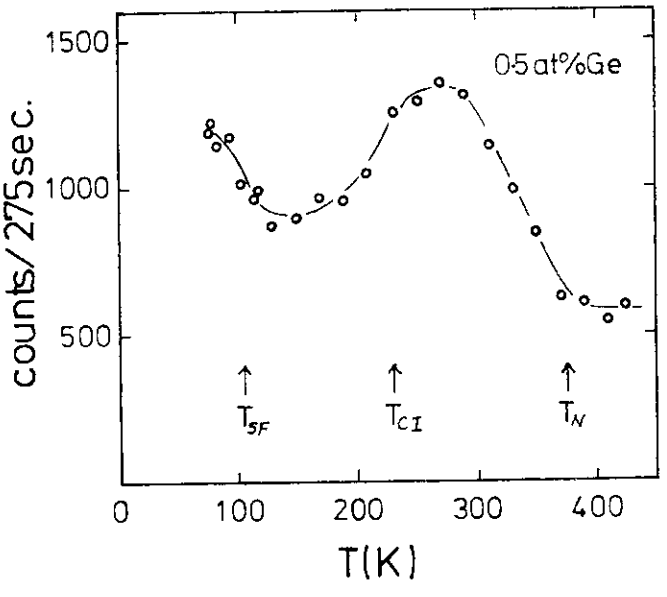

Fig.1. The temperature dependence of the (100) peak intensity of the 0.5 at.% Ge alloy.

and is lower than the liq. N_2 temperature for the 1.0 at.% Ge sample. T_{SF} also decreases by the addition of Ge. This phase diagram is almost consistent with the phase diagram determined by thermal expansion experiments by Suzuki[1].

Temperature and Concentration Dependence of Q

The concentration dependence of the wave number Q of the SDW is shown in Fig.2(b). The value of Q was determined at the temperature just above T_{SF} for 0.25, 0.5 and 0.75 at.% Ge samples, and at liq. N_2 temperature for 1.0, 1.5 and 3 at.% Ge samples. The temperature dependence of Q for the 0.5 at.% Ge sample together with that for pure Cr is shown in a small insert in Fig.2(b). The increase of Q and the discontinuous jump to $2\pi/a$ (commensurate SDW state) can be seen when Ge concentration or temperature is increased.

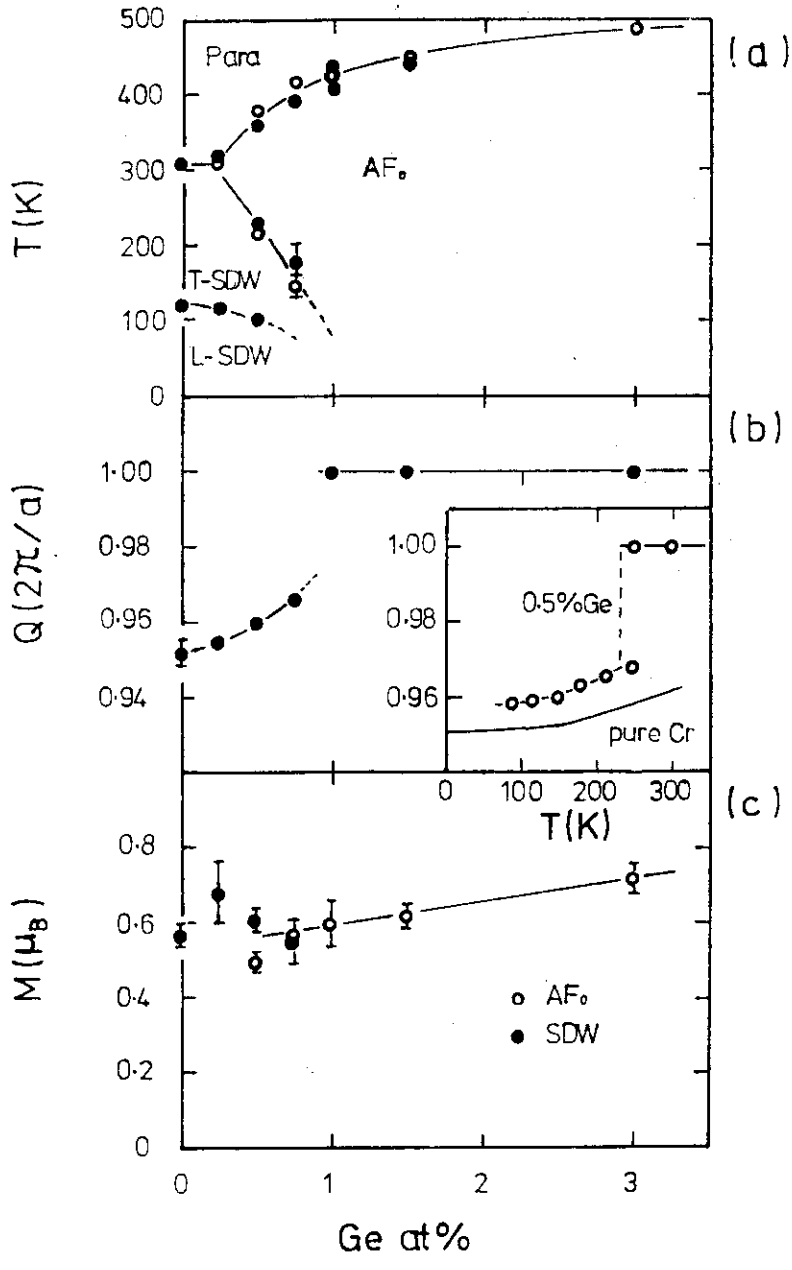

Fig.2. The magnetic phase diagram (a), and the concentration dependence of Q (b) and magnetic moment (c).

Magnitude of the Magnetic Moment

In Fig.2(c) the magnitude of the magnetic moment of CrGe alloys is shown against concentration, where the closed circles and the open circles indicate the amplitude of magnetic moment in the incommensurate SDW and in the commensurate SDW, respectively; the former was determined just above T_{SF}, and the latter was determined at the liq. N_2 temperature for the 1.0, 1.5 and 3 at.% Ge samples and just above T_{CI} for 0.5 and 0.75 at. % Ge samples. In Fig.2(c), one can see that the magnetic moment increases with Ge concentration and at the commensurate- incommensurate transition the amplitude of the incommensurate SDW (not the average value of the magnetic moment) is almost equal to the magnitude of the magnetic moment in the commensurate SDW. This is also the case for the C-I transition in CrMn alloys.

Remarks

The present results are compared with the experimental results for CrSi alloys[2]. For CrGe alloys both the magnetic moment and the Néel temperature increase with increasing Ge concentration, while in the case of CrSi alloys, the magnetic moment increases and the Néel temperature decreases by the addition of Si. On the other hand, the concentration dependence of Q is similar in both alloy systems.

References

1) T.Suzuki: J.Phys.Soc.Jpn. 45 (1978) 1852.
2) J.W.Cable: J.Magnetism.MagneticMaterials. 5 (1977) 112.

III9 Magnetic Phase Diagram of Dilute IrCr Alloy

Yorihiko Tsunoda, Satoshi Iida, Shuzo Kawarazaki and Hiroshi Shiraishi*

Faculty of Science, Osaka University and Software Kaihatsu Company*

The Néel temperature of Cr is drastically affected by the addition of a small amount of 5d-transition elements which locate at the right hand side of Cr in the periodic table(Re, Os, Ir and Pt). For the IrCr system, the concentration dependence of the Néel temperature has been reported by means of electrical resistivity[1] and magneto-volume effect[2] measurements, though these results contain some discrepancies. In order to determine the magnetic phase diagram of IrCr system, neutron diffraction studies have been made by using the single crystals of dilute IrCr alloy with the Ir contents of 0.2, 0.4 and 0.6 at. %. These specimens have been prepared by arc-melting method. Measurements were performed by using TOG conventional double axis diffractometer installed at JRR-3, JAERI, Tokai and at the temperature range between 78 K and 530 K.

The magnetic phase diagram determined by the present measurements is shown in Fig. 1 with the previous works of electrical resistivity and magneto-volume effect[1,2]. Data points at 0.3 % Ir in this figure were determined by means of thermal expansion measurements by present authors in order to clarify the discrepancies in the previous authors. The triple point in this system is found to be around 305 K and 0.2 % Ir. One characteristic behavior is that the Néel temperature at the triple point is lower than that of pure Cr by an amount of 5 $\sim$ 6 K. This feature was confirmed also by the temperature dependence of satellite intensity of second harmonic wave in SDW (strain wave) by X-ray measurements. In contrast to IrCr case, the Néel temperatures at the triple point for ReCr[3] and PtCr[4] alloys are higher than that of Cr. In the latter case, magnetic properties have been successfully explained from the standpoint of rigid band model, i.e., these 5d-transition elements act on Cr as an electron doner just as the case of MnCr alloy. However, for the IrCr alloy, present measurements indicate that we cannot stand on the same viewpoint as ReCr and PtCr systems.

Neutron satellite intensity at (1 - δ, 0, 0) for 0.2 % Ir shows an abrupt change at the Néel temperature indicating a first order phase

transition. The same behavior was reported for ReCr alloy[3]. First order transition from ISDW to paramagnetic phase in dilute Cr alloys seems to be a common feature for many kinds of impurity elements.

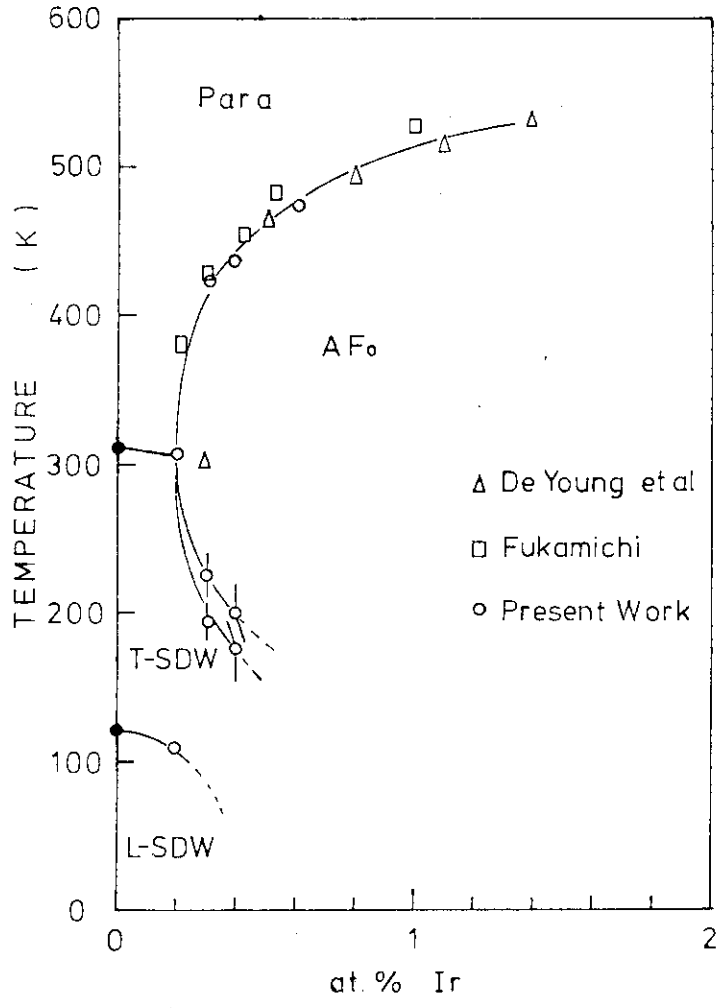

Fig 1. Magnetic phase diagram of dilute IrCr alloy.

1) T.F.DeYoung, S.Arajs and E.E.Anderson AIP conf. Proc. 5, 517 (1971).
2) K.Fukamichi and H.Saito Kinzoku-gakkaishi 40 22 (1976).
3) B.Lebeck and K.Mikke J. Phys. Chem. Solids 33 1651 (1972).
4) J.G.Booth, K.R.A.Ziebeck and R.Chagnon J. Phys. F Metal Phys. 8 1303 (1978).

III10 Pressure Effect of S.D.W. in Cr Alloys

J. Mizuki, Y. Endoh and Y. Ishikawa

Department of Physics, Tohoku University

We have extended the high pressure neutron diffraction studies using the conventional clamped method to investigation of the S.D.W. in several Cr alloys. We have been much interested in the empirical relation between the pressure derivative of Néel temperature (Tn) versus that of the S.D.W. wave vector (Q).

We made numbers of experiments with different pressure, different alloys as well as different concentration. Numbers of plots were thus obtained in the pressure derivatives of Tn and those of Q diagram. It turned out that a simple universal curve could be drawn for most of data except for data from Al-Cr alloys. (Fig. 1.)

The pressure derivatives of S.D.W. wave vector are found to be dependent on the alloy concentration for Fe- or Si-Cr alloys. When the solvent elements are dilute such that ordered states are only incommensurate to the lattice, 1/Q (dQ/dp) has same value as that of pure Cr. However the wave vector changes larger with increase of the pressure when the commensurate states appear in these alloys.

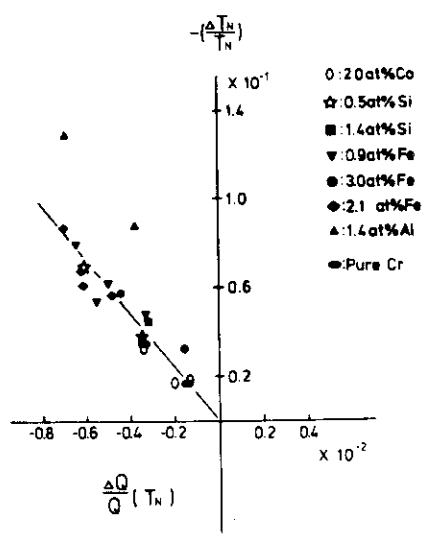

Fig. 1. The change of the Néel temperature of P-1 transition vs. that of the S.D.W. wave vector with the pressure. Quantities are scaled by the value for the atmospheric pressure.

IIIl1 Neutron Experiment on a Randomly Mixed Antiferromagnet with Competing Spin Anisotropies

Koichi Katsumata*, Makoto Kobayashi*† and Hideki Yoshizawa**

*Research Institute of Applied Electricity, Hokkaido University, Sapporo 060, and **The Institute for Solid State Physics, The University of Tokyo, Roppongi, Minato-ku, Tokyo 106

In a previous paper[1], two of the present authors(K.K. and M.K.) et al. have reported the concentration versus transition temperature phase diagram of a random mixture of two antiferromagnets with competing spin anisotropies, $FeCl_2 \cdot 2H_2O$ and $CoCl_2 \cdot 2H_2O$. The phase diagram was determined from the measurements of specific heat and susceptibility on single crystals of $Fe_{(1-x)}Co_xCl_2 \cdot 2H_2O$, and exhibited three kinds of ordered phases, namely, the Co-rich and Fe-rich antiferromagnetic phases and a new phase.

We report here a neutron diffraction experiment on the mixture. This experiment clearly demonstrates a decoupling of the spin components[2] near the tetracritical point which occurs in the concentration versus transition temperature phase diagram. It is also shown experimentally that the new phase observed in the intermediate concentration region is the "mixed ordering" phase[2](or equivalently the "oblique antiferromagnetic" phase[3]).

The experiment was carried out by using the ISSP spectrometer installed at JRR-3, JAERI, Tokai. The single crystal used was about $5\times5\times20mm^3$ in size. The long dimension, which was the c-axis, was set perpendicular to the scattering plane.

In Fig.1 are shown the temperature dependences of the intensities of the magnetic (100) and (010) peaks for x=0.568, which is close to the tetracritical concentration. The

---

†Present address: Nippon Telegraph and Telephone Public Corporation.

arrows in Fig.1 indicate the transition points determined from the specific heat measurement.[1,4] This figure shows clearly that the spin components off the b(b*)-axis diminish rapidly with temperature around T_L, while the components away from the a*-axis survive above T_L, and become zero around the higher transition temperature, T_N. Thus, the decoupling of the spin components near the tetracritical point is demonstrated experimentally.

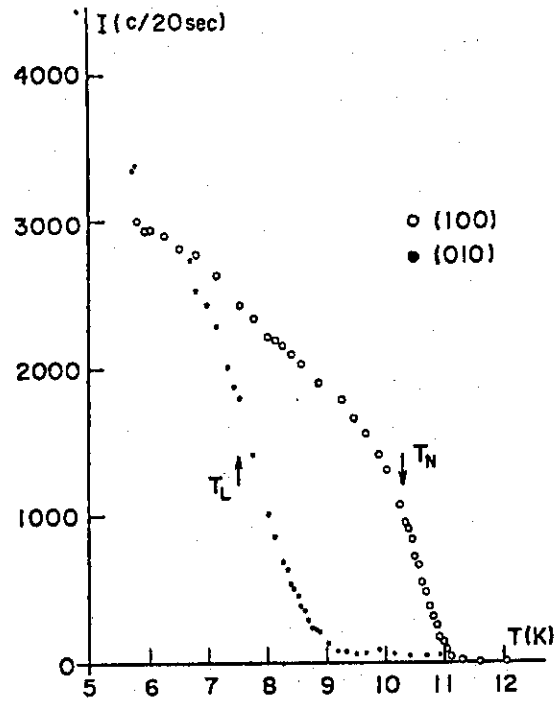

Fig.1. Temperature dependences of the intensities of the magnetic (100) and (010) peaks for x=0.568. Backgrounds coming from the harmonics of the nuclear peaks are subtracted.

The transition regions in Fig. 1 are rather broad, corresponding to the broad peaks occurring at the transition points in the specific heat measurement.[1,4] It should be noted that the homogeneity of the single crystals was examined by x-ray diffraction on powdered samples, and that clusters with a macroscopic size were not observed.

A random mixture with competing spin anisotropies has been studied in the mean-field approximation.[3,5-7] Matsubara and Inawashiro[3] have predicted the existence of a new type of ordered phase called "oblique-antiferromagnetic(OAF)" phase in the random mixture of two anisotropic antiferromagnets. The OAF phase, in which the directions of antiferromagnetically coupled spins are at an angle from the easy axes of the pure substances, corresponds to the "mixed ordering" phase of Aharony and Fishman[2], in the sense that the inclination of the sublattice magnetization both from the easy axes of the pure substances means the simultaneous ordering of the spin components which are associated with competing spin anisotro-

pies. From Fig.1 we see that the sublattice magnetizations make an angle both with the a* and b(b*) axes at temperatures below T_L. The sudden change in the (010) intensity with temperature in Fig.1 represents, in terms of the OAF model, a reorientation of the spin direction towards the b-axis.

An antiferromagnetic ordering of the spins in the new phase of $Fe_{(1-x)}Co_xCl_2 \cdot 2H_2O$ is clearly demonstrated in the experiment under a magnetic field. When we apply an external magnetic field along the c-axis, which is near the direction of the sublattice magnetizations, a spin-flopping transition occurs as in the case of pure antiferromagnets with weak anisotropy. In this experiment we have observed, for the first time, that the metamagnetic transition[8] which is observed in the pure substances does not occur in the new phase, and a spin-flopping transition takes place instead. A competition of the strong anisotropy energies[8] of $CoCl_2 \cdot 2H_2O$ and $FeCl_2 \cdot 2H_2O$ causes the anisotropy in the new phase to be very small.

The authors wish to express their thanks to Prof. K. Hirakawa for his many helpful discussions and encouragements. Thanks are also due to Dr. Y. Tsunoda and Dr. M. Kohgi for their many helpful discussions and advices.

References

1) K.Katsumata, M.Kobayashi, T.Satō, and Y.Miyako: Phys. Rev. B19(1979)2700.
2) A.Aharony and S.Fishman: Phys. Rev. Lett. 37(1976)1587, S.Fishman and A.Aharony: Phys. Rev. B18(1978)3507.
3) F.Matsubara and S.Inawashiro: J. Phys. Soc. Japan 42(1977) 1529.
4) M.Kobayashi, K.Katsumata, T.Satō, and Y.Miyako: J. Phys. Soc. Japan 46(1979)1467.
5) P.A.Lindgård: Phys. Rev. B14(1976)4074; B16(1977)2168.
6) T.Oguchi and T.Ishikawa: J. Phys. Soc. Japan 45(1978)1213.
7) F.Matsubara and S.Inawashiro: J. Phys. Soc. Japan 46(1979) 1740.
8) For details, see K.Katsumata: J. Phys. Soc. Japan 39(1975) 42, and references cited therein.

III12 Magnetic Field Effect on Neutron Diffraction of NiS_2

Tomonao Miyadai, Katsuya Kikuchi and Koichi Takizawa

Department of Physics, Faculty of Science, Hokkaido University

NiS_2 has a complicated magnetic structure at low temperatures; there coexist both the 1'st kind-and the 2'nd kind-antiferromagnetic (AF) orderings of fcc Lattice, and further a weakferromagnetic (WF) moment appears in addition to them. We have investigated, for a few years, the spin structure and the mechanism of WF in NiS_2. We proposed a non-collinear spin structure[1] which can explain the neutron diffraction intensities, results of polarization analysis and also the Mossbauer study. As for the mechanism of WF, we also presented an experimental evidence[2] supporting Yoshimori's theory[3] in which four spin interactions play an essential role. According to this mechanism, the direction of WF moment should couple with the direction of the AF domain. So that the distribution of AF domains is expected to change when we change the distribution of WF domains by applying a magnetic field. We have tried to observe the change with magnetic field in the intensity of AF reflections. This will present a dirct evidence for the coupling of AF and WF. Indeed, we observed[4] a small decrease in the intensity of (200)M1 reflection when a magnetic field was applied along [001] and also [010] directions (perpendicular to the scattering vector).

Here, in order to obtain further information on the effect of the magnetic field, we measured at about 5 K the change in intensity of several M1- and M2-reflections on application of the magnetic field along various directions. The measurements were made at a wave length of 1.0 A by means of PANSIspectrometer at JRR-2. The measured reflections and the directions of the magnetic field used are given in Table I, in which predictions from our spin structure model[1] are also given. Since our model allows six kinds of AF domains, we assumed the random distribution of them. As seen in Table I, the agreement between the observed and the calculated changes in the intensity is not good. However, the observations given in Table I are not conclusive at the present stage. We measured the hysteresis for the application of magnetic field; at 5 K the change by an initial application of a field remained unchanged after switching off the exiting current of the magnet. Further, the change still remained after

the sample crystal had been heated up to about 60 K (above T_N) and again cooled down to 5 K under a remanent field of the magnet. At present, we cannot completely exclude such a possibility that the observed change be apparent. It is, however, sure that the change by a magnetic field is not larger than 20 to 30 % and that the line profile is scarcely affected by a magnetic field. Further experiments are necessary for establishing the magnetic field effect on AF reflections of NiS_2.

The present authors would like to express their sincere thanks to Prof. Y.Ito and Dr. M.Nishi for neutron diffraction measurements.

1) K.Kikuchi et al., J. Phys. Soc. Japan 44 (1978) 410
2) K.Kikuchi, J. Phys. Soc. Japan 47 (1979) 484
3) A.Yoshimori and H.Fukuda, J. Phys. Soc. Japan 46 (1979) 1663
4) K.Kikuchi, T.Miyadai and Y.Ito, Proc. ICM'79 (Munich)

Table I

hkl	WF-domain	Field Direction	Intensity Change in % Observed	Calculated
(200)M1	x	[100]	+16	-13
	z	[001]	(-15)	-13
	y,z	[011]	+24	+ 7
(220)M1	x	~[100]	- 6	+26
	z	[001]	- 6	-12
$(02\bar{2})$M1	y,z	[011]	- 2	+ 6
$(11\bar{1})$M2	y,z	~[111]	+13	0
$(31\bar{1})$M2	x	[311]	- 3	0

M1= the 1'st kind, M2= the 2'nd kind.
hkl is referred to twice the chemical unit cell.

III13 Single Domain Formation of Magnetic Screw Structure by Magnetoelectric Cooling

Kiiti Siratori*, Jun Akimitsu**, Eiji Kita* and Masakazu Nishi***

*Department of Physics, Osaka University, **Department of physics Aoyama Gakuin University, ***Institute for Solid State Physics, University of Tokyo.

The screw spin structure has two types of domains: right-handed and left handed screw. The effect of unequal domain population in a helimagnet to the polarization of neutrons was discussed theoretically as early as 1962. Experimental attempts of finding unequal domain population were, however, made with little success[2], since no method had been found to control screw domains. In this note, we report the first success of screw domain control by the magnetoelectric cooling, i.e., cooling of the specimen through the Néel point in simultaneously applied magnetic and electric field.

In the case of incommensurate conical spin structure, linear magnetoelectric effect is expected from its magnetic symmetry and was really observed in $ZnCr_2Se_4$.[3] In such a case, antiferromagnetic domains can be controlled by the magnetoelectric cooling.[4]

This was directly confirmed by the polarized neutron diffraction technique. Experiment was carried out at PANSI[5] of I.S.S.P., installed at the JRR-2 reactor at J.A.E.R.I., Tokai.

Single crystal of $ZnCr_2Se_4$ used in the present experiment takes the proper screw spin

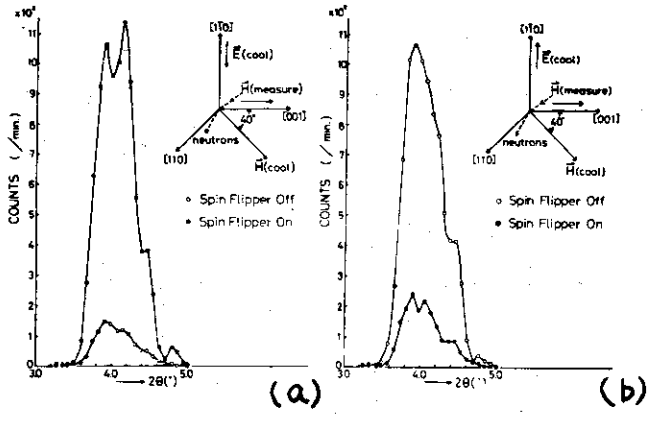

Fig . Polarization dependence of 0,0,k_0 reflection at 8k, after the magnetoelectric cooling.
(a): The cooling electric field was along $[\bar{1}10]$.
(b): The cooling electric field was along $[1\bar{1}0]$.

structure along [1 0 0] below its Néel point of approximately 20K.[6)]

Polarization dependence of the diffracted neutrons at $(0,0,k_o)$ in $ZnCr_2Se_4$ is shown in Fig 1 after the magneto-electric cooling with the electric field of 2.5 kV/cm along $[\bar{1}10]$ (a) and $[1\bar{1}0]$ (b) and a horizontal magnetic field of 12kOe, 40° tilted from [001] to [110].

The intensity of the satellite observed in the present experiment is given as[7)]

$$\frac{d\sigma}{d\Omega} = A|F|^2\{2 - 2(\hat{s}\cdot\hat{e})\cdot(\hat{e}\cdot\hat{K})\} \quad .$$

Here, $\hat{e}$ is the unit scattering vector, $\hat{K}$ is $\vec{k}_o/|\vec{k}_o|$, $\hat{s}$ is the polarization of the incident neutrons and F is the structure factor. The cross section is zero when $\hat{K}$ and $\hat{s}$ are parallel and is $4A|F|^2$ when they are antiparallel. Figure 1 indicates that $\hat{K}$ is antiparallel to $\hat{s}$, or screw is left-handed, in approximately 95% of the specimen in case (a). The situation was reversed in case (b). This means that diffracted neutrons are 95% polarized if the incident neutrons are unpolarized.

This result suggests that single domain screw magnet can be available as a neutron polarizer.

References

1) A. W. Overhauser: Bull. Amer. Phys. Soc. 7 (1962) 241.
Yu. A. Izumov: Zh. Eksp. Theor. Fiz. 42 (1962) 1673.
Soviet phys. - JETP 15 (1962) 1162.
2) G. P. Felcher, G. H. Lander and T. O. Brun: J. Phys. Colloq. (Paris) 32 (1971) 1-577.
3) K. Siratori, E. Kita and K. Kohn: Unpublished.
4) T. J. Martin: Phys. Lett. 17 (1965) 83.
5) Y. Ito, S. Takahashi, Y. Kawamura, K. Motoya and M. Nishi: Tich. Rep. ISSP No.951 (1979).
6) J. Akimitsu, K. Siratori G. Shirane, M. Iizumi and T. Watanabe: J. Phys. Soc. Jpn. 44 (1978) 172.
7) M. Blume: Phys. Rev. 130 (1963) 1670.

III14 Magnetization of Ferromagnetic Metals at the Interface to Other Materials

M. Sato[#], K. Abe[*], Y. Endoh[**], J. Hayter[+] and R. D. Lowde[++]

[#]Institute for Solid State Physics, Tokyo University, Tokyo,
[*]Institute for Solid State Physics, Tokyo University, Tokyo, present address, Device Developement Center, Hitachi Ltd, Kodaira, Tokyo,
[**]Department of Physics, Fuculty of Science, Tohoku University, Sendai, Japan, [+]Institut Laue Langevin,38042 Grenoble, France,
[++]Materials Physics Division, AERE Harwell, OXON, United Kingdom

The problem of the surface magnetization of the ferromagnetic metals has been a subject of many works.[1),2)] It is one example of many interesting basic problems in surface physics. The experimental result of Liebermann et al.[3)] that the surface layer(s) of Ni has no magnetic moment("dead layer") stimulated the active studies on this subject. From the theoretical side Fulde et al.[2),4)], for example, suggested the possibility of the "dead layer" for Ni by their simple discussion which gave us the interesting physical insights on this problem. Teraoka et al.[5)] suggested the enhancement of the surface susceptibility or the surface magnetizationof the bcc transition metals.

To measure the surface magnetization, there are many techniques which are reviewed in ref. 2. Gradmann[6)] studied the surface magnetization of $Ni_{48}Fe_{52}$ alloy by the magnetization measurement of epitaxial films. Shinjo et al.[7)] studied thid problem by Mössbauer spectroscopy. Here we report experimental results on the interface magnetization of Fe-SiO and Ni-SiO multilayer films and of Co particles precipitated in Cu. These were studied by the neutron small angle scattering technique. As was shown in the previous papers,[8),9)] both the nuclear and the magnetic moment distributions can be known independently by this method. Its important merit is that we can extract the information of the surface magnetization by using only the difference of these two kinds of distributions. In the present case,we observed only the interface magnetization, which we believe , gives us useful information on the surface

problem.

In the present experiment, we observed no anomalous surface effect at the Fe-SiO and Co-Cu interfaces at room temperature and a certain reduction of the magnetization at the Ni-SiO interface at 9 °K.

The detailed data and analyses can be seen in the ISSP report[10] and the paper which will be published somewhere else.

It should be noted that some part of this experiment were carried out at Institut Laue Langevin, Grenoble, France.

References

1) U. Gradmann: Appl. Phys. 3 (1974) 161, See also references theirin.
2) P. Fulde: Itinerant Electron Magnetism, edited by R.D. Lowde and E. P. Wohlfarth, North Holland, Oxford(1977), p251, See also references theirin.
3) L. N. Liebermann, J. Clinton, D. M. Edwards and J. Mathon: Phys. Rev. Letters 25 (1970) 232
4) P. Fulde, A. Luther and R. E. Watson: Phys. Rev. B8 (1973) 440
5) Y. Teraoka and J. Kanamori: Proc. Int. Conf. Phys. Transition Metals, Tront (1977)
6) U. Gradmann and Muller: Phys. stat. sol. 27 (1968) 313
7) T. Shinjo, T. Matsuzawa, T. Takada, S. Nasu and Y. Murakami: J. Phys. Soc. Japan 35 (1973) 1032 and T. Shinjo, S. Hine and T. Takada: Proc. 7th Int. Vac. Congr. and 3rd Int. Conf. Solid Surface.
8) M. Sato and K. Hirakawa: J. Phys. Soc. Japan 39 (1975) 1467
9) M.Sato and K. Abe: Solid State Commun. 26 (1978) 95 and erratum 26 (1978)
10) M. Sato, K. Abe, Y. Endoh, J. Hayter and R. D. Lowde: ISSP Technical Report: to be published

III15 Polarized Neutron Diffraction Study of CoMnP Single Crystal

H. Fujii, S. Komura, T. Takeda, T. Hokabe* and T. Okamoto

Faculty of Integrated Arts and Sciences, Hiroshima University, Hiroshima 730, Japan, *Faculty of General Education, Kagoshima University, Kagoshima 890, Japan

The system $(Co_{1-X}Mn_X)_2P$ exhibits only ferromagnetism for $0.1 \leq X \leq 0.55$ in all ordering temperature ranges, shows both ferromagnetism and metamagnetism with decreasing temperature for $0.56 \leq X \leq 0.66$ and shows only antiferromagnetism for $0.66 \leq X \leq 0.8$. The Curie temperature increases with X to a maximum of 583 K at X = 0.5 (CoMnP) and then decreases to about 240 K at X = 0.66[1]. We have carried out polarized neutron diffraction measurements on CoMnP single crystal in order to obtain information on the origin of the various magnetisms in the system $(Co_{1-X}Mn_X)_2P$. The crystal structure belongs to the orthorhombic C23 type with two nonequivalent metal sites in which Co atom occupies the tetrahedral site and Mn atom the pyramidal site. Spin flipping ratios were measured at room temperature for 45 different (h0l) reflections up to $\sin\theta/\lambda \sim 0.70$ A^{-1} in a field of 5.2 KOe with an incident neutron wavelength of 1.00 A. Three single crystals used are in a form of rectangular pillar with the dimensions 0.2 x 1 x 10 mm^3, 1 x 1 x 10 mm^3 and 2 x 2 x 7 mm^3.

For the determination of magnetic moments of Co and Mn atoms, a least-squares fit to the observed ratios of the magnetic to the nuclear structure factors was made. The atomic positional parameters presumed to be close to those of Co_2P were also optimized. In the analysis, as trial form factors for Co and Mn, we used the spherical form factors for the various atomic states calculated by Watson and Freeman[2] and compared the least squares errors for various combinations. The final values for the moments were $0.06 \pm 0.02\ \mu_B$ and $2.66 \pm 0.02\ \mu_B$ for Co and Mn, respectively. These values are in good agreement with the presumed values from the composition dependence of the saturation magnetization[3]. The averaged magnetic form factor was determined on the basis of the values of the magnetic moments on Co and Mn atoms. The magnetic form factor obtained is found to be close to that for Mn^{2+} atom in the range of $\sin\theta/\lambda < 0.4$ but that for Mn^{3+} atom for $\sin\theta/\lambda > 0.4$ as shown in Fig. 1. This fact suggests that the unpaired 3d-elctrons are quasi-localized on the atoms. In addition, the form factor scatters fairly in the range $\sin\theta/\lambda > 0.4$. This means that the asphericity of the form factor is observed.

The above experimental results suggest that the spontaneous ferromagnetism in the range of $0.1 \leq X \leq 0.55$ is associated with the ferromagnetic exchange interaction between Mn moments on pyramidal sites. The metamagnetism in the interval of $0.56 \leq X \leq 0.66$ seems to be originated from an existence of antiferromangetic interaction between Mn moments on tetrahedral and pyramidal sites.

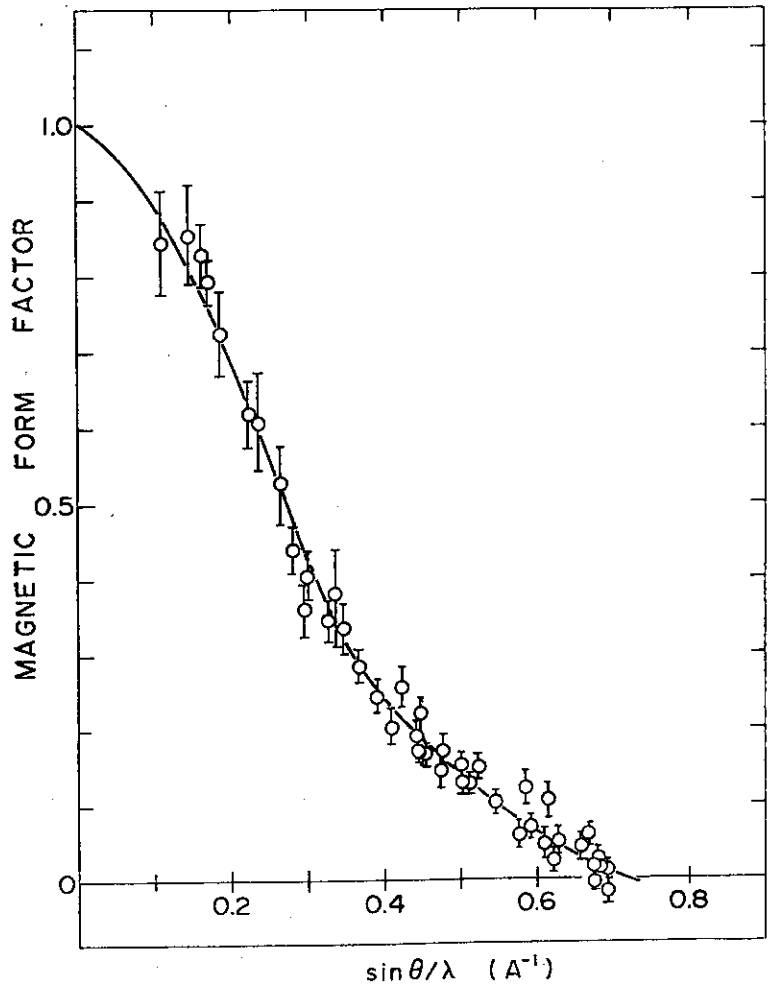

Fig. 1 Magnetic form factor common to Co and Mn atoms.

References

1) R. Fruchart, S. Roger and J. P. Senateur, J. Appl. Phys. 40 (1969) 1250.

2) R. E. Watson and A. J. Freeman, Acta Cryst. 14 (1961) 27.

3) J. B. Goodenough, J. Solid State Chem., 7 (1973) 428.

III16 Magnetic Form Factor of Ni-Pt Alloy System†††

Yutaka Nakai*, Izumi Tomeno*†, Jun Akimitsu**†† and Yuji Ito**

*Faculty of Science, Osaka University, **The Institute for Solid State Physics, The University of Tokyo.

It would be interesting to know the behaviors of Ni and Pt magnetic moments in the Ni-Pt alloy system, which is believed to be a homogeneous ferromagnet near its critical concentration region. This should be contrasted to the Ni-Pd alloy system, which is known as a system of heterogeneous ferromagnetism.

In view of this, we measured the magnetic form factors of the Ni-rich Ni-Pt alloys by means of the polarized neutron diffraction to determine the atomic magnetic moments of Ni and Pt, using form factor analysis technique. For the theoretical treatment of the problem, we rely on the Coherent Potential Approximation (CPA) developed by Hasegawa and Kanamori[1], in which we used a Hartree-Fock Hubbard Hamiltonian with suitable parameters, in order to describe the magnetic moments of Ni and Pt, obtained by the present experiment. Partial state densities of d-electrons for Ni and Pt atoms in the alloy near the critical concentration were also calculated.

The measurements of the polarization ratio were performed by using ISSP and POLTO polarized neutron diffractometers situated at JRR-3 and later using PANSI spectrometer at JRR-2 in JAERI. The polarization ratios were corrected for the secondary extinction, incomplete polarization of incident neutrons and incomplete flipping efficiency. Magnetic structure factors for each specimen were analyzed, using the following formula by means of least squares method.

$$\begin{aligned}\mu f(K) = {} & c_{Ni}\,\mu_{Ni}\,(2/g_{Ni})\{\langle j_0\rangle_{Ni} + A_{hkl}(\,5/2\cdot\gamma_{Ni} - 1\,)\,\langle j_4\rangle_{Ni}\} \\ & + c_{Ni}\,(\,g_{Ni} - 2\,)/\,g_{Ni}\,\mu_{Ni}\langle j_0\rangle^{o}_{Ni} \\ & + c_{Pt}\,\mu_{Pt}\{\,\langle j_0\rangle_{Pt} + A_{hkl}(\,5/2\cdot\gamma_{Pt} - 1\,)\langle j_4\rangle_{Pt}\},\end{aligned}$$

where fitting parameters μ_{Ni}, μ_{Pt}, γ_{Ni} and γ_{Pt} are magnetic moments and the proportions of E_g state for Ni and Pt atoms, respectively. The best-fit parameters are seen in Fig. 1, where the conduction electron contribution, μ_{cond}, was calculated by

$$\mu_{cond} = \mu_{mag} - (\,c_{Ni}\,\mu_{Ni} + c_{Pt}\,\mu_{Pt}\,),$$

with μ_{mag}, the bulk magnetization of the corresponding specimen.

Next we employ the CPA for the Ni-Pt and the Ni-Pd alloys[2] to explain the experimental results, assuming that the Hamiltonian has disorder only on the diagonal term. We used the Hamiltonian with suitable parameters, in order to describe the present experimental results. In the vicinity of the critical concentration, the partial state densities of Ni and Pt atoms in the Ni-Pt alloy were calculated to be almost the same with each other, as seen in Fig. 2, while the partial state densities of Ni and Pd atoms in the Ni-Pd alloy turned out to be quite different. This fact must have relevance to the homogeneous ferromagnetism of the Ni-Pt alloy in contrast to the heterogeneous ferromagnetism of the Ni-Pd alloy.

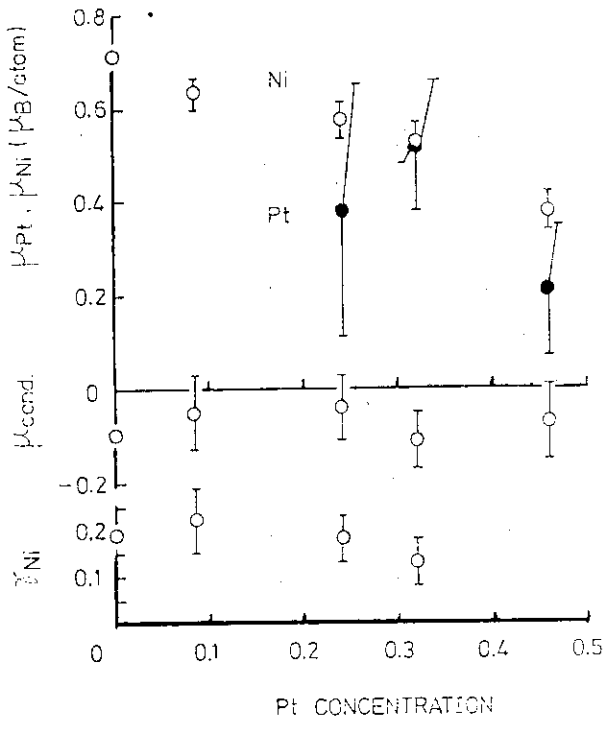

Fig. 1. Concentration dependence of μ_{Ni}, μ_{Pt}, μ_{cond} and γ_{Ni}.

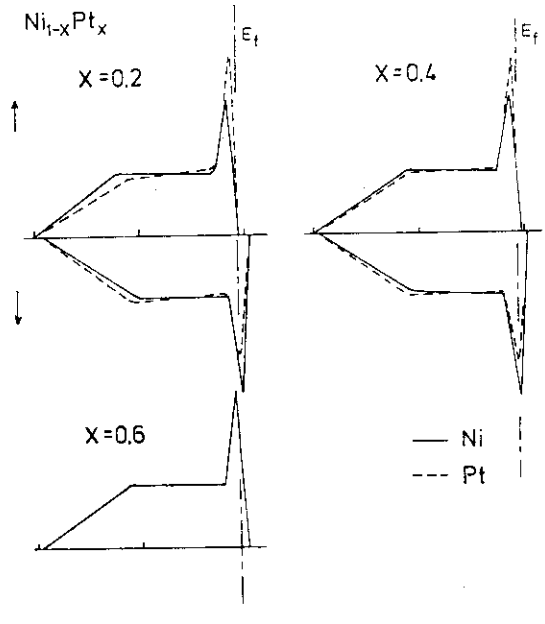

Fig. 2. Calculated partial state densities of d-electrons.

References

†Present address: Tokyo Shibaura Electric Co., Ltd.

††Present address: College of Science and Engineering, Aoyama Gakuin University.

†††to be published in J. Phys. Soc. Jpn. 47 No. 6 (1979).

1)H.Hasegawa and J.Kanamori: J. Phys.Soc. Jpn. 33(1972) 1599, 1607.

2)J.W.Cable and H.R.Child: Phys. Rev. B1(1970) 3809.

III17 Magnetic Moment Distribution in FCC Co-V Alloys

Yoshihira Aoki, Yasuo Yamaguchi, Noriaki Kazama and Hiroshi Watanabe

The Research Institute for Iron, Steel and Other Metals,
Tohoku University, Sendai

The present work has been undertaken to know the magnetic moment distribution in the disordered fcc Co-V alloys by means of the polarized-neutron elastic diffuse-scattering technique at room-temperature. In the Co-rich Co-V alloy system, the disordered fcc state is difficult to be stabilized at room-temperature in the composition range of less than 10 at.% V, because of the martensitic transformation of fcc to hcp (2). In addition, the composition of the fcc alloys which have a ferromagnetic Curie point above room-temperature is limited up to about 20 at.% V (3). From these situations, three specimens containing 13.8, 15.6 and 17.5 at.% V were prepared.

The polarized-neutron elastic diffuse-scattering was measured at room-temperature by means of the POLTO polarized neutron diffractometer with a neutron wavelength λ=1.03 Å. The magnetic field vertically applied was 12.5 kOe. The absolute value of cross-sections was calibrated by the use of a standard V metal with a dimension of 25×25×1 mm^3. The corrections such as absorption, imcomplete incident beam polarization and sample depolarization were made, but the multiple scattering correction for both spin states was neglected because no appreciable difference in the spin-dependent transmission was observed. The bulk moment was measured at room-temperature by means of a sample-vibrating magnetometer.

On the basis of the method used by Shull and Wilkinson (1), the magnetic moment of the individual atoms, $\bar{\mu}_{Co}$ and $\bar{\mu}_{V}$, was calculated from the difference cross-sections and the bulk moments, both of which were obtained at room-temperature. The observed difference cross-sections are shown in Fig. 1 for three alloys containing 13.8, 15.6 and 17.5 at.% V. The average magnetic moment of the individual atoms is given in Fig. 2, together with the bulk moment of $\bar{\mu}$. Solid curves in Fig. 1 indicate the difference cross-sections calculated by the use of $\bar{\mu}_{Co}$ and $\bar{\mu}_{V}$ in Fig. 2. Statistical errors are shown by bars in Figs. 1 and 2.

As seen in Fig. 2, the V atoms have a negative magnetic moment at the Co-rich side of the composition range covered. The absolute value of the

V moment decreases rapidly with increasing V content and vanishes in the composition range of about 16 at.% V or more. The V moment which is negative with respect to the Co moment may be expected in connection with the appearance of empty virtual bound states above the Fermi level (4,5,6). The Co moment also decreases monotonously with increasing V content in the similar manner to the composition dependence of the bulk moment. The decrease in the Co moment with increasing V content may be explained on the assumption of the negative moment disturbances produced by the V atoms on their Co neighbours (7).

References

1) C.G. Shull and M.K. Wilkinson, Phys. Rev. 97 (1955) 304.
2) M. Hansen and K. Anderko, Constitution of Binary Alloys, 2nd ed., McGraw-Hill (1958) p.516.
3) Y. Aoki and M. Yamamoto, Phys. Stat. Sol. (a) 33 (1976) 625.
4) J. Friedel, Nuovo Cimento Suppl. 2 (1958) 287.
5) J. Kanamori, J. Appl. Phys. 36 (1965) 929.
6) I.A. Campbell and A.A. Gomes, Proc. Phys. Soc. 91 (1967) 319.
7) J.W. Cable and T.J. Hicks, Phys. Rev. 2B (1970) 176.

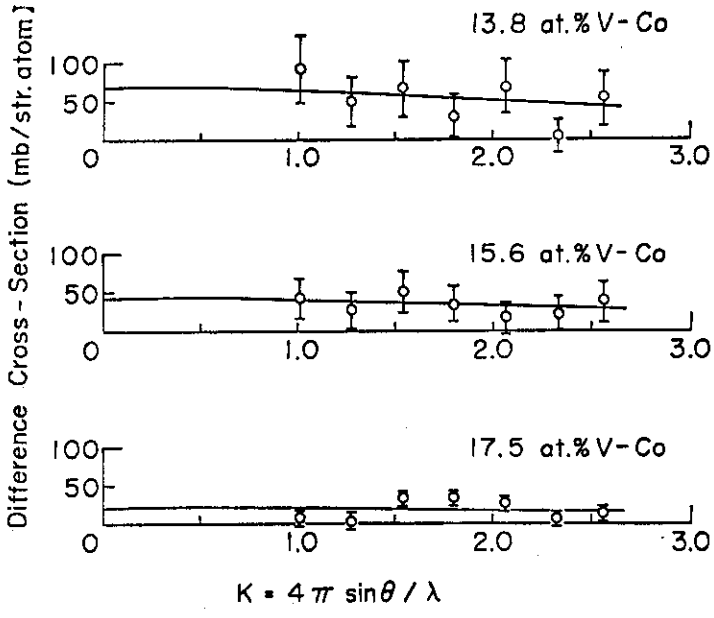

Fig. 1. Difference cross-sections observed at room-temperature by means of polarized neutron technique for three alloys containing 13.8, 15.6 and 17.5 at.% V. Solid curves were calculated from the values of $\bar{\mu}_{Co}$ and $\bar{\mu}_{V}$ given in Fig. 2.

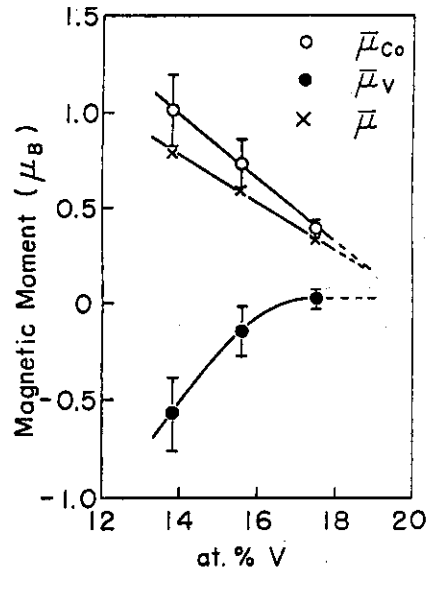

Fig. 2. The composition dependence of $\bar{\mu}$, $\bar{\mu}_{Co}$ and $\bar{\mu}_{V}$ observed at room-temperature in the Co-V alloys.

III18

Magnetic Disturbance around the Interstitial-Site Mn Atom in MnSb

Yasuo Yamaguchi and Hiroshi Watanabe

The Research Institute for Iron, Steel and Other Metals,
Tohoku University, Sendai, Japan

Antimonides of 3d-transition elements with NiAs crystal structure are typical Berthollide compounds with wide single phase regions on the cation rich side.[1] Magnetic properties of these antimonides varies with the cation concentration.[2-4] For ferromagnetic $Mn_{1+\delta}Sb$ ($0 \leq \delta \leq 0.22$), the magnetization decrease with increasing the cation concentration:

$$\mu = (3.55 - 2.78 \times \delta)\ \mu_B \ /\ \text{formula}$$

The excess Mn atoms, which occupy the interstitial sites at random,[5] have been shown to have no magnetic moment with themselves,[6] but have an effect to decrease the magnetization per formula.

In the present study, we measured intensity of the diffuse scattering of polarized neutrons from $Mn_{1.2}Sb$ in order to study the spatial distribution of the magnetic disturbance around the interstitial Mn atom in MnSb. With incident neutrons polarized parallel and antiparallel to the sample magnetization and perpendicular to the scattering vector, the magnetic disordered scattering from interstitial atoms in a ferromagnetic crystal is given by

$$\frac{d\sigma^{\pm}}{d\Omega} = \delta(1-\delta)\cdot \left| \Delta F_N(k) \pm 0.270 \cdot \Delta F_M(k) \right|^2 \qquad (1)$$

in barns per formula unit, where δ is concentration of the excess atoms, $\Delta F_N(k)$ and $\Delta F_M(k)$ are respectively the alterations of the nuclear and magnetic structure factor introduced by an excess atom on the interstitial site, and k is the scattering vector.

The difference of the intensities of the diffuse scattering between spin up and spin down of the incident neutrons have been measured at 293K along two different directions of the scattering vector, [0.2,0,1] and [1,-0.6,0,7]. The experimental results are shown in Fig. 1 compared with the calculations for three different models. The interstitial Mn atom has been reconfirmed to have no magnetic moment by itself, magnetic moment of the first neighbouring Mn atoms around the interstitial Mn is found to be reduced about 13%, and the magnetic disturbance around the interstitial Mn

atom is closed within the first neighbouring regular-site Mn atoms.

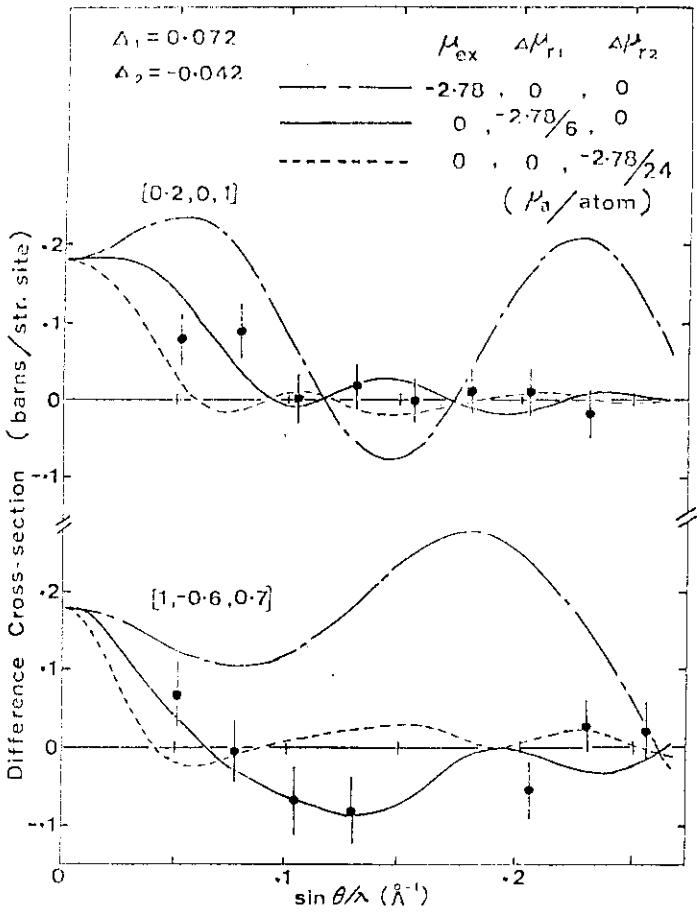

Fig. 1. Difference of differential cross section between up and down spin of incident neutrons scattered by a slice of a single crystal of $Mn_{1.2}Sb$ along two different directions of scattering vector. Experimental values (heavy circles with error bars) are compared with model calculation of reduction of the magnetization due to excess Mn (— ·—), first neighbouring Mn (————), or second neighbouring Mn (----).

References

1) A. Kjekshus and W.B. Pearson: Progress in Solid State Chem., ed. H. Reiss (MacMillan, New York, 1964) p.83.
2) T. Okita and Y. Makino: J. Phys. Soc. Japan 25 (1068) 120.
3) K. Yamaguchi, H. Yamamoto, Y. Yamaguchi and H. Watanabe: J. Phys. Soc. Japan 33 (1972) 1292.
4) H. Schmid: Cobalt 7 (1960) 26.
5) I. Teramoto and A.M.J.G. van Run: J. Phys. Chem. Solids 29 (1968) 347.
6) Y. Yamaguchi, H. Watanabe and T. Suzuki: J. Phys. Soc. Japan 41 (1976) 703.

III19 Atomic Magnetic Moments in a Ternary Alloy Fe-Co-Ni†

Noboru Schibuya, Yutaka Nakai, Katsuhito Yamasaki and Nobuhiko Kunitomi

Department of Physics, Osaka University, Toyonaka, Osaka 560

Recently, theoretical treatments based on the coherent potential approximation (CPA) have successfully explained the physical properties of non-dilute random substitutional alloys. Jo et al. have applied this method to a fcc ternary ferromagnetic Fe-Co-Ni alloy.[1] As a method of the experimental verfication of CPA, the study of the ternary alloy system Fe-Co-Ni has two significances compared with the study of the binary alloy system. First, in the ternary alloy system we can investigate series of specimens with the same numbers of 3d-electrons per atom and different compositions of constituent atoms. According to the rigid band approximation (RBA) the magnetic properties should be the same for specimens with an equi-electron number, whereas by the CPA treatment the magnetic moment of individual atoms were calculated to be different even in a series of specimens with equi-electron number. Second, we can prepare the specimens with the same concentration of Co varying the concentration of the other two constituent atoms. One of the main features of the CPA analysis in the Fe-Co-Ni may be the conspicuous variation of the magnatic moment of Co in the series of specimens with constant Co concentration. Since the magnetic moment of Co in a Fe-Co-Ni alloy can almost uniquely be determined from the diffuse scattering cross section of polarized neutrons and the bulk magnetization, we can directly compare the results of CPA calculation with those of experiment.

Because there exists a contingent condition that the coherent nuclear scattering amplitudes of Fe and Ni, b_{Fe} and b_{Ni}, are nearly equal, the difference cross section is expressed as,

$$\Delta\left(\frac{d\sigma}{d\Omega}\right) = 4\alpha[c_{Co}(b_{Ni}-b_{Co})(\bar{\mu}-\mu_{Co})+c_{Fe}(b_{Fe}-b_{Ni})(\mu_{Fe}-\bar{\mu})].$$

If b_{Fe} is exactly equal to b_{Ni}, only the first term remains and the atomic magnetic moment of Co, μ_{Co}, can be determined accurately. In the actual case of Fe-Co-Ni, b_{Fe} and b_{Ni} are slightly different, so the contribution from the second term should be estimated. But this term usually much smaller than the first term, we calculated it as a correction.

The measurements were made at room temperature by using a conventional type polarized neutron diffractometer POLTO at JRR-3. The differ-

ence cross section was obtained by flipping the spin direction of neutrons. The background noise due to multiple scattering was calculated by the computer simulation method. The magnetic moments of Co are shown in Fig. 1 arranged along the equi-electron density line and along the constant Co line.

Along the equi-electron line the experimental values of μ_{Co} increase gradually with the Co concentration rather than being constant. This fact suggests that the CPA explains the experimental results better than the RBA, because the latter predicts a constant Co moment along equi-electron line. Along the constant Co line the characteristic variation of μ_{Co} is clearly seen in the region of dilute Co concentration. Increasing the Fe concentration from Ni side, the theoretical and experimental values of μ_{Co} decrease rapidly. In the intermediate concentration range of Ni and Fe, the experimental values increase after passing a minimum, whereas the theoretical values are almost unchanged. Near the α-γ phase boundary μ_{Co} decreases again with increasing Fe concentration in both experimental and theoretical cases.

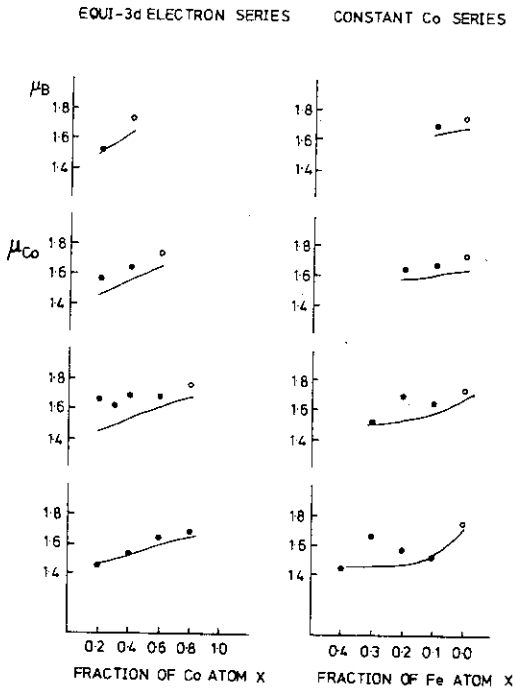

Fig. 1. Magnetic moment of Co atom. The full and open circles indicate present and other experimental results, respectively.[2,3] The solid curves are calculated.

References

† N. Schibuya, Y. Nakai, K. Yamasaki and N. Kunitomi: J. Phys. Soc. Jpn. 46(1979) 475.

1) T. Jo, H. Hasegawa and J. Kanamori: J. Phys. Soc. Jpn. 35(1973) 57.

2) J. W. Cable, E. O. Wollan and W. C. Koehler: Phys. Rev. 138(1965) A755.

3) M. F. Collins and D. A. Wheerer: Proc. Phys. Soc. 82(1963) 633.

IV1 Neutron Scattering Investigation of the Magnetic Excitations in $CoBr_2$

Hideki Yoshizawa, Koji Ubukoshi and Kinshiro Hirakawa

The Institute for Solid State Physics, the University of Tokyo

Although anomalous magnetic properties of 2D XY ferromagnets have fascinated many theorists, it is rather difficult to find experimental papers on such systems, because few materials which behave like the good 2D XY ferromagnet have been discovered so far. Recently, José et al.[1] investigated 2D XY model with symmetry-breaking field and have shown that the XY system with six-fold symmetric anisotropy may possibly have a temperature region in which the susceptibility diverges but accompanying with no spontaneous magnetizations. Thus the study of substances with the hexagonal layer structure is of great interest in finding the peculiar characteristics of the 2D XY model.

We studied the magnetic excitations in $CoBr_2$ by inelastic neutron technique and checked the two-dimensionality and the planar anisotropy.

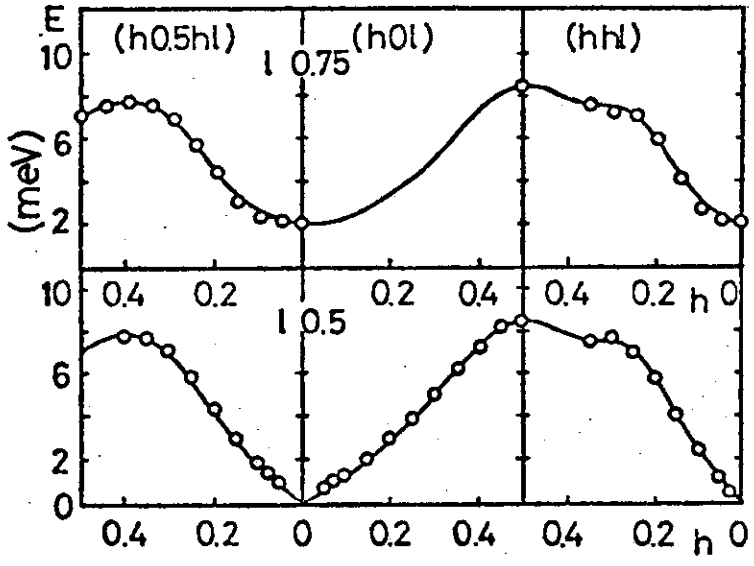

Fig. 1 The observed spin wave dispersion relation at T= 5 K, where the curves are calculated using the dispersion formula derived from the spin Hamiltonian (1).

The spin dynamics of $CoBr_2$ can be described by the following anisotropic exchange Hamiltonian with an effective spin S=1/2[2],

$$H=-\sum_{nn}(J_1S_iS_j-D_1S_{ix}S_{jx})-\sum_{nnn}(J_2S_iS_j-D_2S_{ix}S_{jx})-\sum_{third\ nn}(J_3S_iS_j-D_3S_{ix}S_{jx})$$
$$-\sum_{nn}{}'(J'S_iS_m-D'S_{ix}S_{mx}). \qquad (1)$$

By fitting the dispersion curve given by (1) to the observed spin wave energies, the coefficients are determined as follows,

intraplanar exchange J_1=2.01, J_2=0.019, J_3=-0.338 meV,

interplanar exchange J'=-0.97 meV,

planar anisotropy D_1=1.14, D'=-0.06 meV, $D_2=D_3\approx 0$.

As shown by these numerical values, $CoBr_2$ has fairy strong XY characters (D_1/J_1=0.567), but the two-dimensionality is definitely poor ($-J'/J_1$= 0.483).

Another interesting feature of $CoBr_2$ is the removal of the degeneracy of the excitation spectrum. Loveluck and Lovesey [3] have shown that the planar anisotropy removes the degeneracy between the 'in-plane' correlation and the 'out-of-plane' correlation in the case of a antiferromagnetic chain. We have pointed out, however, that in a 3D planar antiferromagnets, the easy plane anisotropy should also remove the degeneracy between the two correlation modes. In fact, we have succeeded to observed these excitations separately in $CoBr_2$, which correspond to the non-degenerate spin wave derived by Lines[2].

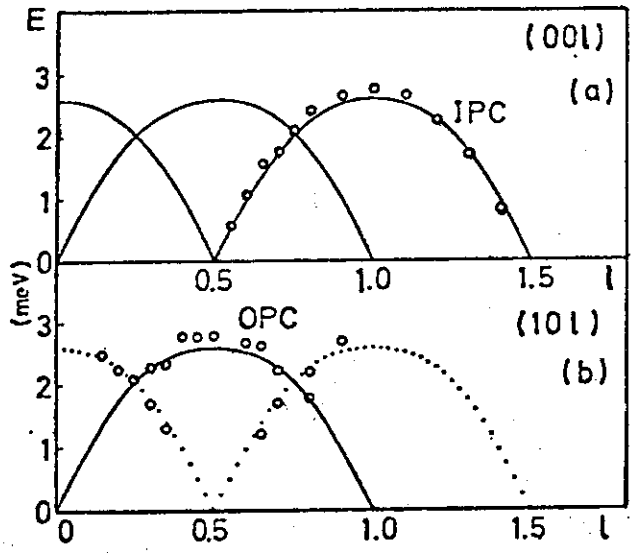

Fig. 2
The non-degenerated dispersion relations observed (a) along the [001] direction and (b) along the [101] direction.

1) J.V.José, L.P.Kadanoff, S.Kirkpatrick and D.R.Nelson: Phys. Rev. B16(1977)1217

2) M.E.Lines: Phys. Rev. 131(1963)540,546

3) J.M.Loveluck and S.W.Lovesey: J. Phys. C. 8(1975)3857

IV2

Observation of Condensation of Magnons in Quasi-2D, Planar Ferromagnet K_2CuF_4

Kinshiro Hirakawa and Hideki Yoshizawa

Institute for Solid State Physics, The University of Tokyo,
Roppongi, Minatoku, Tokyo

K_2CuF_4 is a good example of 2D,planar ferromagnet[1)2)]. It is mostly of Heisenberg type with the intraplane exchange J = 11.4K,[3)] but a little (~1%) XY-like anisotropic exchange J_A gives rise to an easy planar anisotropy in the c-plane. The inter-plane exchange J' is,however, exceedingly smaller than the J, J'/J being $6\sim8\times10^{-4}$. It undergoes a transition at T_c=6.25K below which ferromagnetic order is observed by neutron scattering.

We examined carefully the intensities of both ferromagnetic Bragg scattering as well as the off-Bragg diffuse scattering due to magnons in the direction of c*-axis as a function of magnetic field applied parallel to the easy plane. Though this system is very nearly Heisenberg type, the fluctuations at such a low temperature as $kT < (S\xi)^2 J_A$ are very nearly of XY-like , where ξ is the correlation length in the 2D plane measured by the a-unit. So, this system might give us important informations about the phase transition of the 2D XY system with S = 1/2.

As the spin wave dispersion curve along the c*-axis is so flat and the frequency is so low, one can expect a high density of magnons which is inversely proportional to the dispersion frequency. This magnon density as a function of $q_c (\equiv q)$ can be observed as a quasi-elastic diffuse scattering. The observed q dependent intensity is well explained by the XY-like (sinusoidal) dispersion curve rather than the Heisenberg one. The linear temperature dependence of the intensity and very sensitive behaviour against the applied field also confirm that the diffuse scattering is of the magnon scattering seen as Quasi -elastically. There seems no energy gap at q = 0 showing very good easy plane type as indicated by the divergent nature toward q = 0. The diffuse scattering intensity falls down remarkably by the

magnetic field. But, the field dependence of the Bragg scattering is quite striking. It decreases once as shown in Fig.1 and slowly increases again. After careful examination, it was proved that the Bragg intensity fallen off corresponds to the conventional one, i.e. it goes up at OK to the one for the full length of the spin magnetic moment $g\mu_B S$ with S = 1/2 as shown in Fig.2. Thus the difference from the zero field intensity as indicated by the shade is the anomalous extra intensity which has not been found before. We attribut it to a condensed state of magnons whose wave vectors are q and -q because at the Bragg point the resultant q should be zero. Contrary to the off-Bragg uncondensed magnons whose number is proportional to the temperature, the condensed magnons increases with desreasing temperature in the manner proportional to the square of the spontaneous magnetization. it can be erased by very weak internal fields, as is evident from the fact that for higher external field than the demagnetization field for the

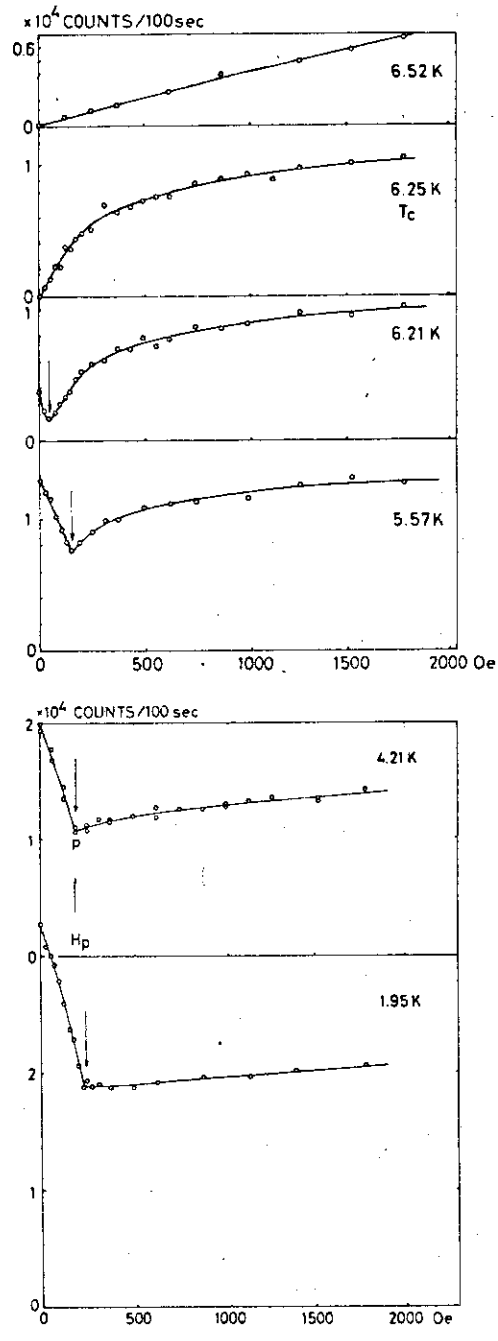

Fig. 1 A series of the field dependence of the Bragg intensity at (004) at various temperatures. The nuclear scattering has been subtracted. The arrows indicate the calculated demagnetization field which varies being proportional to $M_s(T)$ at $H_{int}=0$.

saturation, the giant fluctuation is completely erased. Below that field self-shielding by the infinite susceptibility occurs. We think that this occurence of giant fluctuation is the so-called " Stanley Kaplan transition" discussed so far. It is interesting to note that the temperature dependence of the fluctuation is very nearly the same form with the Monte Calro simulation for the 2D plane rotator model worked out recently by Miyashita et al.[4)]

(For details, see K.Hirakawa and H.Yoshizawa; J. Phys. Soc Japan 47(1979)368)

References

1) I. Yamada; J. Phys. Soc. Japan 33(1972)979

2) K. Hirakawa and H. Ikeda; ibid 35(1973)1328

3) S. Funahashi, F. Moussa and M. Steiner; Solid State Comm. 18(1976)433

4) S. Miyashita, H. Nishimori, A. Kuroda, and M. Suzuki; Progr. Theor. Phys. 60(1978)1669

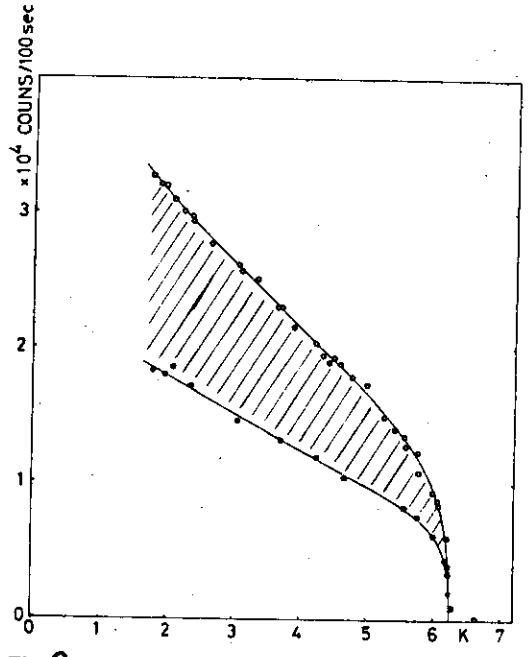

Fig. 2 Temperature dependence of the Bragg intensity (open circles) and the Bragg intensity (filled circles) obtained by picking up the point *p* in Fig. 5. The latter corresponds to the conventional type of Bragg scattering.

IV3 Fe-Fe Interaction in $KFeS_2$ — a Linear Chain Antiferromagnet and a Spin Analogue of Two Iron Ferredoxins — by Neutron Inelastic Scattering

Masakazu Nishi, Yuji Ito and Satoru Funahashi*
Institute for Solid State Physics, University of Tokyo,
*Physics Division, JAERI

Following the previous magnetic structure determination of $KFeS_2$, a spin analogue compound for the active sites of ferredoxins[1], we have carried out measurements of the spin wave excitation of this compound in order to study the Fe-Fe interaction specifically. Experiments were performed with using PANSI and ND-1 triple axis spectrometer of ISSP as well as CTNS triple axis spectrometer of JAERI, all situated at JRR-2 reactor. Measurements were done with the constant-Q mode of $(\zeta,0,1)$, $(0,\zeta,1)$, $(0,0,1+\zeta)$ and $(0,0,3+\zeta)$ using various incident neutron energies at temperatures 77K and 150K. In fig.1 examples of the observed spin wave intensities at $\zeta=\pm0.08$ along c*-axis are shown. The apparent peak shifts towards the higher energy position as the scattering vecter Q increases. This is due to the resolution effect convoluting the large resolution elipsoid with the steep spin wave dispersion surface along c*-axis indicative of the strongly coupled intra-chain iron atoms. Calculation of neutron intensity with the assumed dispersion relation shows that the peak position observed at larger Q value is closer to the true spin wave energy than that measured at smaller Q.

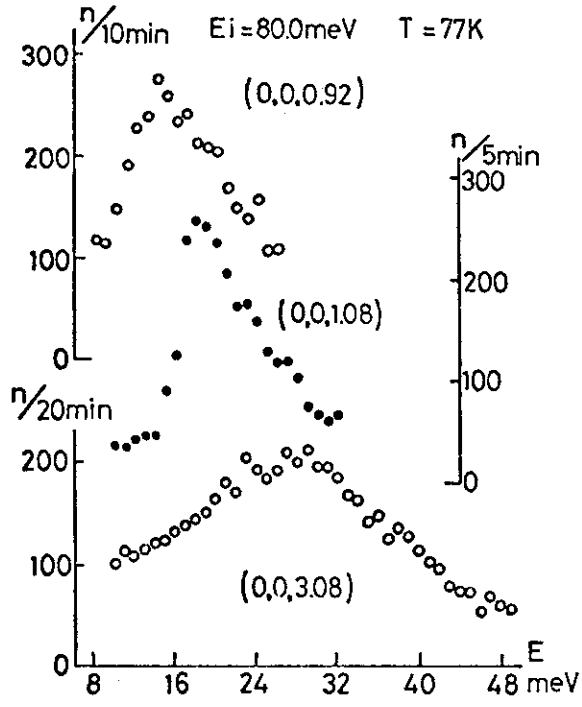

Fig.1

As a preliminary step, the observed dispersion relation was fitted with the Heisenberg Hamiltonian with few

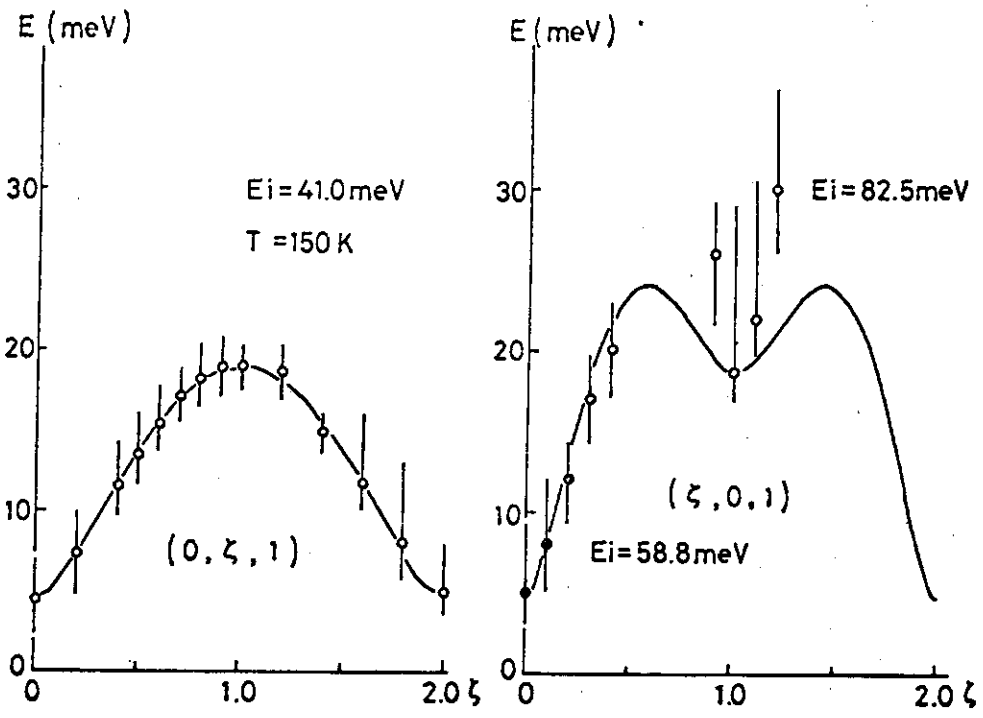

Fig.2

exchange parameters for the interaction between iron atoms. For this, the fitting parameters were restricted to the coupling constants between the intra-chain nearest neighbor(n.n.) iron atoms, J_0, inter-chain exchange between n.n. iron atoms along the a-axis, J_2, that of inter-chain n.n. iron atoms along the face center of the a-b plane, J_4 and the energy of the anisotropy field, $g\mu_B H_A$.
In fig.2 and fig.3 the measured dispersion relations along the three principal directins are shown together with the curves given by

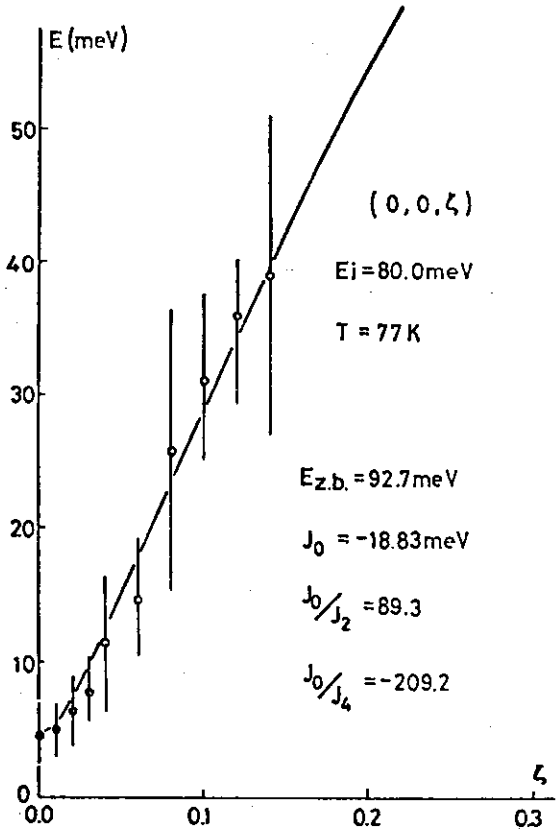

Fig.3

solid lines fitting by the least square procedures. They were determined using the above mentioned parameters by this fitting as J_0=-18.83 meV,J_2=-0.22 meV,J_4=0.09 meV and $g\mu_B H_A$= -0.12 meV. The ratio of the intra-chain coupling constant to that of the inter-chain is about hundred indicating a one-dimentional character of interaction. The fitting was not so satisfactory along the a*-axis. Better agreement could be obtained by taking into accounts the proper resolution correction and also by increasing the number of coupling constants. The obtained value of intra-chain n.n. coupling constant for $KFeS_2$,J_0=152 cm^{-1} should be compared with that of the oxidized spinach ferredoxin,J= 183 cm^{-1} determined from the magnetic susceptibility measurements[2]. Good agreement of these values confirms $KFeS_2$ as being a spin analogue compound for the active site of the two iron oxidized ferredoxins,and lends support for the similar electronic structure for the FeS_2 cluster of these two substances.

To clarify the electronic structure of $KFeS_2$ further,the magnetic form factor of iron atoms is now tried to be extracted out from the measured integrated intensities of observed spin wave excitations as was done in ref.3).

References

1) M.Nishi and Y.Ito : Solid State Commun. 30 (1979) 571.
2) G.Palmer et al : Biochim.Biophys.Acta, 245 (1971) 201.
3) S.K.Sinha et al : Phys.Rev.B15 (1976) 1415.

IV4 Magnetic Excitations in TbZn

Yoshikazu Hamaguchi, Hiroshi Betsuyaku and Satoru Funahashi

Physics Division, Japan Atomic Energy Research Institute

The magnetic excitations in TbZn were measured at several temperatures by using the triple-axis spectrometers in JRR-2. A single crystal was grown by the Bridgman method and cut into the shape of 30*10*10 mm. Incident neutron energies of 14.8, 24 and 35 meV were chosen suitable for the expected transfer energy and resolution. Measurements were made with constant-Q mode with fixed incident energy. Dispersion curves observed at 10K are shown in Fig. 1. At the Γ point the energy gap is 2 meV and the dispersion law is initially quadratic in scattering vector q and isotropic. At larger values of q the dispersion curve separate in two branches. Upper branch shows the usual behaviour of the ferromagnet coupled with long range oscillatory exchange interactions and the single-ion anisotropy. The intensity of both branches is almost the same. Temperature dependence of the energy spectrum was studied at both Γ and X points. At the Γ point the energy gap decreases linearly with **increasing** temperature and tends to zero at T_r (about 60K in our sample). At the X point the intensity of upper branch decreases almost linearly with increasing temperature and tends to zero at T_r, but the energy decreases slightly. The energy of the lower branch remains up to T_r but the intensity increases with increasing temperature. Near T_r sudden change of the energy spectrum has been observed. T_r is a spin-rotation temperature.

The dispersion relations at 78K are shown in Fig. 2. Due to the broadening of the energy line width an energy accuracy is not so good in the high energy region. They were analyzed within the dynamical susceptibility formalism of Buyers et al[1]. For the CEF (crystalline electric field) Hamiltonian we used the values of W=1.0 K/atom and x=-0.30 which

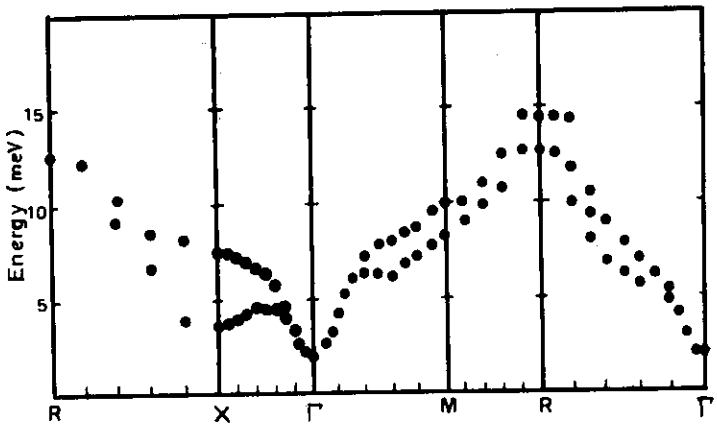

Fig.1: Dispersion curves for TbZn at 10K

were determined from T_r [2]. Magneto-elastic term and quadrupolar couplings were neglected for simplisity. The single-ion Hamiltonian was diagonalised self-consistentently to obtain the eigenvalues and the eigenvectors as a function of temperature. The solid curves drawn in Fig. 2 were obtained by using the most probable J(q), the Fourier transform of which gives the interion interactions. A slight disagreement between J(q=0) (0.50 meV) with J(0) deduced from T_c (0.63 meV) is due to neglecting the quadrupolar couplings. We calculated the dispersion relations at 10K under the assumption that the interion interaction and the CEF parameters were not strongly modilied by spin rotation, but the agreement with the experimental data was poor. At 10K we observed several very weak incommensurate magnetic peaks besides the fundamental ones. Some of them are consistent with the presence of the small $TbZn_2$ single-crystal inclusions, oriented with thier C axis along the 001 of TbZn. Some modifications of the simple ferromagnetic structure may be the origin of unusual dispersion relations below T_r.

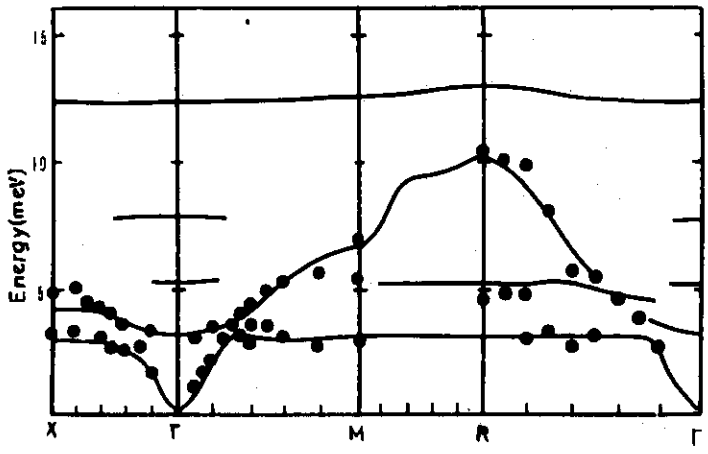

Fig.2: Dispersion curves at 78K. Theoretical curves are drawn with solid lines as explained in the text.

In conclusion the CEF parameters obtained from T_r and oscillatory Heisenberg exchange interactions can explain the magnetic excitations in TbZn above T_r fairly well, but it should be necessary to introdece additional terms to explain those below T_r. The behaviour of magnetic excitations in TbZn is not similar to that in HoZn [1~3].

References

1) W. J. Buyers, T. M. Holen and A. Perreault, Phys. Rev. B 11 (1975) 266.
2) P. Morin, J. Pierre and J. Chaussy, Phys. stat. sol.(a) 24 (1974) 425.
3) J. Pierre, D. Schmitt, P. Motin and B. Hennion, J.Phys.F 7 (1977) 1965.
4) B. Hennion and J. Pierre, J.Phys.F 8 (1978) 2617.
5) P. Morin, J. Rouchy and E. du Tremolet de Lacheisserie, Phys. Rev. B 16 (1977) 3182.

IV5 Spin Wave Excitations in Fe_2P

S. Komura, K. Tajima*, H. Fujii, Y. Ishikawa* and T. Okamoto

Faculty of Integrated Arts and Sciences, Hiroshima University, Hiroshima, Japan * Department of Physics, Faculty of Sciences, Tohoku University, Sendai, Japan

Fe_2P becomes ferromagnetic below Tc = 209 K by the first order transition and has a large magnetic anisotropy with easy axis along the c-axis [1]. The crystal structure is of hexagonal C22 type with two non-equivalent Fe sites; tetrahedral Fe_I is surrounded by four P atoms and pyramidal Fe_{II} by five P atoms, both tetrahedrons and pyramids forming canal pairs along the c-axis.

A polarized neutron diffraction study [3] has shown that magnetic moment of Fe_I is 0.9 μ_B and that of Fe_{II} 1.7 μ_B and that the magnetic form factor of Fe_I is very close to that of a free iron atom and that of Fe_{II} close to Fe^{4+}. A recent neutron diffraction study has revealed that an incommensurate spin structure with propagation vector along [110] is established in a 3% Mn substituted Fe_2P.

For the purpose of clarifying the mechanism of the first order transition as well as the substantial change of the magnetic structure by the Mn impurities, we have measured the spin wave dispersion relations with a triple axis spectrometer TUNS using 13.7 meV incident neutron energy. The spin wave and phonon dispersion relations along [100] = a^*-axis, [110] = b^*-axis and [001] = c^*-axis were obtained for several temperatures from 77 K to above Tc. The results for [001] and [100] are shown in Fig. 1, the latter being very similar to those for [110].

The phonon dispersion relations are temperature independent, whereas the spin wave dispersion relations are strongly temperature dependent, especially for [100] and [110]. The spin wave energies along [100] and [110] are not only much less than those along [001], but heavily softened with increasing temperature. It is interesting to note that even at 227 K which is above Tc over-damped spin wave excitations were observed along [100] and [110] with finite but very small excitation energies of the order of 0.2 meV.

The above experimental results strongly suggest that the configurations of one-dimensional ferromagnetic chains along [001] are little affected by temperature and would persist even above Tc, whereas the two-dimensional ferromagnetic order in the (001) plane is perturbed significantly by

temperature below Tc and it collapses the three-dimensional ferromagnetic order above Tc.

It seems that the magnetic interactions in the (001) plane is rather favourable for the antiferromagnetic (presumably incommensurate) spin ordering and that the ferromagnetism is realized by the strong ferromagnetic interactions along [001]. This point of view would consistently explain the first order transition of Fe_2P as well as the experimental observations that an addition of small amount of Mn impurities in Fe_2P stabilized the incommensurate structure with the propagation vector along [110] as a result of weakening the ferromagnetic interaction along [001]. Further experiments are however required to verify this conjecture.

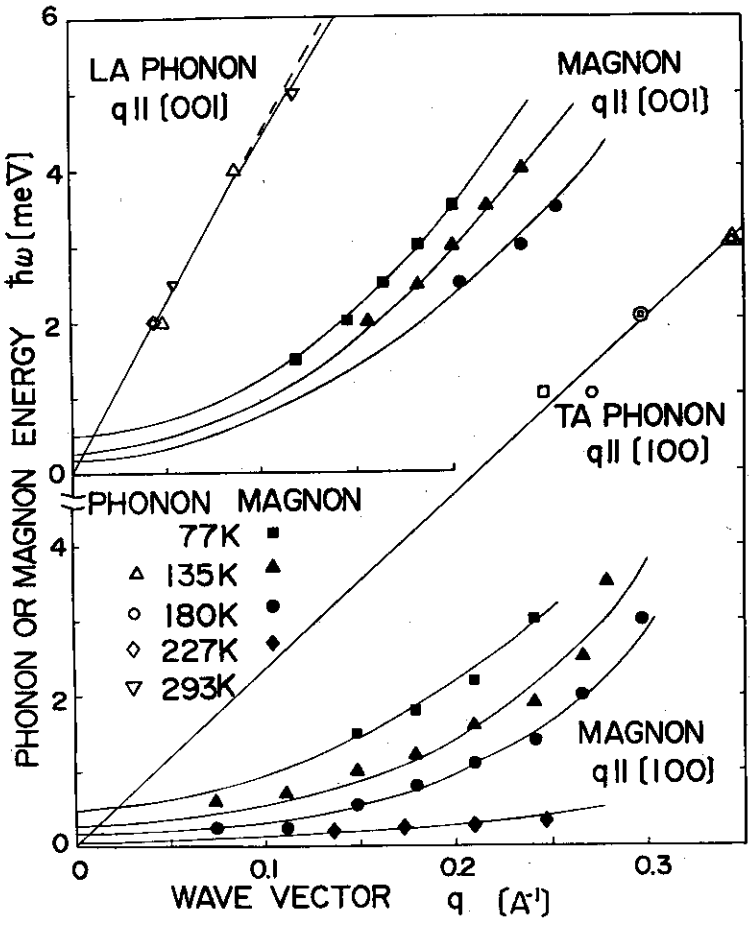

Fig. 1 Spin wave and phonon dispersion relations along [001] and [100] in Fe_2P at various temperatures.

References

[1] H. Fujii, T. Hōkabe, T.Kamigaichi and T. Okamoto, J. Phys. Soc. Japan 43 (1973) 41

[2] B. Carlsson. M. Gölin and S. Rundgvist, J. Solid State Chem. 8 (1973) 57

[3] H. Fujii, S. Komura, T. Takeda, T. Okamoto, Y. Ito and J. Akimitsu, J. Phys. Soc. Japan 46 (1979) 1616

IV6 Spin Wave Scattering Studies of Ferro to Spiral Transition in MnP

Keisuke Tajima, Hisashi Obara and Yoshikazu Ishikawa
Department of Physics, Tohoku University

Manganese phosphide MnP is a ferromagnetic intermetallic compound below 291K but it transforms into a double spiral state at T_s=47K[1-5]. The crystal structure is of a distorted orthorhombic type (a>b>c) and the c-axis is the direction of the easy magnetization in the ferromagnetic state. The spiral structure below 47K was investigated in detail by neutron diffraction [2-4] and it has been found that the spins rotate in the b-c plane with a propagation vector $0.117(\frac{2\pi}{a})$ along the a-axis. The magnetic phase diagram under magnetic field was also determined by neutron deffractions [4,6] and magnetization measurements [5].

In order to investigate the mechanism of the ferro-spiral transition in MnP, the neutron spin wave scattering experiments were performed with a triple axis spectrometer (TUNS). Spin wave dispersions have been measured along the a- and b-axis mainly around the (200) reciprocal lattice point at the several temperatures below and above T_s and results obtained are shown in Fig.1. In the ferromagnetic state, the dispersion in the b-axis exhibits a quadratic relation E_0+Dq^2 which changes little with temperature. The dispersion in the a-axis, however, shows a strong temperature dependence. At 77K, which is 30K above T_s, dispersion curve has a minimum at $\zeta\sim0.1$ and this minimum is accentuated at 50K. In the spiral state at 38K, the Brillouin zone center splits into two positions, $Q=\pm0.117(\frac{2\pi}{a})$ and the dispersion curve becomes linear at small q region. The dotted curve with square marks in Fig.1 is the dispersion curve from the Brillouin zone center of $Q=-0.117(\frac{2\pi}{a})$.

The analysis has been made based on the Heisenberg model by assuming a single spiral structure. The Hamiltonian is given by

$$H = -2\sum_{i>j} J_{ij}S_iS_J + D_1\sum_i S_{iz}^2 + D_2\sum_i(S_{ix}^2 - S_{iy}^2), \qquad (1)$$

where J_{ij} is the effective inter planer exchange interaction parameter and D_1 and D_2 are the axial and inplane one ion anisotropy constants respectively. The spin wave dispersion relation was obtained by diagonalizing the eq.(1),

$$h\omega = 2S\{[J(0)-J(q)-4D_2][J(0)-J(q)+D_1-2D_2]\}^{1/2}, \qquad (2)$$

(ferromagnetic state)

or,

$$h\omega = 2S\{[J(Q)-\tfrac{1}{2}J(Q-q)-\tfrac{1}{2}J(Q+q)][J(Q)-J(q)+D_1]\}^{1/2}, \qquad (3)$$

(spiral state)

where J(q) is the Fourier transform of J_{ij}. D_2 is neglected in the calculating process of the eq.(3). The energy gap at q=0 in the ferromagnetic state at 77K was estimated to be (0.5±0.3)meV. The exchange parameters were determined by a least squares fitting of the eqs.(2) or (3) to the experimental data of 150K, 77K and 38K. Only a nearest interplaner parameter was taken into account for the analysis of the dispersion curve along the b-axis, whereas for the a-axis, the nearest and 2nd nearest exchange parameters J_1^a and J_2^a respectively were found to be sufficient to reproduce the experimental data in the measured q range (60% of the Brillouin zone boundary). The exchange parameter along the b-axis was found to be almost constant through the transition. The temperature dependence of the exchange parameters along the a-axis is displayed in Fig.2. Positive J_1^a is almost constant between 38K and 150K, while negative J_2^a decreases smoothly by increasing temperature. In the Heisenberg model, the spiral structure becomes stable when $J_1^a < -4J_2^a$; $|J_2^a| > J_{20}^a = 2.6$meV. This relation hold below T_s as is marked by a chained line in Fig.2. From this analysis, we can make a conjecture that the free energy of the ferromagnetic state of MnP is quite close to that of the spiral state and the transition is caused by small change of J_2^a.

References

1) E. Huber and D. Ridgley, Phys. Rev. 135 (1964) A1033
2) J. Forsyth, S. Pickart and J. Brown, Proc. Phys. Soc. 88 (1966) 333
3) G. Felcher, J. appl. Phys. 37 (1965) 1056
4) H. Obara, Master Thesis, Tohoku Univ. March(1979)
   H. Obara, Y. Endoh, Y. Ishikawa and T. Komatsubara, to be published.
5) T. Komatsubara, T. Suzuki and E. Hirahara, J. Phys. Soc. Japan 26 (1969) 208
6) Y. Ishikawa, T. Komatsubara and E. Hirahara, Phys. Rev. Lett. 23 (1969) 532

Fig.1. Spin wave dispersion relations along the a- and b-axis at various temperatures below and above T_s. Solid lines are the results of a least squares fitting by using eqs.(2) or (3) except for 50K. Dotted line indicates the dispersion curve at 38K arising from another Brillouin zone. ζ is the reduced wave vector. The arrow indicates the zone center in the spiral state.

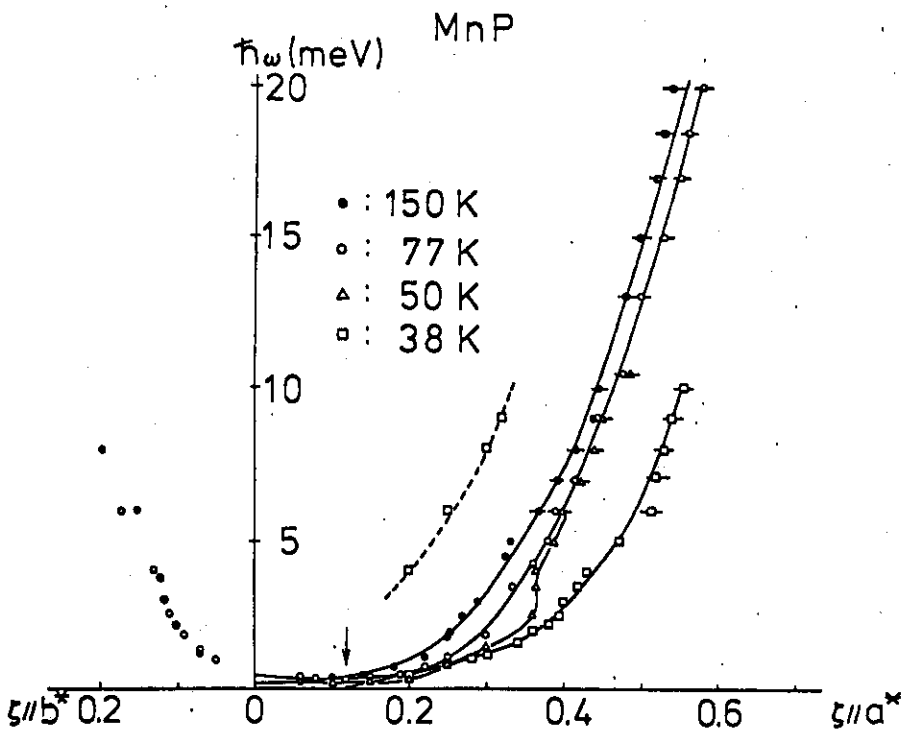

Fig.2. Temperature dependence of the interplaner exchange parameters along the a-axis. Chained line indicates the boundary of ferro-spiral transition for J_2^a. See text.

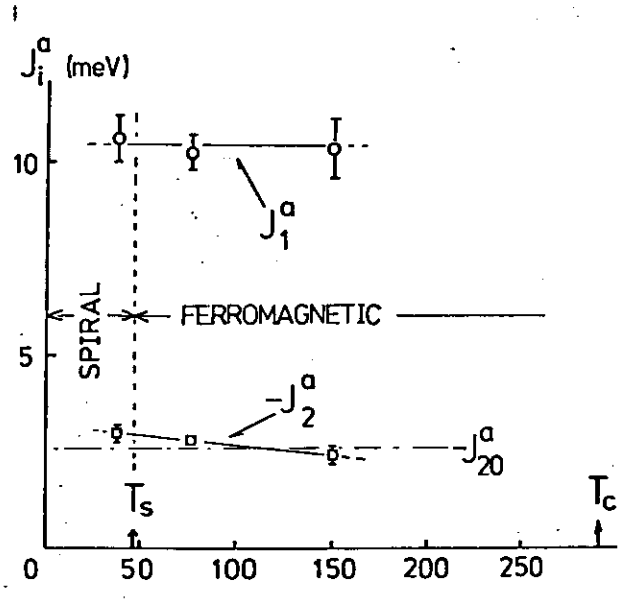

IV7

Neutron Scattering from FeSi

M. Kohgi and Y. Ishikawa
Department of Physics, Tohoku University

1. Introduction The intermetallic compound FeSi is known as a material which exhibits the anomalous behaviors in magnetic and thermal properties; a pronounced maximum of the susceptibility in the neighborhood of 500°K and an anomaly of the specific heat near 280°K[1], in spite of lack of long range magnetic ordering[2]. Recently, Takahashi and Moriya[3] have proposed a model which takes account of the effect of spin fluctuations in a nearly ferromagnetic semiconductor. According to the theory, the amplitude of local spin density increases strongly with temperature up to saturation where the spin fluctuations may be regarded as a set of local moments interacting with each other.

The purpose of this work is to explore any evidence of the existence of the local magnetic moment in FeSi at high temperatures by means of neutron inelastic scattering techniques.

2. Experimental results The neutron scattering experiments were carried out on a triple axis spectrometer TUNS at JRR-2. The sample is a large single crystal (∿20mmϕ×40mm) made by Czochralski method at Institute for Iron, Steel and Other Metals, Tohoku Univ. The incoming neutron energy was fixed at 40mev.

In order to see the temperature dependence of the scattering, constant-K scans were carefully performed at T=77°K, 300°K and 600°K with K=(0.6, 0.6, 0), where the contribution from phonon scattering is negligible up to the energy transfer of E=18mev. The observed spectra are composed of a peak around E=0 and a nearly constant background. The profiles of the peaks agree with that obtained with the same scan for a vanadium standard sample within the experimental errors at all the experimental temperatures. The temperature dependence of the intensity and the half width of the peak and the magnitude of the background are shown in Fig.1 by open circles, triangles and squares, respectively. The intensity of the nuclear incoherent scattering component at 0°K of FeSi estimated from the vanadium measurement is also shown in the figure by an arrow with an error bar. Note that the observed peak intensity at 77°K agrees with the calculated nuclear incoherent component within the experimental errors. These facts indicate that the central peaks of the constant-K scans come almost only from the nuclear incoherent elastic scattering.

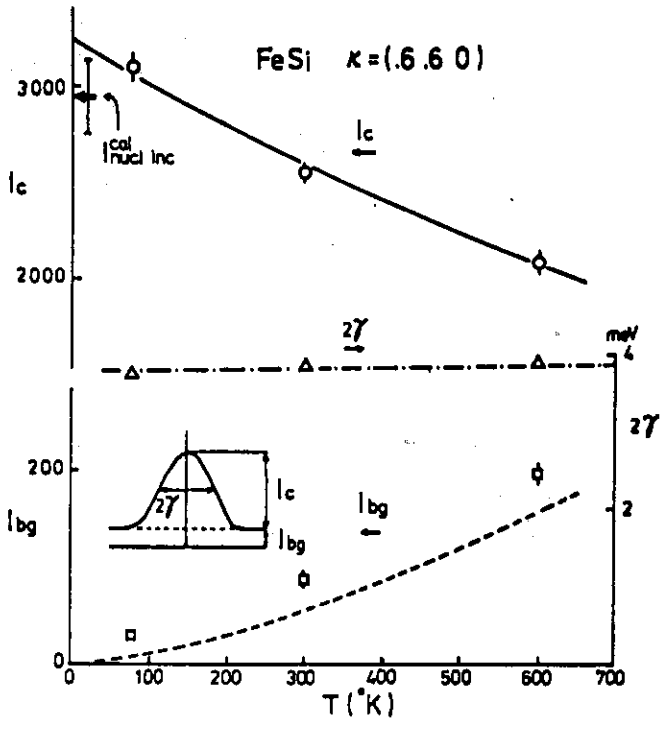

Fig.1. Temperature dependence of peak intensity (circles), half width (triangles) and background (squares) for the constant-K scans with K=(0.6, 0.6, 0). The solid line shows the best fit Debye-Waller factor to the peak intensities. The broken line shows the calculated multi-phonon contribution to the background at E=0.

Scans along the [001], [110] and [111] directions around the (110) reciprocal lattice point with E=0 were performed at T=300°K. Their intensities are constant within the experimental errors except near (110) and the zone boundaries where the strong contamination of the Bragg reflections exists. Therefore it can be said that there is no evidence of the wavelength dependence of the scattering along the principal axes at least at T=300°K.

3. Discussion and conclusion As the high temperature susceptibility of FeSi obeys the Curie-Weis law with $p_{eff}=2.1\mu_B$ per Fe and $\Theta_p=-340°K$, it is reasonable to expect that the "induced local moment" has the magnitude of order of S=1/2. The integrated intensity of paramagnetic scattering in this case is evaluated to be about 3.5 times that of the nuclear incoherent elastic scattering of FeSi.

Our experimentsl results has shown, however, that the intensity of the incoherent elastic peak rather decrease with increasing temperature up to 600°K as shown in Fig. 1. The decrease in intensity can be explained only by the nuclear incoherent scattering component, if we assume the Debye temperature Θ_D of Fe atom is 70°K. The solid line in Fig.1 shows that the calculated Debye-Waller facter using this parameter. We also estimated the contribution of the multi-phonon scattering to the background by the Gaussian

approximation[4] with Θ_D=70°K and using the observed peak intensity. The broken line in Fig.1 is calculated in this way, which agrees reasonably with the observation. Therefore it may safely be said that there is no appreciable contribution of paramagnetic scattering to the observed scattering peak, in another words, in order that the observed spectrum contains the paramagnetic scattering from the local moment system with S=1/2, the energy spread of the scattering should exceed 200mev, which would be too large for the local moment system with the magnetic interaction of order of 340°K.

In conclusion our experimental results suggest that the paramagnetic state above 600°K in FeSi cannot be interpretated in terms of the simple localized spin model with S=1/2, not in accordance with what Takahashi and Moriya has anticipated in their theory.

References

1) V. Jaccarino, G.K. Wertheim, J.H. Wernick, L.R. Walker and S. Arajs: Phys. Rev. 160 (1967) 476.
2) H. Watanabe, H. Yamamoto and K. Ito: J. Phys. Soc. Japan 18 (1963) 995.
3) Y. Takahashi and T. Moriya: J. Phys. Soc. Japan 46 (1979) 1451.
4) W. Marshall and S. Lovesey: Theory of Thermal Neutron Scattering (Oxford University Press. 1971) p.95.

IV8 Magnetic Excitations in An Amorphous Invar Alloy $Fe_{86}B_{14}$

Y. Ishikawa, K. Yamada, K. Tajima and K. Fukamichi*
Physics Department, Tohoku University and *The Research Institute for Iron, Steel and Other Metals, Tohoku University Sendai

Amorphous ferromagnetic alloys $Fe_{1-x}B_x$ have been reported to exhibit the Invar properties[1]; the thermal expansion becomes very small below the Curie temperature. Previous neutron scattering works have revealed that the spin dynamics of the crystalline Invar alloys, $Fe_{65}Ni_{35}$ and Fe_3Pt are common and are quite anomalous compared with non Invar ferromagnetic alloys as $Fe_{50}Ni_{50}$ or Pd_2MnSn[2,3]. The temperature dependence of the magnetization is much faster than what is expected from the observed spin wave excitations by neutron scattering, instead of the fact that no other excitations have been detected. Therefore the presence of the "hidden excitation" was anticipated[2,3]. The magnon line width Γ varies with wave vector q and temperature T as $\Gamma \propto q^2 T^\alpha$ with $\alpha<1$, in contrast with the non Invar alloys where a relation $\Gamma \propto q^4 T^2$ predicted by the classical spin wave theory really holds[2,3]. We have then anticipated that these anomalous dynamical properties would be closely related with the Invar mechanism.

In order to get a further conclusive result on this point, we extended our studies to the amorphous Invar alloys, and the spin wave excitations in $Fe_{1-x}B_x$ have been measured by neutron scattering.

The sample used in the experiment was prepared by splat cooling technique with 95% enriched B^{11} to reduce the neutron absorption. A bundle of ribbons 1-2mm wide were encased in a thin aluminum cylindrical tube 20mm in diameter and 30mm in height and the neutron scattering experiments were carried out on a triple axis spectrometer TUNS at JRR-2, Tokai. Pyrolytic graphite (002) crystals were used as both monochromator and analyzer and the scattering around the (0, 0, 0) reciprocal lattice point was observed using an incident neutron energy of 14.5mev and 60'-10'-10'-30' collimation. The sample has a norminal composition of $Fe_{86}B_{14}$ with the Curie temperature Tc=570K.

Examples of energy scans at $q=0.08\text{Å}^{-1}$ at different temperatures are displayed in Fig.1, which shows that rather well defined spin waves persist even at T/Tc=0.8. After making correction for instrumental resolution (though it is still in a stage of preliminary calculations), a quadratic

relation $\hbar\omega_q = Dswq^2$ was found to hold to $q=0.12\mathring{A}^{-1}$. In Fig.2 is shown the temperature dependence of the spin wave stiffness constant $D_{sw}(T)$ which was found to obey a relation to T/Tc=0.8

$$D_{sw}(T)=D_0(1-a(T/Tc)^{5/2}) \qquad (1)$$

with $D_0=122\pm4$mevA^2 and $a=0.74\pm0.05$. The value of D_0 obtained is nearly in agreement with that obtained for a similar amorphous alloy $Fe_{83}B_{16.5}Si_{0.5}$ ($D=125$mevA^2)[4].

Previous magnetic studies of this alloy system have also shown that the spin wave stiffness constant D_M obtained from the magnetization measurements is about 65mevA^2 for this composition[5]. Therefore the descrepancy between D_{sw} and D_M is quite significant for this material.

It has been reported that in some ferromagnetic amorphous alloys (Co_4P, $Fe_{75}P_{15}C_{10}$, $(Fe_{93}M_0)_{80}B_{10}P_{10}$) D_M is smaller than D_{sw}[6,7], but there is also a material for which D_M nearly accords with D_{sw} and no conclusive interpretation has ever been proposed on this phenomenon[8]. It is noted, however, that no amorphous alloys cited above show such a large descrepancy in D by two methods as found in this sample and we may safely conclude that the descrepancy is at least partly due to the Invar mechanism. We have also no data to prove that the first class of amorphous alloys mentioned above have no Invar properties. In this connection the study of the magnetic excitations in non Invar alloys is now highly required.

References

1) K. Fukamichi, H. Hiroyoshi, M. Kikuchi and T. Masumoto, Journ. Mag. Magnetic Materials 10 (1979) 294.
2) Y. Ishikawa, S. Onodera and K. Tajima, ibid 183.
3) Y. Ishikawa, Proc. International Conf. Neutron Scattering and Magnetism (Julich) September (1979).
4) J.J. Rhyne, J.W. Lynn, F.E. Luborsky and J.L. Walter, J. Appl. Phys. 50 (1979) 1583
5) R. Hasegawa and R. Ray, Phys. Rev. B20 (1979) 211
6) J.D. Axe, G. Shirane, T. Mizoguchi and K. Yamaguchi, Phys. Rev. 15 (1972) 2763
7) H.A. Mook, N. Wakabayashi and D. Pan, Phys. Rev. Letters 34 (1975) 1021
8) R.J. Birgeneau, J.A. Tarvin, G. Shirane, E.M. Gorgy, R.C. Sherwood, H.S. Chen and C.L. Chien, Phys. Rev. B18 (1978) 2192

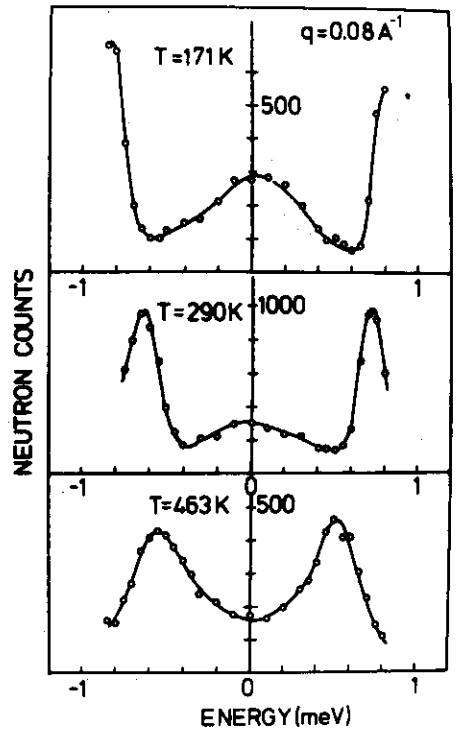

Fig.1. Energy scans of $Fe_{86}B_{14}$ at q=0.08Å^{-1} and at different temperatures.

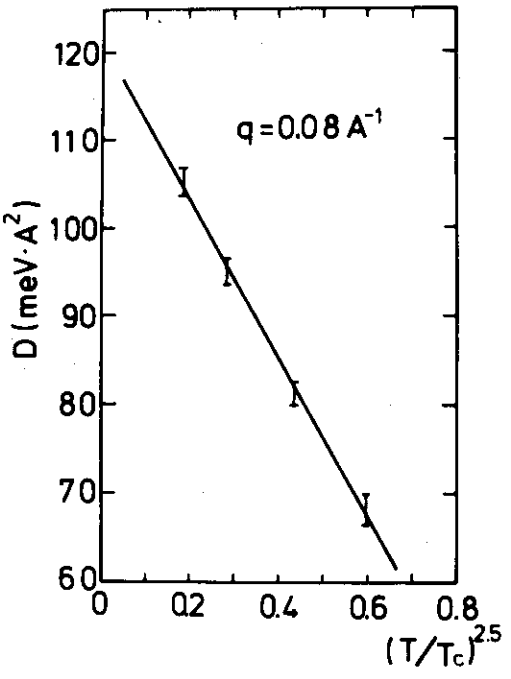

Fig.2. Temperature dependence of spin wave stiffness constant plotted against $T^{5/2}$.

IV9 SPIN WAVE EXCITATIONS OF AMORPHOUS FERROMAGNET $Fe_{40}Ni_{40}P_{14}B_6$

Kiyoichiro Motoya*, Masakazu Nishi*, Yuji Ito* and
Tadashi Mizoguchi**

*Institute for Solid State Physics, The University of Tokyo
**Department of Physics, Gakushuin University

Spin-wave excitations in an amorphous ferromagnetic metal $Fe_{40}Ni_{40}P_{14}B_6$ were measured by means of a pseudorandom spin modulated time of flight neutron scattering technique.

The amorphous metal ribbons ≈2mm wide, ≈30mm long and ≈40μm thick were arranged to make a square sheet and then 73 sheets were piled up. The total sample thickness ≈3mm was determined taking account of the large thermal neutron absorption cross section of ^{10}B. The sample sheets were mounted in a frame, the effective area of which was 20mm × 20mm. The measurements were made using PANSI spectrometer[1] installed at JRR-2. The experimental arrangement is shown in Fig.1. A monochromatic unpolarized beam reflected by a P.G. monochrometer was successively reflected and polarized by a Heusler polarizer. This "double monochrometer" arrangement was necessary for the present measurements because of the small scattering angle. The neutron spin polarization was pseudorandomly reversed by a Mezei spin flipper which was driven by a transistorized current source. The length of the pseudorandom code was chosen as 31 units and the unit pulse duration was 5 μsec. The neutron counting time was 1 μsec. The magnetic field of 3 kOe was applied to the sample parallel to the scattering vector. In this configuration, either the spin-wave creation or the spin-wave annihilation scattering process can be observed depending upon the neutron polarization

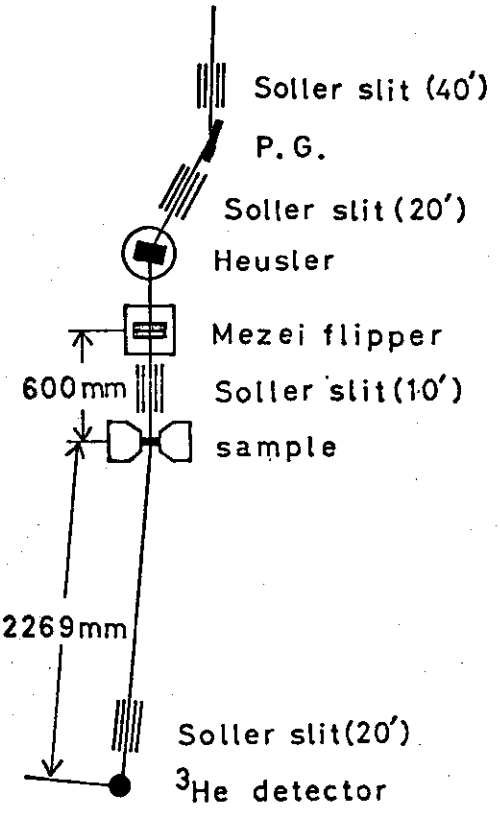

Fig.1. Sketch of the experimental arrangement.

direction[2]. The influence of various back ground noises was highly reduced by the cross correlation technique. For a fixed incident neutron energy and a scattering angle, the data were collected over about 20 hours. Measurements were made at room temperature with the incident neutron energy of 13.7,16.9,20.5,31.4,41.7 and 56.8 meV with the scattering angle 2θs being fixed at 0.55° or at 0.95°. Figure 2 shows the cross correlation value of the measurement taken with Ei=31.4 meV and 2θs=0.95°.

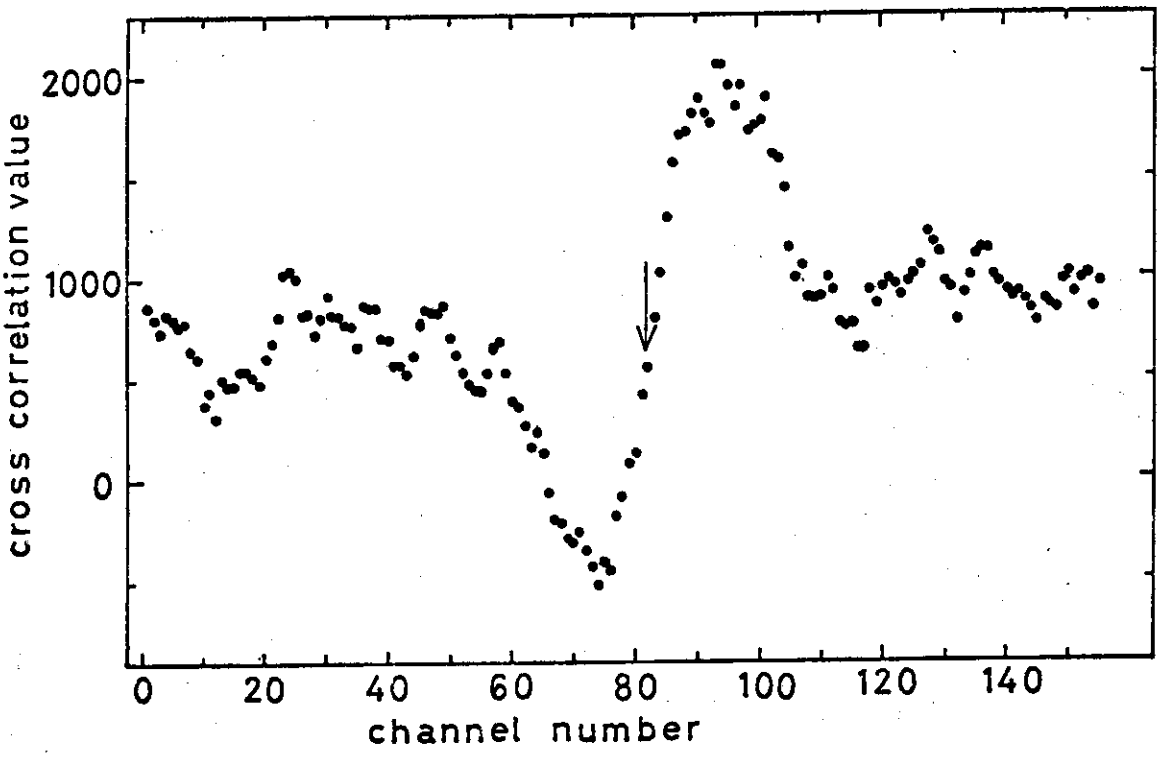

Fig.2. Cross correlated spectrum of the measurement taken with Ei=31.4 meV and 2θs=0.95°. The arrow indicates the time channel corresponds to the elastic scattering.

Positive and negative cross correlation value correspond to the magnon creation (flipper ON) and magnon annihilation (flipper OFF) process, respectively.

The observed spin-wave dispersion is shown in Fig.3, in which open circles and solid circles are the points obtained from the spin-wave annihilation and spin-wave creation process, respectively. The curve represents the best fit equation

$$E = \Delta + D\,q^2 \qquad \text{with}$$

$D = 111$ meV·A^2 and $\Delta = 0.044$ meV.

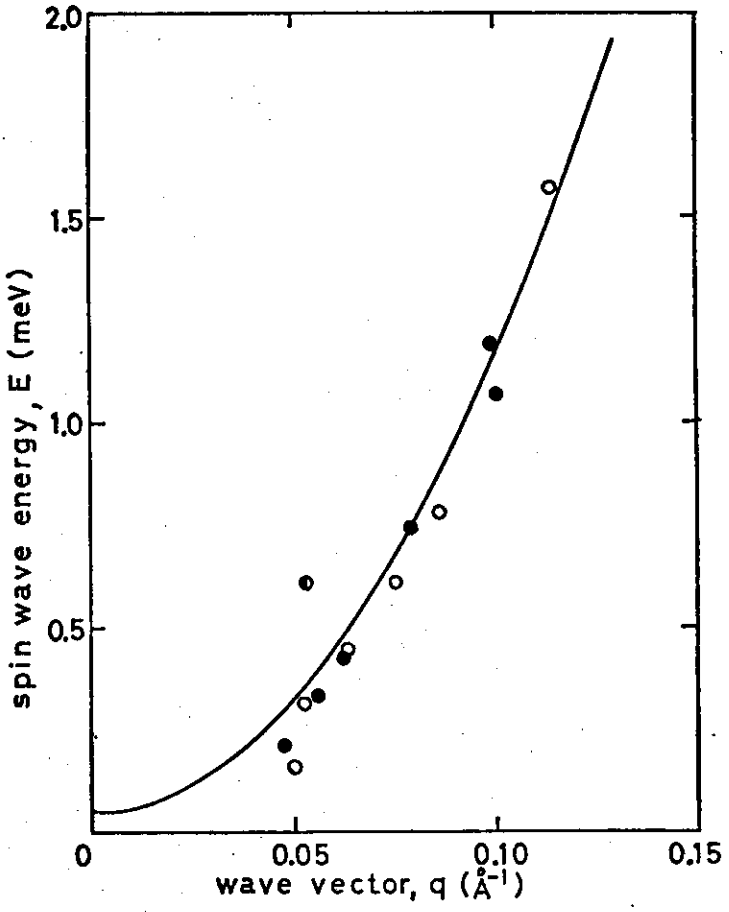

Fig.3. Spin-wave dispersion of amorphous $Fe_{40}Ni_{40}P_{14}B_6$ at room temperature. Open circles and solid circles are the points obtained from the spin-wave annihilation and spin-wave creation process, respectively.

References

1) Y.Ito, S.Takahashi, Y.Kawamura, K.Motoya and M.Nishi, nukleonika 24 (1979) 699

2) E.J.Samuelsen, T.Riste and O.Steinsvoll, Phys.Letters 6 (1963) 47

V1 The Neutron Diffraction Study of Liquid GeTe and As_2Te_3

O. Uemura, M. Tsushima, T. Kamikawa and T. Satow

Faculty of Science, Yamagata University

The radial distribution analyses for GeTe and As_2Te_3 are made at temperature above the melting point by the neutron diffraction technique. Furthermore, the local order in amorphous(a-) GeTe is determined by analyzing the intensity data of the electron diffraction of its thin film. The structure factors S(K) and radial distribution functions(RDF) of these liquids were compared with those of amorphous states.

S(K) for both the amorphous and liquid states of GeTe are given in Fig. 1. The S(K) of a-GeTe is characterized by an apparent small-angle prepeak which does not exist in the S(K) of the amorphous state of either pure Ge or pure Te and the strongest second peak. The S(K) of l-GeTe is somewhat different, either in the position or in the height of peaks, from that of the amorphous state. In particular, the corresponding second peak becomes extremely low when melting. The S(K) of l-GeTe is also quite different from that of typical liquid metals which follows the hard sphere model where the first peak in the S(K) is remarkably high[1].

Values of the interatomic distance(ID) and the coordination number(CN) evaluated from the RDF are listed in Table 1, which suggest that the local order in the amorphous and the liquid states is not like the distorted rock-salt structure of GeTe which possesses a relatively ionic character[2]. It seems that the amorphous material is more covalentic than crystalline GeTe. Furthermore, it can be expected from the value of CN 3.7, that fourfold-coordinated Ge atoms and four-fold or less than four-fold coordinated Te atoms exist in a-GeTe, although an exact coordination relationship between constituting atoms cannot be determined only by a single diffraction experiment. The CN in l-GeTe cannot be determined exactly due to the broadening and asymmetry of the first peak in the liquid RDF, but it seems to be nearer to the value of the amorphous state and to be much smaller than that of typical liquid metals.

S(K)s for l-As_2Te_3 at 424 and 625°C are shown in Fig. 2, together with the X-ray diffraction result on $As_{45}Te_{55}$ glass by Cornet and Rossier[3]. The general characteristic of functional form of the S(K), i.e. either in the height or in the position of peaks, is nearly equal in the amorphous and liquid states. The nearest-neighbor shell of the RDF shows a relative-

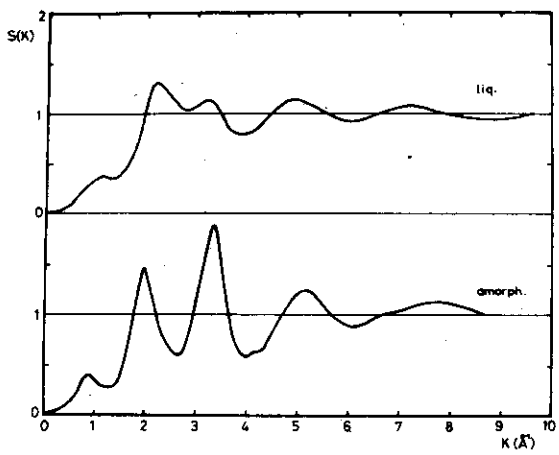

Fig. 1 The S(K) of liquid(770°C) and amorphous GeTe.

Table 1 The ID and CN of GeTe in the liquid and amorphous states.

Specimen	r_1	r_2	CN
l-GeTe	2.83	4.15	4.1*
			3.6**
a-GeTe	2.67	4.15	3.7

* Observed area of the first peak.

** Twice the area of the left segment of the first peak.

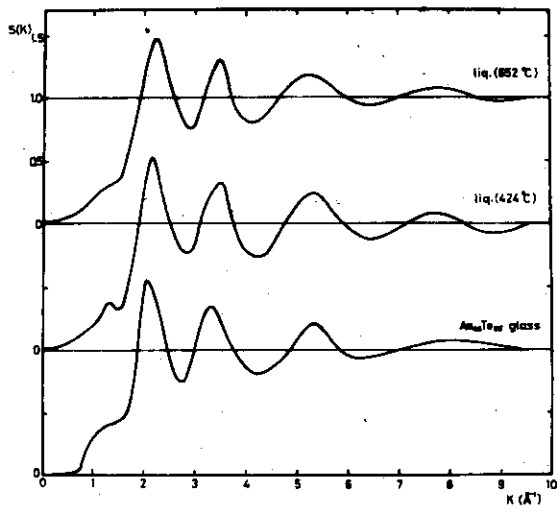

Fig. 2 The S(K) of l-As_2Te_3 at 424 and 652°C and a-$As_{45}Te_{55}$[3].

Table 2 The ID and CN of As_2Te_3 in the liquid and amorphous states.

Specimen	r_1	r_2	CN
l-As_2Te_3(424°C)	2.66	4.02	2.7
l-As_2Te_3(652°C)	2.66_5	4.02	2.6
a-As_2Te_3	2.66	3.98	-

ly sharp and symmetrical form in both the liquid and amorphous states.

Table 2 lists the result of radial distribution analysis, together with the corresponding data of c-As_2Te_3. The results of structural analysis shown in Table 2 suggests that the amorphous structure of As_2Te_3 within the first two coordination spheres has the local order which would be expected when the sample was cooled to toom temperature while maintaining it in the liquid state. It is also shown in Table 2 that in As_2Te_3 the short-range order in the disordered state (the amorphous and liquid states) is different from that in the crystalline state. c-As_2Te_3 includes As atoms surrounded octahedrally by Te atoms and threefold-coordinated As atoms[4]. Therefore, it has a longer mean interatomic distance and a larger CN than those in the disordered state, different from As_2S_3 and As_2Se_3 which show a similar local order in both the disordered and crystalline states.

[1] N.W. Ashcroft and J. Lekner: Phys. Rev. 145 (1966) 83.

[2] J. Goldak and C.S. Barrett: J. Chem. Phys. 44 (1966) 3323.

[3] J. Cornet and D. Rossier: J. Non-Cryst. Solids 12 (1973) 85.

[4] G.J. Carron: Acta Cryst. 16 (1963) 338.

V2 The Neutron Diffraction Study of Liquid As_2Se_3 and $GeSe_2$

Osamu Uemura, Daisaku Muno and Tsuneo Satow

Department of Chemistry, Faculty of Science, Yamagata University

Neutron diffraction experiments were performed on liquid As_2Se_3 and $GeSe_2$ at high temperatures. The structure factors S(K) and radial distribution functions(RDF) of these liquids were compared with those of amorphous states.

The S(K) for liquid $GeSe_2$ at 771°C are shown in Fig. 1, in which the S(K) of amorphous(a-) $GeSe_2$[1] is also plotted. There is no difference between the general forms of both S(K). As in the amorphous state a clear pre-peak is observed in the liquid(l-) $GeSe_2$ around K=1.05 $\AA^{-1}$ corresponding to the strongest diffraction line in the orthorhombic $GeSe_2$. Height of the first peak maximum in the liquid state is considerably low compared with that in the amorphous state. This result is often seen in covalent bonded liquid semiconductors such as l-Se[2]. On the other hand, in the case of e.g. l-Sb_2Se_3 which has rather high electrical conductivity, the first peak maximum of the liquid S(K) becomes much higher than the second one compared with the case of the amorphous state[3]. It seems from these results that hte distorted tetrahedra of $GeSe_4$ in the solid $GeSe_2$ in which one Ge atom is bonded to four Se atoms, each Se atom being shared between two tetrahedra, are scarcely destroyed in the liquid state.

The peak positions and the coordination number(CN) of nearest neighbor atoms evaluated from the RDF are listed in Table 1 together with the result of a-$GeSe_2$. The result of radial distribution analysis also suggests that the covalent bond between unlike atoms wiakens little on melting.

Fig. 2 gives the S(K) for l-As_2Se_3 at 400, 515 and 630°C together with amorphous data[4]. The peak maxima of the S(K) in the liquid state diminish and their widths broaden slightly with increasing temperature. These trends are found to be evident in the first peak maximum. This result corresponds to that of Crozier et al.[5] obtained by the EXAFS technique that the disorder term in As_2Se_3 increases with the increase of temperature in the liquid region. A similar conclusion to the case of l-$GeSe_2$ can be decuced from the following characters of the S(K) in l-As_2Se_3. 1) Its functional form is similar to that in the amorphous phase. 2)Pre-peak is distinctly observed at thesame position as that in the amorphous S(K). 3)The ratio of the first and second peak maxima is considerably small. 4) The first minimum near 2.9 $\AA^{-1}$ is shallower than the second one near 4.6 $\AA^{-1}$.

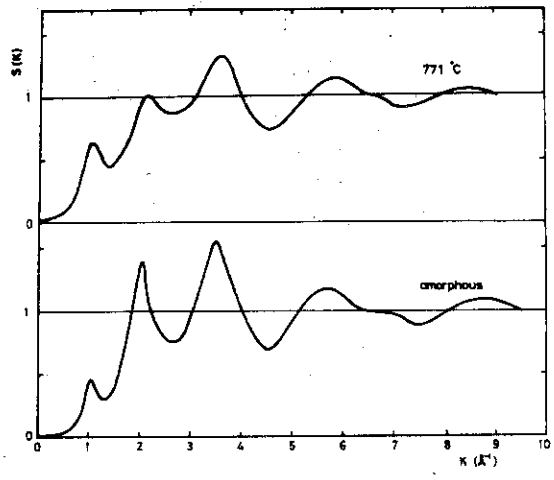

Fig. 1 The S(K) for a- and l-$GeSe_2$.

Table 1 The interatomic distance(ID) and the CN of l-As_2Se_3 and l-$GeSe_2$.

Specimen	ID(Å)	CN	Ref.
l-$GeSe_2$(771°C)	2.40_5	2.8	
a-$GeSe_2$	2.36_5	2.6	[1]
l-As_2Se_3(400°C)	2.41_0	2.7	
l-As_2Se_3(515°C)	2.43_0	2.7	
l-As_2Se_3(630°C)	2.43_5	2.6	
a-As_2Se_3	2.43	2.4	[4]

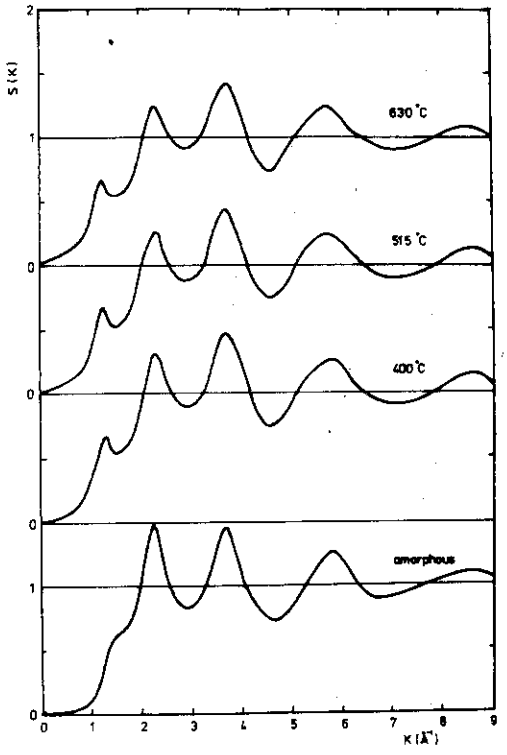

Fig. 2 The S(K) for a-As_2Se_3 at room temperature[4] and the liquid one at 400, 515 and 630°C, respectively.

The nearest neighbor distances and the CN obtained from the RDF are also described in Table 1, as well as the data of a-As_2Se_3[4]. There is little difference in the ID between both states if the increase of thermal motion in the liquid state is taken into consideration.

It is also observed that the RDF of both materials are characterized by the well-defined first neighbor shell because of the deep minimum on its right-hand side although in the liquid state. These results indicate that strong covalent bondings between unlike atoms in the solid state still remain when melting.

[1] O. Uemura, Y. Sagara and T. Satow: phys. stat. sol.(a) 32 (1975) K91.

[2] Y. Waseda, K. Yokoyama and K. Suzuki: Phys. Cond. Mat. 18 (1974) 293.

[3] T. Satow, O. Uemura, S. Akaike and S. Tamaki: J. Non-Cryst. Solids 29 (1978) 215.

[4] Y. Sagara, O. Uemura, S. Okuyama and T. Satow: phys. stat. sol.(a) 31 (1975) K33.

[5] E.D. Crozier, F.W. Lyte, D.E. Sayers and E.A. Stern: Canad. J. Chem. 55 (1977) 1969.

V3 Neutron Diffraction on Liquid Binary Alloys with Miscibility Gaps. III. Ga-Pb System

Yoshimi Tsuchiya*, Shin'ichi Takeda**, Keiichi Iida**
Koji Honma*** and Hideo Okazaki***

*Department of Physics, Faculty of Science, Niigata University,
**College of Bio-Medical Technology, Niigata University,
***College of General Education, Niigata University.

In the previous reports,[1] we have shown that the interference functions of liquid Zn-Bi and Bi-Ga systems have anomalous temperature dependence. From the concentration-concentration fluctuation, $S_{cc}(Q)$ of Bi-Ga, it is inferred that this anomalous behaviour of interference function is connected with the temperature dependence of concentration fluctuation. To make sure the above results, we have measured the interference functions for liquid Pb-Ga system as a function of temperature and concentration.

Pb-Ga system at 50 at% of Ga has the critical point of the two liquid separation, T_c, at 606° C.[2] The liquid specimen was confined in quartz tube. The system was heated by nickrome wire heater and its temperature was controlled within ± 1° C using the so called PID regurator. The neutron diffraction measurements were carried out using ISSP-ND II diffractometer at JRR-3 reactor with Ge single crystal monochrometer.

After correction due to the quartz tube, background counting, absorption, etc, the results were analyzed under the assumption that each partial interference function has only weak dependence on the constituents of the alloys.[3] Then according to Bhatia and Thornton,[4] the concentration-concentration fluctuation, $S_{cc}(s)$, $s = Q/2\pi$, was obtained. In Fig. 1, the temperature dependence of $S_{cc}(s)$ for 50 at% Ga alloy is shown. $S_{cc}(s)$ has a

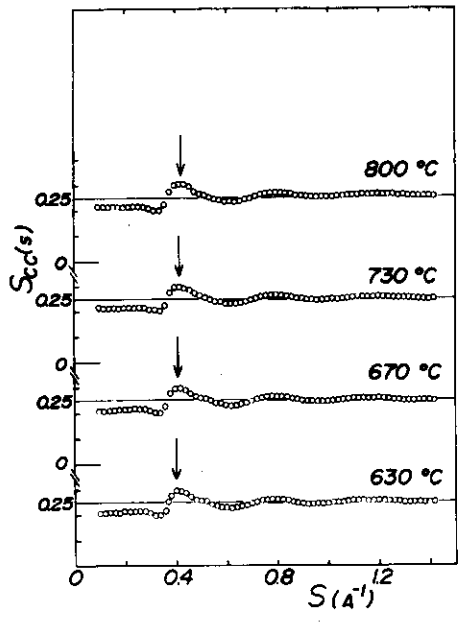

Fig. 1, Temperature dependence of $S_{cc}(s)$ for liquid $Pb_{50}Ga_{50}$ alloy.

typical s-dependent characteristic; namely it has a small peak at about s = 0.4 A^{-1} and approaches to C(1-C) = 0.25 (C; Ga concentration) in the higher momentum region. As the temperature is approached to the critical temperature, the peak position shifts towards low momentum region. In Fig. 2, the peak position is plotted against the reduced temperature, $(T-T_c)/T_c$. This result may suggest that the anomalous temperature dependence of the interference function for immiscible liquid alloys is due to the temperature dependence of a concentration fluctuation. However, a more sophisticated consideration will be required to connect the observed temperature dependence of $S_{cc}(s)$ to the critical opalescence at the critical temperature.

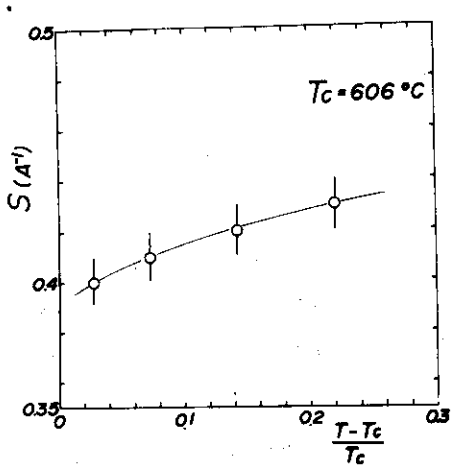

Fig. 2, Temperature dependence of the peak position of $S_{cc}(s)$.

References

1) K. Honma, H. Okazaki, Y. Tsuchiya, S. Tamaki and K. Iida: Phys. Lett. 58A (1976) 29, Y. Tsuchiya, S. Tamaki, F. Tachibana, K. Honma and H. Okazaki: Annual Report on Neutron Scattering Studies in JAERI, JAERI-M 8009 (1978) 98.

2) R. P. Elliott: Constitution of Binary Alloys, First Suppliment (McGraw-Hill, 1965) 453.

3) J. E. Enderby, D.M. North and P. A. Egelstaff: Phyil. Mag. 14 (1966) 961, Y. Waseda and S. Tamaki: Phil. Mag. 32 (1975) 951.

4) A. B. Bhatia and D. E. Thornton: Phys. Rev. B2 (1970) 3004.

VI1 NEUTRON DIFFRACTION TOPOGRAPHIC OBSERVATION OF LAYER-SUBSTRUCTURE IN COPPER ALLOYS

Hiroshi Tomimitsu, Kohji Kamada and Kenji Doi

Physics Division, Japan Atomic Energy Research Institute.

Neutron diffraction topography was applied to the direct observation of the texture in some Bridgman-grown Cu-alloy crystals. The texture in a Cu-5% Ge crystal with 3 cm in diameter and 10 cm in length, the growth direction being nearly parallel to [110], was found composed of a layer-substructure: layers parallel to (001) were arrayed with the spacing of about 1 mm, and extended throughout the crystal nearly parallel to the growth direction. The (001)-layers were attached on its both sides with plates parallel to (100)- and (010)-planes, with the thickness, the interplaner spacing and the height of about 0.5 mm, respectively. These layer-substructures corresponded to the arrayed striations visible on the crystal surfaces. The (001)-layer substructure as revealed with the Cu-5%Ge crystal was also observed in other Cu= based alloys, such as Cu-Ni, Cu-Si, Cu-Al, etc., and it seems to be quite different from both of the cellular- and lineage-substructures hitherto proposed to explain the texture of Bridgman-grown crystals. The model seems to suggest a new type of growth mechanism in Bridgman-grown crystals. The novel techniques of neutron diffraction topography were applied, viz. the successive topographic observation with varying crystal settings and the simultaneous edge-on view of the two of the {100}-planes with Bragg angle exactly set to 45 degree. The image contrast of the topographs was explained with the diffraction theory of the secondary extinction.

This work is going to be published very soon, of which preliminary accounts were published already[1].

Reference

(1) H.Tmimitsu, K.Kamada and K.Doi: Phil.Mag. A38(1978),483.

VI2 A New Result with a Two Crystal Component Neutron Interferometer

Seishi Kikuta, Toshio Takahashi, Kan Nakayama*
Yasuhiko Fujii** and Sadao Hoshino**

Institute of Industrial Science, University of Tokyo, * National Research Laboratory of Metrology, ** Institute for Solid State Physics, University of Tokyo.

In the paper published[1] previously, the construction of a two-crystal component interferometer was reported with preliminary reuslts of the interference effect. The interference fringe pattern given in the paper shows a rather poor contrast. This reports on the interference fringe pattern, with a higher contrast, which is obtained by constructing another interferometer.

A neutron interferometer composed of two components having the same type as shown in the previous paper was newly made from a single crystal of silicon grown by the floating zone method, which is free from dislocation and of high purity. Both the first and second crystals have the equal thickness of 11.7 mm and a gap between two crystals is 14.2 mm. The symmetric 220 Laue-case diffraction was used with $\lambda = 2.44$ Å. The beam having the angular deviation of $W \fallingdotseq 0.5$ was selected by means of the slit system, the slit width being 2 mm. A phase shifting material, an aluminum parallel plate of 4.980 ± 0.002 mm thick,

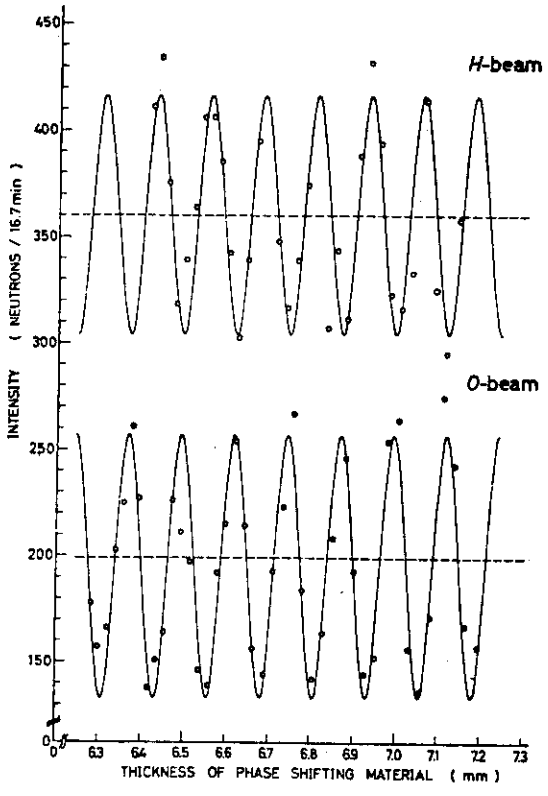

Fig. 1. Intensity oscillations of the O-beam and H-beam with the thickness of the phase shifting material of aluminum.

was inserted in the path I between the first and second crystals shown in Fig. 1 of the previous paper and rotated in a step of 0.216°. Other experimental conditions are the same as those in the previous paper. As shown in Fig. 1, the intensity oscillations of the O-beam and H-beam exhibit visibility higher than those in the previous report, probably because a crystal of higher quality was used. The observed points were fitted by the curve having a form of $a \cdot \sin bt + c$, as shown in Fig. 1. As a result, the material thickness producing a phase shift of 2π was determined as 0.125 ± 0.001 mm and the coherent scattering amplitude of aluminum as $(3.45 \pm 0.02) \times 10^{-13}$ cm.

Reference

1) S. Kikuta, T. Takahashi, K. Nakayama, Y. Fujii and S. Hoshino : J. Phys. Soc. Japan 45 (1978) 715.

VI3 POLARIZED NEUTRON DIFFRACTION FROM DYNAMICALLY AND STATICALLY POLARIZED PROTONS

Kiyoichiro Motoya, Masakazu Nishi and Yuji Ito

Institute for Solid State Physics, The University of Tokyo

If proton nuclei are polarized to some extent, a large spin dependence of scattering amplitude can be advantageously utilized to get informations on protonic positions[1] as well as their collective motions.

We measured the neutron spin dependent scattering of Nd^{3+} doped $La_2Mg_3(NO_3)_{12}\cdot 24H_2O$ single crystal with dynamically polarized protons with known proton polarization enhancement monitored by NMR, and this was compared with the one under the static brute force proton polarization method.

In the case of centrosymmetric crystal and $|f_N| \ll 1$, the flipping ratio R, which is the Bragg intensity ratio upon reversal of the incident neutron polarization, is simply given by

$$R=1+4\delta f_p^u \,/\, (f_p^u\, b_c + F_{oth}),$$

where $\delta = (1/4)\, b_{inc}\, f_N$, $b_{inc} = 5.818 \times 10^{-12}$ cm, $b_c = -0.374 \times 10^{-12}$ cm, f_p^u is the unit structure factor for protons, F_{oth} is the structure factor for others except protons and f_N is the mean proton polarization.

The polarized neutron diffraction measurements were made with PANSI spectrometer installed at JRR-2. A polarized neutron beam of λ = 1.22A reflected by Heusler alloy was used. Data were collected for (0,3,0) and (0,3,12) reflections with several polarization conditions. The results are summarized in Table 1. In selecting the Bragg reflection (0,3,0), we chose it because the proton structure factor F_p $(=f_p^u\, b_c)$ was substantially larger than F_{oth}. This means that the flipping ratio R is rather insensitive to the actual value of f_p^u. In order to determine the protonic positions accurately, we need to measure flipping ratios of reflections for which $|F_p| \simeq |F_{oth}|$. On the other hand, the observed good agreement between the experimental values and the calculated ones for both brute force method and for the dynamic polarization method indicates that the proton polarization value estimated from the observed NMR enhancement factor indeed gives the mean polarization of protons in the unit cell.

The small angle scattering experiment with much higher proton polarization in combination with the pseudorandom neutron spin modulation technique to observe proton polarization distribution is currently undertaken by us.

h,k,l	polarization method	temperature (K)	field (kOe)	proton polarization	R_{obs}	R_{calc}
0,3,0	dynamic	2.27	2.74	-4.44×10^{-3}	1.078(7)	1.075
0,3,0	dynamic	2.22	2.74	$+4.28\times10^{-3}$	0.923(8)	0.927
0,3,0	static	1.68	40.0	$+2.43\times10^{-3}$	0.965(9)	0.958
0,3,0	static	4.21	2.70	$+6.67\times10^{-5}$	1.001(8)	1.000
0,3,12	static	1.63	40.0	$+2.43\times10^{-3}$	0.997(6)	1.000

Table 1. Summary of experimental results. R_{obs} is the measured flipping ratio. R_{calc} is the calculated flipping ratio from the proton polarization value and the atomic positions determined by the X-ray diffraction experiment[2]. Numbers in the parentheses are standard errors.

References

1) J.B.Hayter, G.T.Jenkin and J.W.White, Phys.Rev.Letters 33 (1974) 696

2) A.Zalkin, J.D.Forrester and D.H.Templeton, J.Chem.Phys. 39 (1963) 2881

This work will be published in Solid State Communications.

VI4 Utilization of Pseudo-Bent PG Monochromator in DMNS

Masashi Iizumi and Nobuaki Minakawa
Division of Physics, Japan Atomic Energy Research Institute

DMNS, the double monochromators neutron spectrometer of triple-axis type (Fig. 1) was originally designed to utilize a bent monochromator for one of the pair of monochromator. A pair of flat PG monochromator of 75 mm x 75 mm has been used because a suitable bent monochromator with large area had not been available. Recently a pseudo-bent monochromator was fablicated and brought into use from October, 1978. This report describes the performance of this monochromator.

This pseudo-bent monochromator consists of 7 pieces of flat PG crystals of strip shape (11 mm x 75 mm x 1.6 mm) which were purchased from the Union Carbide Co. and are of the ZXC grade (mosaic spread: 0.8±o.2° FWHM). These pieces were placed on a aluminum frame. The part of the frame receiving the pieces had been machined so as to make a cylindrically concave curvature with radius of 75 cm. The PG pieces were then fixed by thin aluminum plates with screws (Fig. 2). Although we had provided an adjusting mechanism for each piece of graphite in order to allign the (002) planes of the composite crystals with in a tolerable horizontal mosaic spread, the rocking curve with width of 0.9° with no noticable structure was obtained without any adjustment.

This monochromator was then utilized as the second monochromator of DMNS and the performance was checked by various measurements. The energy of neutrons was 14.8 meV and collimation was all 40'. As is shown in Fig. 1, this spectrometer employs an air-cushion drive mechanism in translating back and forth the spectromater part as a whole. This enable one to set the

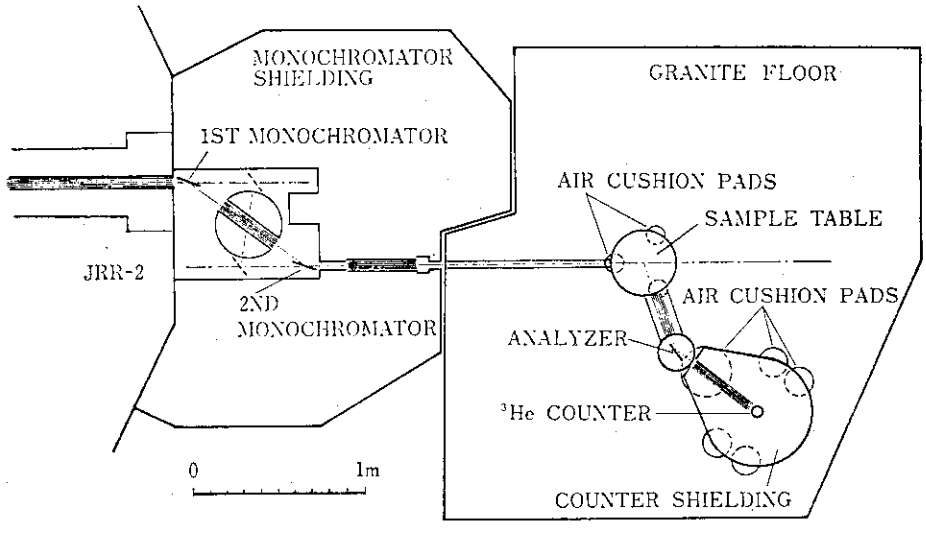

Fig. 1. Plan of DMNS

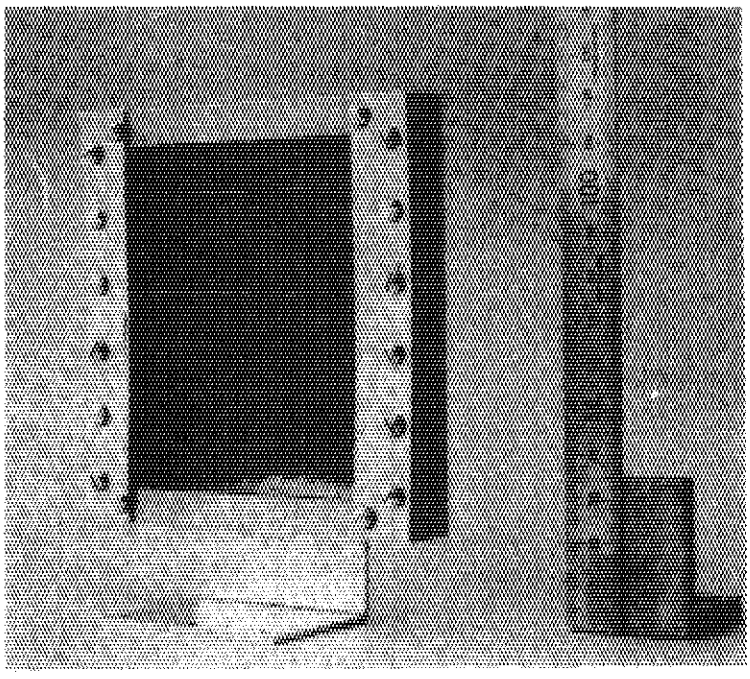

Fig. 2. Pseudo-bent moncchromater

position of the sample table approximately at the image position of the bent monochromator (140 cm from the monochromator). Size of the neutron beam at the sample position was measured by a small fission counter and the result was about 3.5 cm in height and 2 cm in width. The overall efficiency was compared by measuring the one-phonon scattering of a Cu single crystal. Intensity gain turned out to be a factor of five as compared with the flat monochromator previously used. Part of this gain was attributable to the removal of a redundant collimator of 40' placed between two monochromators before the present modification. However most of the substantial gain was brought about by the use of the bent monochromator. The gain was enhanced by the beam channel designed so as to take full advantage of the bent monochromator. As shown in Fig. 3 the cross section of the beam channel indicated by a pair of numbers in the lower part of the figure was designed to be unusually large in height compared with its width; the height was taken to be the same as the vertical size of the monochromator (75 mm).

The gain in intensity at the center of the image position is given approximately by

$$\frac{I_{bent}}{I_{flat}} = \frac{L_0 + L_1}{L_1} \frac{h_m}{h_s}$$

where L_0 is the distance from the source to the monochromator and L_1 is that of the monochromator to the sample. Also h_s is the height of the source, while h_m is that of monochromator. For a certain value of the focussing dis-

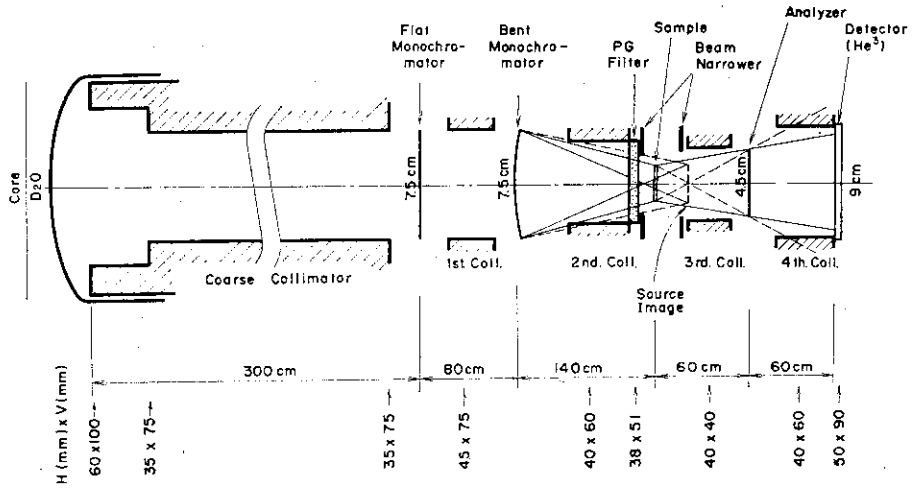

Fig. 3. Vertical cross section of the beam path of DMNS, which was designed to take full advantage of the bent monochrmator and vertically divergent neutron beam. Pairs of numbers at the bottom indicate cross sections of beam path.

tance which is taken in such a way that the source image is generated in the vicinity of the sample position with a practical monochromator-to-source distance, it is most effective to make the monochromator height as large as practical and make the whole part of the monochromator be illuminated by the neutron beam. Sofar as the authors know the present attempt is the first to try to deduce full advantage of such a beam chammel design.

Large cross section of beam channel is liable to cause the increase of background. But in the present spectrometer a careful design of a beam stopper of direct beam and shielding suppress the background at fairly low level (0.8 counts/min).

In order to match the relaxed vertical resolution of the monochromator system by the use of bent monochromator the vertical resolution of the analyzer system was also relaxed by collecting divergent scattered beam by the vertical arrangement of a He^3 counter with 50 mm in diameter and 90 mm in effective height. Effective angular divergence of the neutron beam in the vertical direction was approximately the same for both the monochromator and analyzer systems and is 1.6° in FWHM.

LIST OF PUBLICATIONS

A. Papers Published in Journals

79A1
Katsuhiko Abe and Masatoshi Sato
Application of the Multilayered Films to the Neutron Diffraction Technique
J. Cryst. Soc. Japan, 21 (1979) 165

79A2
J. Akimitsu and Y. Ito
Orbital Ordering in K_2CuF_4 (in Japanese)
Kotaibutsuri (Solid State Physics) 13 (1978) 67

79A3
Hiroshi Betsuyaku
First-Order Phase Transition and Critical Neutron Scattering in Chromium
Phys. Rev. Letters 42 (1979) 546

79A4
Yasuo Endoh
Lattice Dynamics in Ferromagnetic Invar Alloys
J. of Magnetism and Magnetic Materials 10 (1979) 177

79A5
Yasuo Endoh and Yasuhisa Noda
Zero Sound Anomaly in a Ferromagnetic Invar Alloy $Fe_{65}Ni_{35}$
J. Phys. Soc. Japan 46 (1979) 806

79A6
Kazuo Gesi and Masashi Iizumi
Neutron Scattering Study on the Incommensurate Phases in Rb_2ZnBr_4
J. Phys. Soc. Jpn. 45 (1978) 1777

79A7
Kazuo Gesi and Masashi Iizumi
Neutron Scattering Study on the Incommensurate Phases in Ferroelectric Rb_2ZnCl_4 and K_2ZnCl_4
J. Phys. Soc. Jpn. 46 (1979) 697

79A8
S. Haneda, Y. Yamaguchi, H. Watanabe and N. Kazama
Magnetic and Crystallographc Studies on MnAs Submitted by P or Sb
J. Phys. Soc. Japan 46 (1979) 802

79A9
Kinshiro Hirakawa and Hideki Yoshizawa
Observation of Condensation of Magnons in Quasi-2D, Planar Ferromagnet K_2CuF_4
J. Phys. Soc. Japan 47 (1979) 368

79A10
Sadao Hoshino, Takashi Sakuma and Yasuhiko Fujii
The Existence of the Order Phase in Superionic Conductor Ag_3SI
J. Phys. Soc. Japan 45 (1978) 705

79A11
Satoshi Iida, Masaharu Kohno, Yorihiko Tsunoda, and Nobuhiko Kunitomi
Strain Waves in Chromium Alloys
J. Phys. Soc. Japan 44 (1978) 1747

79A12
Masashi Iizumi
Verwey Transition in Magnetite as a Potentially Incommensurate but Eventually Commensurate Phase Transition.
Modulate Structures - 1979, AIP Conf. Proc. 53 (1979) 184

79A13
Masashi Iizumi and Kazuo Gesi
Neutron Scattering Studies of Ferroelectric Crystals with Modulated Structure
Modulated Structures - 1979, AIP Conf. Proc. 53 (1979) 211

79A14
Masashi Iizumi
Neutron Spectrometer of Tanzboden Type (in Japanese)
J. Cryst. Soc. Jpn. 21 (1979) 168

79A15
Y. Ito, J. Akimitsu, M. Matsui and S. Chikazumi
Magnetic Form Factor of $Fe_{0.66}Ni_{0.34}$ Invar Alloy
J. Mag. and Magnetic Materials 10 (1979) 194

79A16
Yuji Ito, Shiro Takahashi, Yoshihisa Kawamura, Kiyoichiro Motoya and Masakazu Nishi
About the newly constructed PANSI - polarization analysis neutron scattering instrument - in Japan
Nukleonika 24 (1979) 699

79A17
Koichi Katsumata, Makoto Kobayashi and Hideki Yoshizawa
Neutron Experiment on the Tetracritical Phase Transition in a Random Mixture with Competing Spin Anisotropies
Phys. Rev. Letters 43 (1979) 960

79A18
Katsuya Kikuchi
Magnetic Study of NiS_2 Single Crystals
J. Phys. Soc. Jpn. 47 (1979) 484

79A19
Seishi Kikuta, Toshio Takahashi, Kan Nakayama, Yasuhiko Fujii and Sadao Hoshino
Construction of Two Crystal Component Neutron Interferometer
J. Phys. Soc. Japan 45 (1979) 1024

79A20

Seishi Kikuta, Toshio Takahashi, Kan Nakayama, Yasuhiko Fujii and Sadao Hoshino

Neutron Bragg-Case Rocking Curves from the Front and Back Surfaces of Silicon Crystal Plate

J. Phys. Soc. Japan 45 (1978) 1065

79A21

Seishi Kikuta, Toshio Takahashi, Kan Nakayama, Yasuhiko Fujii and Sadao Hoshino

A New Result with a Two Crystal Component Neutron Interferometer

J. Phys. Soc. Japan 46 (1979) 1024

79A22

N. Kunitomi, Y. Tsunoda, N. Wakabayashi, R.M. Nicklow and H.G. Smith

The Phonon Dispersion Relations in a Disordered $Ni_{1-x}Pt_x$ System

Sol. St. Comm. 25 (1978) 921

79A23

Masahiro Mori, Yukio Noda and Yasusada Yamada

Incommensurate Jahn-Teller Phase Transitions in $R_2PbCu(NO_2)_6$ (R: K, Rb, Cs, Tl)

AIP Conf. Proc. 53 (1979) 214

79A24

Yutaka Nakai, Kazuo Hozaki, Nobuhiko Kunitomi

Magnetic Moments of Mn Atoms in fcc Co-Mn Alloys

J. Phys. Soc. Japan 45 (1978) 73

79A25

Masakazu Nishi and Yuji Ito

Magnetic Structure of $KFeS_2$-a Linear Chain Antiferromagnet and a Spin Analog of Active Sites of Two Iron Ferredoxins- by Neutron Diffraction

Solid State Commun. 30 (1979) 571

79A26

Takashi Sakuma, Sadao Hoshino and Yasuhiko Fujii

Quasi-elastic Neutron Scattering Study of Aquaous Solutions of $FeCl_3$, $NiCl_2$ and $MgCl_2$
J. Phys. Soc. Japan 46 (1979) 617

79A27
Masatoshi Sato and Katsuhiko Abe
Interface Magnetization of Fe-SiO Multilayer Film Studied by Neutron Bragg reflection
Solid State Commun. 26 (1978) 95 and ibid, Erratum 26 (1978)

79A28
Masatoshi Sato and Katsuhiko Abe
Acoustic Phonon Dispersion in $NiTe_2$
J. Phys. C 12 (1979) L613

79A29
Masatoshi Sato, Katsuhiko Abe and Y. Endoh
Neutron Diffration Studies on the Interface Magnetization of Fe-SiO Multilayer
J. de Physique 40 (1979) C2-72

79A30
Noboru Schibuya, Yutaka Nakai, Katsuhito Yamasaki, Nobuhiko Kunitomi
Neutron and Mossbauer Studies of Atomic Magnetic Moments in a Ternary Alloy Fe-Co-Ni
J. Phys. Soc. Japan 46 (1979) 475

79A31
Yoshihiro Shiozaki, Yutaka Nakai, Nobuhiko Kunitomi
Average Magnetic Moment of Mn Impurities in Ferromagnetic Ni-Co Alloys
J. Phys. Soc. Japan 46 (1979) 59

79A32
Yoshihiro Shiozaki, Yutaka Nakai
Neutron Diffraction Experiment on γ-$Cu_{15}Mn_{85}$ Single Crystal
J. Phys. Soc. Japan 47 (1979) 817

79A33
Hiroshi Tomimitsu, Kohji Kamada and Kenji Doi
Neutron Diffraction Topographic Observation of the Layer-Substructure in a Cu-5%Ge Single Crystal
Phil. Mag. A38 (1978) 483

79A34
Y. Tsunoda, N. Kunitomi, N. Wakabayashi, R.M. Nickiow, H.G. Smith
Phonon Dispersion Relations in the Disordered Ni_{1-x} Pt_x system
Phys. Rev. 19 B (1979) 2876

79A35
O. Uemura, Y. Sagara, D. Muno and T. Satow
The Structure of Liquid As_2Se_3 and $GeSe_2$ by Neutron Diffraction
J. Non-Cryst. Solids, 30 (1978) 155

79A36
O. Uemura, Y. Sagara, M. Tsushima, T. Kamikawa and T. Satow
The Neutron Diffraction Study of Liquid GeTe and As_2Te_3
J. Non-Cryst. Solids 33 (1979) 71

79A37
Toshio Urano, Yutaka Nakai
Magnetic Scattering of Neutrons by the Clusters in Co Rich CoAl Compounds
J. Phys. Soc. Japan 45 (1978) 439

79A38
Y. Yamaguchi and H. Watanabe
Magnetic and Crystallographic Study on the Electronic State of Interstitial Cations in MnSb
J. Phys. Soc. Japan 46 (1979) 1138

79A39
O. Yamashita, Y. Yamaguchi, I. Nakatani, H. Watanabe and K. Masumoto
Polarized Neutron Diffraction Study of $CuCr_2Se_4$ Single Crystal
J. Phys. Soc. Japan 46 (1979) 1145

B. Preprints of Papers Submitted for Publication

79B1
J. Akimitsu and K. Siratori
Single Domain Formation of Magnetic Screw Structure in Particular Application to Neutron Polorizer
to be published in J. Mag. and Magnetic Materials

79B2
M. Akimitsu, J. Akimitsu, T. Mizoguchi and S. Kimura
Magnetic Structure in $Fe_{1-x}O$
to be published in J. Phy. Chem. Solid

79B3
J. Akimitsu, Y. Inada, K. Siratori, I. Shindo and N. Kimizuka
Two Dimensional Spin Ordering in YFe_2O_4
to be published in Solid State Commun.

79B4
Hajime Asano, Kazunori Kishi and Makoto Hirabayashi
Static Displacement of Ta in Ta_2H by Single Crystal X-ray and Neutron Diffraction
to be published in Proc. Int. Conf. Hydrogen in Metals, Minakami, Nov. 1979, Japan Inst. Met.

79B5
Hajime Asano and Makoto Hirabayashi
Hydrogen Ordering in Va Transition Metal Hydrides
Zeitschrift für phys. Chem. in press 1979. Presented at Int. Conf. Hydrogen in Metals, Münster, Germany, March, 1979

79B6
Yasuo Endoh, Mitsuo Kataoka, Humihiko Takei, Yasuhisa Noda and Yoshikazu Ishikawa
Neutron Scattering Study of Cooperative Jahn Teller Effect in Fe_2TiO_4
J. Mag. Magnetic Materials in press

79B7
Yasuo Endoh, Jn'ichiro Mizuki and Yoshikazu Ishikawa
Spin Density Wave in dilute Fe- and Si-Cr under the High Pressure
appear in J. Mag. Magnetic Materials

79B8
H. Fujii, S. Komura, T. Takeda, T. Hōkabe and T. Okamoto
Polarized Neutron Diffraction Study of CoMnP Single Crystal
Int. Conf. on Neutron Scattering and Magnetism 1979 Jülich; to be
published in J. Magnetism and Magnetic Materials

79B9
Satoru Funahashi and Yoshikazu Hamaguchi
Spin-Wave Dispersion Relations in Mn_2Sb
International Conference on Magnetism, Munich, Sept.3-7, 1979;
to be published in J. Magnetism and Magnetic Materials

79B10
Yoshikazu Hamaguchi, H. Betusyaku and S. Funahashi
Magnetic Excitations in TbZn
International Conference on Magnetism in Munich, Sep. 3-7, 1979. JAERI-memo
8508 (1979)

79B11
Makoto Hirabayashi
Structural Phase Transitions in Metal Hydrides
to be published in Proc. Int. Conf. Hydrogen in Metals, Minakami, Nov.
1979, Japan Inst. Met.

79B12
Sadao Hoshino, Takashi Sakuma and Yasuhiko Fujii
A Structural Phase Transition in Superionic Conductor Ag_3SI
ISSP Technical Report A964, May 1979, to be published in J. Phys. Soc.
Japan 47, No.4.

79B13
Mitsuo Kataoka and Yasuo Endoh
Critical Diffuse Scattering due to the Cooperative Jahn Teller Transition
submitted to J. Phys. Soc. Japan

79B14
Katsuya Kikuchi, Tomonao Miyadai and Yuji Ito
Weak Ferro- and Antiferromagnetism of NiS_2
ICM'79 in Munich, Sep. 3-7, 1979; to be published in J. Magnetism and Magnetic Materials

79B15
S. Komura, K. Tajima, H. Fujii, Y. Ishikawa and T. Okamoto
Spin Wave Excitations in Fe_2P
Int. Conf. on Magnetism, 1979 Munich; to be published in J. Magnetism and Magnetic Materials

79B16
Kiyoichiro Motoya, Masakazu Nishi and Yuji Ito
Polarized Neutron Diffraction from Dynamically and Statically Polarized Protons
to be published in Solid State Commun.

79B17
Hisashi Obara, Yasuo Endoh, Yoshikazu Ishikawa and Takemi Komatsubara
Magnetic Phase Transition of MnP under the Magnetic Field
Preprint, to be submitted to J. Phys. Soc. Japan

79B18
Isao Okada, Hajime Asano and Makoto Hirabayashi
Refinement of the Structure of β-V_2D by Single Crystal Neutron Diffraction
to be published in Proc. Int. Conf. Hydrogen in Metals, Minakami, Nov. 1979, Japan Inst. Met.

79B19

M. Sato, K. Abe, Y. Endoh, J. Hayter and R.D. Lowde

Magnetization of Ferromagnetic Metals at the Interface to Other Materials

submitted to J. Phys. C

79B20

K. Siratori, J. Akimitsu, E. Kita and M. Nishi

Control of the Sense of the Screw Spin Structure by Magnetoelectric Cooling

to be published in J. Phys. Soc. Jpn.

79B21

H. Watanabe and Y. Yamaguchi

Electronic State of Cations in NiAs Type Compounds Containing Mn

to be published in J. Magnetism Mag. Materials

79B22

H. Watanabe, Y. Yamaguchi, H. Oda and H. Takei

Magnetic and Neutron Diffraction Study of $SrCoO_{3-x}$

to be published in J. Magnetism Mag. Materials

79B23

Yasusada Yamada, Masahiro Mori, Yukio Noda and Masashi Iizumi

Neutron Diffuse Scattering in Fe_3O_4 due to Molecular Polarons

to be published in Solid State Commun.

79B24

Y. Yamaguchi and H. Watanabe

Magnetic Disturbance around the Interstitial-Site Mn Atom in MnSb

to be published in J. Phys. Soc. Japan 48 (1980) No.2

79B25

Hideki Yoshizawa, Koji Ubukoshi and Kinshiro Hirakawa

Neutron Scattering Investigation of the Magnetic Excitations in $CoBr_2$

Technical Report of I.S.S.P. Ser.A No. 980

C. Papers Read at Meetings

Following papers were read at the Fall Meeting of Physical Society of Japan in Shizuoka, October 3-6, 1978

79C1
Kazuo Gesi and Masashi Iizumi
Neutron Scattering Study on the Incommensurate Phases in Rb_2ZnCl_4 and Rb_2ZnBr_4

79C2
Sadao Hoshino, Takashi Sakuma and Yasuhiko Fujii
Phase Transition of Ag_3SI II. Structure

79C3
Masashi Iizumi and Kazuo Gesi
Incommensurate Satellite Reflections in the Ferroelectric Phase of Ammonium Rochelle Salt.

79C4
Kiyoichiro Motoya, Yuji Ito and Masakazu Nishi
Nuclear Polarization and Polarized Neutron Diffraction of LMN

79C5
Masakazu Nishi and Yuji Ito
Magnetism of $KFeS_2$

79C6
M. Ohashi, Y. Yamaguchi, T. Kaneko, H. Yoshida and H. Watanabe
Neutron Diffraction Study of CrSb Single Crystal

79C7
Masatoshi Sato, Katsuhiko Abe, Yasuo Endoh, Yuji Ito and Masakazu Nishi
Interface Magnetization of Ni-SiO Multilayered Film Studied By the Bragg reflection of Polarized Neutron beam

79C8
Shin'ichi Takeda, Keiichi Iida, Yoshimi Tsuchiya, Koji Honma and Hideo Okazaki
Structure of IVb-Te Liquid Semi-conductors

79C9
Hiroshi Tomimitsu, Kohji Kamada and Kenji Doi
Neutron Diffraction Topographic Observation of Cu-Alloys Made by Bridgman Method

79C10
Yoshimi Tsuchiya, Fumio Tachibana, Koji Honma and Hideo Okazaki
Neutron Diffraction on Liquid Binary Alloys with Miscibility Gaps. III. Ga-Pb system

Following papers were read at the Spring Meeting of Physical Society of Japan in Osaka, Mar. 31-Apr. 3, 1979

79C11
Yasuo Endoh, Yoshikazu Ishikawa, Yasuhisa Noda and Humihiko Takei
Cooperative Jahn Teller Effect in Fe_2TiO_4

79C12
Satoru Funahashi, Hiroshi Nozaki and Isao Kawada
Magnetic Structure of V_5S_8

79C13
Mitsuo Kataoka and Yasuo Endoh
Critical Neutron Scattering from Fe_2TiO_4

79C14
Katsuya Kikuchi, Tomonao Miyadai, Tsunaomi Fukui and Koichi Takizawa
Magnetic Property and Origin of Weak Ferromagnetism in NiS_2

79C15
Kiyoichiro Motoya, Yuji Ito, Masakazu Nishi and Tadashi Mizoguchi
Spin Wave Excitations of Amorphous $Fe_{40}Ni_{40}P_{14}B_6$

79C16
Yutaka Nakai, Nobuhiko Kunitomi, Noboru Shibuya and Nobuyoshi Wakabayashi
Spin Wave in Fe-V Alloy

79C17
Takashi Sakuma and Sadao Hoshino
Phase Transition of Ag_3SBr I.

79C18
Tsutomu Sano, Shuzo Kawarazaki, Satoshi Iida and Nobuhiko Kunitomi
Magnetic Phase Diagram of Cr-Be Alloys.

79C19
Hiroshi Tomimitsu, Kohji Kamada and Kenji Doi
Neutron Diffraction Topographic Observation of Some Copper-Alloys Made by Bridgman Method

79C20
Hiroshi Tomimitsu, Kohji Kamada and Kenji Doi
Neutron Diffraction Topographic Characterization of the Large Crystals of Metallic Alloys

79C21
Yorihiko Tsunoda and Nobuhiko Kunitomi
Lattice Vibration in $Ag_{30}Pd_{70}$ Disordered with respect to the Interatomic Forces.

Following paper was read at the International Conference on Solid Films and Surfaces in Tokyo, July 5-8, 1978.

79C22
Masatoshi Sato, Katsuhiko Abe and Yasuo Endoh
Neutron Diffraction Studies on the Interface Magnetization of Fe-SiO Multilayer

Following paper was read at the Annual Meeting. of Japan Crystallograplic Society in Hiroshima, Nov. 18-19, 1978

79C23

Hiroshi Tomimitsu, Kohji Kamada and Kenji Doi

Neutron Topographic Observation of Copper Alloys